CHAPTER ONE
INTRODUCTION

1.1 Background of the Study

In the interaction of particles with electromagnetic fields, a consequence of force is naturally made manifest. But a force is defined as the product of a mass and the acceleration is possesses as a direction relationship with the force of a prime mover. When particles interact with fields, they get mass (Freeman, 2019). Hence, the vector quantity of a rate of change of velocity (acceleration); as a direct function of a rate of change of a particle's displacement, constitutes a thermodynamic study. This is primordially based on an integral understanding of the nature of interactions between particles or cells and, in a defined case study, the treatment of biological components with selected phytochemical extracts can form a background of a typical surface thermodynamic study. The HIV scourge since 1981 has long ago necessitated the need for Antiretroviral Therapies (ARTs) in its management. There are various quests for finding a lasting solution which tried to comply with global standards by the World Health Organization (WHO) and its allies. However, when faced with a positive test result to HIV, and a risk of contracting tuberculosis, a patient's first thought is an antiretroviral drug or therapy. This essentially entails that the drug blocks the virus contraction, penetration, replication and transmission thereby providing a functional cure of HIV in an infected person.

The consequences of contracting this virus can be considered to include the bitter psychological trauma which is always high, the lack of education to constantly go and test for any HIV infection, the non-availability of economic power to get a private HIV test kit and the opportunity to consult with a professional for the prescriptions of required antiretroviral drugs that can provide functional cure or therapy. Hence, infection with the HIV, a pathogenic retrovirus, can cause acquired immunodeficiency syndrome (AIDS) (Barre-Sinossi, et al., 1983). According to Maddon et al., (1986), macrophage, neuron and other cells can be infected by HIV, compare with (Chukwuneke, 2015). Dalgleish, et al., (1985) affirmed that CD4+ lymphocytes are the major target cells for HIV. This is because HIV has strong affinity to the CD4 molecules on the surfaces of CD4+ cells. HIV infection in a human body destroys so many CD4+ lymphocytes that the body begins to lose its natural immune function, therefore an AIDS patient is highly vulnerable to various infections like tuberculosis, neuronal dysfunction, tumors, and so on. Treatment success has been limited by poor tolerance of the

treatments by patients and the emergence of resistant strains of HIV. A need thus exists for an effective HIV treatment that will be well tolerated and relatively cheap.

Great efforts have been dedicated to remedial and preventive methods for many years, but there seem to be no working vaccine or cure for HIV/AIDS yet. An ideal vaccine should be innocuous and capable of inducing neutralizing antibodies as well as persistent immune responses in the mucous membrane and the blood (Levy, 2000). Drugs are being developed against new targets in different stages of HIV replication cycle. These drugs include new HIV reverse transcriptase inhibitors and HIV protease inhibitors, as well as new anti-HIV agents aimed at other targets (De, 2000). The use of antiretroviral drugs is actually expensive. Several therapies are currently available for initial therapy for HIV-infected patients but this research is focused at herbal drugs or additives that might have potential efficacies and tolerability profiles, and in a new therapeutic combinations that might result in synergetic activity. Before now China, India, Nigeria, the United States of America (USA) and WHO have all made substantial research investments in traditional herbal medicine as recorded by (Jon et. al., 2008). The WHO declaration of health for all by the year 2000 emphasized the importance of traditional medicine in achieving primary health care. According to WHO, the use of plant remedies is increasing in the developed countries of the world. In industrialized countries, consumers are seeking viable alternatives to synthetic medicines with their associated dangers of side effects and over medications. During the last decade, the WHO health assembly passed a number of resolutions in response to the resurgence of interests in the study and use of traditional medicine (van oss, et al., 2011).

The historic tradition of herbal extraction by man is still the empirical method known to provide health care for man. Traditional herbal medicines which have been in existence for more than two thousand years with various testimonies of success for curing many kinds of diseases, from my assessment is now gaining popularity. Judging from Jon (2008), it does appear that in many countries a variety of herbs and natural substances have been systematically experimented upon, recorded and incorporated into regular systems of medicine that later became the material-medica of traditional medicine.

Until the beginning of the 19th century, medical practices were what are now called traditional medicine. Originally medicine was obtained from plants available in the immediate environment and over the millennia, the most effective remedies amongst them were selected

by trial and error cum empirical reasoning. These then became part of medical tradition. Eventually, the renaissance period brought great scientific upheavals that began to introduce Cartesian Scientific Material into human activities and notably into the theory and practice of health care. Its method was to break up complex phenomena into their component parts and to deal with each one in isolation. This approach resulted in a search for a single cause for the disease and, correspondingly modern pharmacological experimental investigations were aimed at finding a single active compound of mineral elements or principle that could be isolated from a medicinal plant. The introduction of this kind of abstract medicine in the form of basic chemicals and pharmaceuticals during the 18^{th} and 19^{th} centuries resulted in methods for bringing quick relief to suffering and this won instant admiration and popularity. This system known as Allopath or Modern Medicine made rapid advances during the 19^{th} and 20^{th} centuries as a result of the advances made in biological, chemical and pharmacological sciences (van oss, et al., 2011).

It is against this background that this research employs an in-vivo experiment, to initiate interactions between collated blood and herbal drug samples and to measure their individual absorbance and corresponding transmittance values using a digital ultraviolet Spectrophotometer. In this specialized thermodynamic investigation, mathematical analysis of all values measured is done with dielectric constants and computed with the Lifshitz formula using the Microsoft 2018 version of the Excel software. Hamaker constants (A_{11}, A_{22} or A_{33}), Hamaker combined constants (A_{12}, A_{13} or A_{23}), the Combined Hamaker coefficients (A_{131}, A_{232}, and A_{132}), the harmonized combined Hamaker coefficients ($A_{132harm.}$); which are various measures of change in free energy of adhesion (ΔF^{adh}) were also computed. The ΔF^{adh} value being negative ($-\Delta F^{adh}$) and A_{132} being positive ($+A_{132}$), indicates attraction between particles involved in blood-drug interactions. It is this attraction that is the desired outcome which is the thermodynamic criterion for lymphocyte-drug attraction. But the converse ($+\Delta F^{adh}$ and $-A_{132}$) indicates repulsion. It is this repulsion that is another desired outcome which is the thermodynamic criterion for drug-coated, lymphocyte-HIV repulsion.

With this idea, a disease causing particle (pathogen) can be influenced to become repelled by a biological cell particle(s). This sort of influence (which can be catalyzed using a drug(s)), is here predicted thermodynamically. Prediction being favorable, informs that, contact which allows penetration, which initiates interaction, which leads to infection, can be discouraged. Hence, the prediction that is vital is that of calculating iteratively, A_{33} (Hamaker constant) that

would render A_{131abs} and A_{132abs} (Absolute Combined Hamaker coefficient or the interactive term, of two and three particles in interaction respectively) negative. To achieve this condition of negative A_{33}, herbal additive(s) in the form of drugs would be used. A specialized thermodynamic prediction of interactions between a Mycobacterium Tuberculosis (M-TB) and HIV infection of human sputum using ANOVA/Minitab software, has been carried out by Chukwuneke (2015). Therefore, to characterize surfaces involving Blood-HIV-Herbal extracts, the surface energetics (the science of surfaces) of the interactions between surfaces; of a blood cell, a herbal extract and a HIV particle depend on many factors. These factors include the chemical properties of the herbal extract, the concentration of the different herbal extracts, the subsequent incubation with blood samples that would be collected from a number of HIV infected and uninfected persons for the light absorbance capacity measurements that has a relationship with; the CD4+ counts of the blood samples, the spectrophotometric analysis of would-be interacted samples and the statistical computations of all sample slides to arrive at a value of A_{132abs}. for an uninfected-infected particles of lymphocyte and serum most especially.

The concept of surface thermodynamics would be used in this work to determine quantitatively, the interaction between the HIV particles and herbal extract drug-coated T-cells in an in-vivo experiment, and subsequently a UV spectrophotometer analysis of samples' slides to investigate the therapeutic blockage mechanism of the herbal extract-coated lymphocytes to HIV using the model of the negative Hamaker Coefficient. A sign of the Hamaker coefficient i.e. being negative or positive indicates the nature of the interaction and measured coefficients indicate the level of drug-lymphocyte coating. Ultimately, this study examines the efficacy of three plant biomaterials acclaimed to possess antiviral potentials. They are: Mangifera indica (leaf), Garcinia kola (seed) and Azadiratchta indica (leaf). A combination of the three herbs would also be used. They are: Garcinia kola + Azadiratchta indica + Mangifera indica. The herbal extracts and their combinations' efficacy would be examined in relation with HIV-lymphocyte interactions, and hence a defense for a thermodynamic efficacy determination of drugs before use. The results of this study is hoped to be very valuable to drug manufacturers in the search for more effective antiretroviral drugs with little or no side effects.

For the purpose of this study, the Absolute Hamaker Coefficients for each herbal extract on both infected and uninfected samples of blood would be measured and the Absolute Hamaker Coefficients compared with values with a recent research work on: "Surface Energetics Study of the Interactions between HIV and Blood Cells Treated with Antiretroviral Drugs" (Ani,

2015). Interesting also of this study is its efforts to use the spectroscopy method in analyzing surface interactions in order to gain insight towards the measured value with a numerical sign that rendered HIV infection ineffective. These would mainly form the research intentions for the surface thermodynamics study with bio-particles and the research expected results for an extension of the frontiers of knowledge: as a Thermodynamic prediction for efficacy or effectiveness of biomaterials.

1.2 Statement of Problem

The ineffectiveness of HAART has been attributed to the capacity of HIV to develop resistance to it due to rapid genetic variations (Achebe, 2010). Therefore, the mechanism by which drugs can block the virus by coating lymphocytes seems weak and it becomes necessary to study the surface thermodynamics of the interactions between the virus and the drug-coated lymphocytes. The problem or challenge is in formulating drugs that can functionally eliminate the HIV and hence, the questions arise as to how effective are the available antiretroviral drugs, how effective would herbal alternative therapies be in comparison to known synthetic antiretroviral drugs. The answers to such questions would be found in a study of the surface effects in HIV-drug interaction systems.

1.3 Aim and Objectives of the Study

The aim of this research is the thermodynamic study of the interactions between HIV and blood cells in herbal extract media.

The following objectives were pursued:

i) To extract the herbal additives used as drug samples.
ii) To measure the absorbance and transmittance values of blood, drug and blood-drug samples.
iii) To determine the Hamaker constants and coefficients for particles in blood-drug interacting systems.
iv) To determine the changes in free energies of adhesion of particles in blood-drug interacting systems.
v) To determine the thermodynamic efficacy of the selected antiviral herbal extracts using the concept of negative Absolute combined Hamaker coefficient.

1.4 Significance of the Study

The significant long term impacts of the research, among others includes: the establishment of a template for surface thermodynamics analysis using methods for validating the effectiveness of abundant natural substances in offering therapy for healthiness, the discovery of low cost herbal extracts that are comparable to known HAART regimens that can become additives to HIV infected serum for a functional cure and serving as a reference material for thermodynamic studies of other biological systems.

1.5 Scope of the Study

The research coverage areas include the: identification of antiviral plants, extraction of crude active principles and characterization, serial dilution of compounds for inoculation of blood samples, slides preparations of samples for UV spectrophotometer radiation, and the final analysis of thermodynamic parameters of: wavelength, absorbance, transmittance, reflectance, refractive index (real and imaginary parts), dielectric constants (real and imaginary parts), absorption and extinction coefficients using the Hamaker criterion to establish the degree of potency of the antiviral active compounds.

CHAPTER TWO
LITERATURE REVIEW

2.1 Conceptual Frameworks

This defines all relevant concepts within the scope of the research that are according to earlier authors and the definitions establishment by the researcher.

2.1.1 Concept of Surface Energy and the Thermodynamics Free Energy Approach

In time, space and methodology components of the thermodynamics of surface energy, as a thermodynamic prediction tool for changes in surface free energy of interacting particles which can approximately estimate the magnitude of the natural forces of attraction and repulsion as functions for efficacy or quality, the ideal gas law of 1834 by Èmile Clapeyron who is also known as Van der Waal, has provided basic primordial ideas for most established theories on particle-particle attraction and repulsion. But in recent times, other scholars of heat energy have made remarkable contributions to a better understanding of heat energy in the subject of thermodynamics, at the surface level i.e., surface thermodynamics.

The external view or appearance of all bodies of matter that have length and width is considered as the surface. The atoms of a matter that make up a body exist at the interior as well as at the exterior surfaces. If the body is a solid, its molecules are held together by a strong bond of cohesion from the interior and uniformly out to the exterior. This gives the solid its shape and makes it stable without flowing or vaporizing. But if the body is a liquid, its atoms are free to move and its molecules only exhibit a strong inward attraction (cohesion), thus forming an elastic skin on its open exterior surface. This property of a liquid is what is known as surface tension or free surface energy.

A virus is assumed to be a particle with a surface. The white blood cell (lymphocyte) is also considered a particle with a surface. Herbal extracts whether in their solid forms or as solutions equally have surfaces and their intermolecular bonds of cohesion and their surface tensions are both manifestations of some level of energy. Hence, the philosophic doctrine which attributes all natural phenomena to the action of energy defines energetics (Webster dictionary, 2010). Energetics/Thermodynamics study is the study of the science of the laws and phenomena of

energy in all its forms. This is to say that, all matter possess some form of 'surface free energy' or 'surface thermodynamics'.

The thermodynamic approaches to surface effects or tensions were based on the fact that a surface layer between a bulk liquid and its vapour phase has its own composition which affects the surface tension of the mixture. Recall that the surface tension has been defined as the reversible work of formulation of a unit area of surface at constant temperature (T), volume (V) and chemical potential (μ), and number of component for multi-component systems.

The surface tension is the two dimensional analogue to the pressure on a surface. However, one can calculate any increase in surface tension (surface free energy) using the Gibbs elasticity theoretical model:

$$dU = TdS - PdV + \mu dN + A\sum \sigma_{ij} d\varepsilon_{ij} \qquad (2.1)$$

where:

$U \rightarrow$ internal energy of one-component solid

$T \rightarrow$ absolute temperature

$S \rightarrow$ entropy

$P \rightarrow$ pressure

$V \rightarrow$ volume

$\mu \rightarrow$ chemical potential

N $\rightarrow$ refractive index of a surface area.

$A \rightarrow$ surface area

$\sigma_{ij} \rightarrow$ component of the surface stress (force per unit length)

$\varepsilon_{ij} \rightarrow$ component of the surface strain (deformation)

i & j $\rightarrow$ tensors along i direction in a j perpendicular surface

$A\sum\sigma_{ij}d\varepsilon_{ij}$, is the proportionality factor γ called the surface tension.

Therefore, in equ. (2.1), the elasticity model can be written as:

$$dU = TdS - PdV + \mu dN + A\gamma \tag{2.2}$$

Integrating both sides of equ. (2.2):

$$U = TdS - PdV + \mu dN + A\gamma \tag{2.3}$$

But under constant absolute: temperature, entropy, pressure, volume, refractive index and chemical potential:

$$\frac{dU}{dA} = \gamma \tag{2.4}$$

U , A and γ play key roles, but the internal energy of one-component solid U , is a function of the S, V and N . Then,

$$dU = \left(\partial u/\partial s\right)_{VN} dS + \left(\partial u/\partial v\right)_{NS} dV + \left(\partial u/\partial N\right)_{VS} dN \tag{2.5}$$

Or

$$dU = TdS - PdV + \mu dN \tag{2.6}$$

Since the wavelength of the key properties constitutes the extensive property i.e.,

$U(\lambda S, \lambda V, \lambda N)$ or $\lambda U(S, V, N)$ this then lead to the Euler's equation with equ.(2.6) as:

$$U = TS - PV + Nd\mu = 0 \tag{2.7}$$

In considering the surface energy differently from the bulk, the pressure in the bulk of an isotropic solid is equal in all directions, whereas the pressure on the surface plane is highly anisotropic. Assuming negligible vapour pressure and solubility of a solid that may be present in a liquid, the number of surface active molecules that reside on the surface of a system was calculated by the Gibbs adsorption equation.

$$\Gamma = \frac{-1}{RT} d\gamma/dc \tag{2.8}$$

At constant temperature,

$$-d\gamma = \sum_i \Gamma_i d\mu_i \tag{2.9}$$

Where:

Γ is the surface excess concentration (mol/m^2)

R is the gas constant

c is the concentration of the substance in the bulk solution.

$d\gamma/dc$ is the change in surface tension with change in concentration.

Based on the above deduction, Gibbs and Duhem deduced the equation for interfaces:

$$\partial\gamma_{SV} = -S_{SV}\partial T - \Gamma_{SV}\partial\mu \tag{2.10a}$$

$$\partial\gamma_{SL} = -S_{SL}\partial T - \Gamma_{SL}\partial\mu \tag{2.10b}$$

$$\partial\gamma_{LV} = -S_{LV}\partial T - \Gamma_{LV}\partial\mu \tag{2.10c}$$

Where: $\Gamma_{LV,}$ Γ_{SL} and Γ_{SV} are the interfacial excess concentrations showing that the three interfacial tensions are functions of T and μ and are not mutually independent. Therefore, the corresponding Gibbs-Duhem equation taking into account the surface was given as:

$$Ad\gamma + Sdt - Vdp + Nd\mu + A\sum\left(\gamma\sigma_{ij} - \sigma_{ij}\right)d\varepsilon_{ij} \tag{2.11}$$

Dividing the thermodynamic quantity in a bulk and specific part, and applying the Gibbs-Duhem relation for the bulk, the specific surface entropy which is given by the temperature dependence of γ implies that:

$$S_S = -A\left(\partial\gamma/\partial T\right)_S \tag{2.12}$$

Typically, $\gamma = \gamma_0(1 - T/T_c)^n$

$_n \approx 1$, for metals, T_c is the critical absolute temperature at which the solid phase vanishes.

In conclusion, the surface tension and surface stress ideally are not identical in solids. But in liquids, the surface tension is independent of small strains, since the liquid adapt to perturbations. The tendency to minimize surface energy is a defining factor in the morphology and composition of surfaces and interfaces. Minimization of energy leads to a spherical equilibrium shape iniso-tropic liquid (in the absence of gravity). In crystalline solids, the surface tension depends on the crystal plane and direction. This idea must have been employed to favor particle engulfment and repulsion as the case may be.

2.1.2 Hamaker Theory

In one of his classical papers, Hamaker stated that, the London-van der Waals forces (van der Waals, 1873), of attraction between Spherical Particles, are in essence synonymous with the Hamaker coefficients (Hamaker, 1937).

He then stated that, "if two particles are embedded in a fluid and the London-van der Waals' force between particles and fluid is greater than between the particles themselves, it might be thought that the resultant action will be repulsion rather than an attraction" (Hamaker, 1937).

This theory is quite significant in establishing a thermodynamic criterion for this Virus-Drug interaction prediction and as such, this tool is obviously valuable in HIV study. Therefore, to explain the idea of Hamaker coefficients, it is necessary to consider the explanation of the deviations of an ideal gas law by Èmile Clapeyron who is also known as van der Waal in equation 2.2 below. Originally, the ideal gas law is given as:

$$PV = RT \tag{2.13}$$

Where: P is the ideal gas pressure, V is the ideal volume, R is the universal gas constant for a spherical particle of gas, T is the ideal temperature.

At high pressure, van der Waal introduced the 'corrections' below (Hamaker, 1937) to the ideal gas law of 1834 stated in equ. (2.13):

$$\left(\mathbf{P} + \frac{\mathbf{a}}{\mathbf{v}^2}\right)\left(\mathbf{V} - \mathbf{b}\right) = \mathbf{RT} \tag{2.14}$$

Where: P, R and T are as defined, $\frac{a}{v^2}$ is the correction term to pressure, **V**is the volume, b is the correction term to volume. The term $\frac{a}{v^2}$ indicates that the kinetic energy of the molecules which strike the container wall is less than that of the bulk molecules. This effect is due to the fact that the surface molecules are attracted by the bulk molecules. In other words, molecules must attract each other by some kind of cohesive force, as van der Waals stated. Since then, these forces of molecular attraction have been known as van der Waals forces.

London (1930) derived an expression for the mutual attraction energy of two molecules in vacuum. Hamaker, in 1937 equally considered that, for the mutual attraction of two molecules in an assembly of molecules, a solid particle must attract other particles. Thus, the interaction energies are obtained by the summation of all interaction energies of all molecules present. This resulted in a van der Waals pressure of attraction (attractive energy) between two semi-infinite (solid) particles at a separation distance, d in vacuum. The equation for this expression is given by equation (2.15) in terms of the Hamaker constant as:

$$F_{vdw} = \frac{-A_{ii,jj,kk}}{6\pi d^3} \qquad (2.15)$$

Where: $-A_{ii,jj \text{ or } kk}$ is the negative Hamaker constant for two identical particles ($_{11,\ 22 \text{ or } 33}$). Hence, $A_{11} \Rightarrow$ Hamaker constant for the interaction between two identical particles of an Uninfected Lymphocyte (1). $A_{22} \Rightarrow$ Hamaker constant for the interaction between two identical particles of a HIV Infected Lymphocyte (2). $A_{33} \Rightarrow$ Hamaker constant for the interaction between two identical particles of either an Uninfected Serum with Drugs (3) or an Infected Serum with Drug (3). The Hamaker constants are non-geometrical contributions to the forces of attraction based on molecular properties only. $\frac{1}{6\pi}$ is a constant of proportionality with respect to the circle, d is a minimum separation distance for a semi-infinite plate.

Multiplying (2.15) by πd (a function of the dielectric constant) for a spherical particle of radius R of a separation distance d, the attractive energy is then given by:

$$F_{vdw} = \frac{-A_{11}R}{6d^2} \qquad (2.16)$$

Where: A_{11} is a Hamaker constant, which is the non-geometrical contribution to the force of attraction, based on molecular properties only. The constant A_{11} is given by:

$$A_{11} = \pi^2 q_1^2 \beta_{11} \tag{2.17}$$

Where: q_1 is the number of atoms per cm^3; β_{11} is the London/van der Waals constant for the interaction between two identical molecules.

But for a combination of two different particles (1 & 2), as in (HIV & Lymphocyte) then:

$$\beta_{12} \approx \sqrt{\beta_{11} \cdot \beta_{22}} \tag{2.18}$$

Similarly,

$A_{ij} = \sqrt{A_{ii} \times A_{JJ}}$: [UNinf. Lympho.-INf. Lympho. (with HIV particle)]

$A_{ik} = \sqrt{A_{ii} \times A_{kk}}$: [UNinf. Lympho.-UNinf. Serum (with & without Drugs)]

and: [UNinf. Lympho.-INf. Serum (with & without Drugs)]

$A_{jk} = \sqrt{A_{jj} \times A_{kk}}$: [INf. Lympho.-UNinf. Serum (with & without Drugs)]

and: [INf. Lympho.-INf. Serum (with & without Drugs)]

If the combined Hamaker coefficient of three particles, A_{132} is NEGATIVE, it indicates a thermodynamic criterion for Drug-coated lymphocyte repulsion of HIV. The converse indicates a thermodynamic criterion for Lymphocyte attraction of Drug.

A_{131} exists for the combined Hamaker coefficient for uninfected blood-based particles of lymphocyte and serum. This according to Hamaker is always either POSITIVE or ZERO.

consequently, for a combination of three materials, when the gap between two of the particles 1 & 2 is filled with a medium 3, for example water or serum containing herbal extract(s), from Hamaker's calculations, it follows that:

$A_{132} = A_{12} + A_{33} - A_{13} - A_{23}$ or,

$$A_{132} = \left(\sqrt{A_{11}} - \sqrt{A_{33}}\right)\left(\sqrt{A_{22}} - \sqrt{A_{33}}\right) \quad (2.19)$$

Where, A_{132} is a corresponding combined Hamaker coefficient.

Equation (2.19) shows that for a three-component system involving three materials 1, 2 & 3, A_{132} can become negative, when $A_{132} < 0$ or when $\sqrt{A_{11}} > \sqrt{A_{33}}$ and $\sqrt{A_{22}} < \sqrt{A_{33}}$ or when $A_{11} < A_{33} < A_{22}$ or when $A_{11} > A_{33} > A_{22}$

Hamaker had stated that London/van der Waals forces were always attractive for two particles of the same material embedded in a liquid fluid. He added that if the particles were of different composition (as is of HIV, blood and drug in serum), the resultant force would be repulsive. This indicates as well changes in free energy and hence, a thermodynamic prediction of interacting systems.

Table 2.1: Changes in Free Energy and Thermodynamic Predictions for synthetic Particles (Omenyi, 1978).

Material	ΔFNET (mJ/m2)	Prediction
Biphenyl/Silicon	-3.4	Engulfing
Biphenyl/Teflon	-2.6	Engulfing
Biphenyl/Polystyrene	-0.1	Engulfing
Biphenyl/Nylon	+2.5	Rejecting
Biphenyl/Acetyl	+3.5	Rejecting
Naphthalene/Silicone glass	-3.5	Engulfing
Naphthalene/Teflon	-2.7	Engulfing
Naphthalene/Polystyrene	-0.4	Engulfing
Naphthalene/Nylon	+2.1	Rejecting
Naphthalene/Acetyl	+2.3	Rejecting

The results of table 2.1showed that negative free energy change (for synthetic particles) resulted in particle engulfment (viewed as attraction between particle and advancing solid-liquid interface) while positive free energy change gave rise to rejection (viewed as mutual repulsion between particle and solid-liquid interface). This paved the way for the application of the Hamaker's theory. Deryagin (1954) reported that for dissimilar particles, cases were

possible in which the resultant forces could be less than zero. Visser (1981) gave conditions for A_{132} to become negative.

2.1.3 Thermodynamic Relation to Hamaker Equation

The experiment work of Neumann et al., (1979) presented a thermodynamic relation to the derivation of the Hamaker coefficient, based on the work of Omenyi (1978). This approach showed that the thermodynamic free energy of adhesion, ΔF^{adh} of a particle, P on a solid, S when both are separated by a liquid, L of thickness, d_0 is given by:

$$\Delta F^{adh} = \gamma_{PS} - \gamma_{PL} - \gamma_{SL} \tag{2.20}$$

Where: γ_{ij} is the interfacial free energy. Also:

$$\Delta F_{PLS}^{adh}(d_0) = \gamma_{PS} - \gamma_{PL} - \gamma_{SL} \tag{2.21}$$

γ_{PS} is the interfacial free energy between P and S;

γ_{PL} is the interfacial free energy between P and L;

γ_{SL} is the interfacial free energy between S and L.

In terms of the Hamaker coefficients, the free energy of adhesion is

$$\Delta F_{PLS}^{adh}(d_0) = -\frac{A_{PLS}}{12\pi d_0^2} \tag{2.22}$$

Thus the combined Hamaker coefficient can be calculated once the interfacial free energies are evaluated, using equation (2.23) :

$$A_{132} = 12\pi d_0^2(\gamma_{PS} - \gamma_{PL} - \gamma_{SL}) \tag{2.23}$$

The numerous interfacial tension equations that are found in literatures are divided into two groups; those based on the equation of state and those based on surface tension components approach.

2.1.3a Based on Equation of State

The equation of state was demonstrated with the assumption that solid-liquid tension is the parameter whose value depends on the properties of the solid and the measuring liquid. Hence, the so-called equation of state is given by

$$F\left(\gamma_S \cdot \gamma_L \cdot \gamma_{SL}\right) = 0 \tag{2.24}$$

or

$$\gamma_{SL} = f\left(\gamma_S \cdot \gamma_L\right) \tag{2.25}$$

i. **Berthelot model:** initiated this direction of studies and assumed that the interfacial adhesion work (W_{SL}) was equal to the geometric mean of the cohesion work of a solid (W_{SS}) and, the cohesion work of a measuring liquid W_{ll}.

$$W_{SL} = \left(W_{SS} \cdot W_{ll}\right)^{\frac{1}{2}} \tag{2.26}$$

Then, using the relation, the Berthelot model is given as:

$$W_{SL} = 2\gamma_S ;\ W_{ll} = 2\gamma_L \tag{2.27}$$

This is in relationship with the Dupre equation given by

$$W_{SL} = \gamma_S + \gamma_L - \gamma_{SL} \tag{2.28}$$

A hypothesis in the form of the following equation could be expressed as:

$$\gamma_{SL} = \gamma_S + \gamma_L - 2\left(\gamma_S \cdot \gamma_L\right)^{\frac{1}{2}} \tag{2.29}$$

In an attempt to determine γ_S the model in equ. (2.30) is as expressed:

$$\gamma_{SL} = \gamma_S + \gamma_L - 2\left(\gamma_S \cdot \gamma_L\right)^{\frac{1}{2}} \tag{2.30}$$

or

$$\gamma_{SL} = \gamma_S + \gamma_L \tag{2.31}$$

ii. Neumann model: the combined rule for Neumann's geometric mean to Young's equation is stated thus;

$$(1 + Cos\theta)\gamma_{LV} = 2\sqrt{(\gamma_{SV} \cdot \gamma_{LV})} \times \exp\left\{-\beta(\gamma_{LV} - \gamma_{SV})^2\right\} \tag{2.32}$$

Neumann et al. (1983) derived three other forms of the equation of state; the first one was obtained from the fundamental thermodynamic relations concerning the intermolecular interactions:

$$\gamma_{SL} = \frac{\left\{(\gamma_S)^{\frac{1}{2}} - (\gamma_L)^{\frac{1}{2}}\right\}}{\left\{1 - 0.015(\gamma_S \cdot \gamma_L)^{\frac{1}{2}}\right\}} \tag{2.33}$$

The second one was a Neumann modified Berthelot hypothesis expression,

$$\gamma_{SL} = \gamma_S + \gamma_L - 2(\gamma_S \cdot \gamma_L)^{\frac{1}{2}} \exp\{1 - \beta_1(\gamma_L \gamma_S)\} \tag{2.34}$$

The third further modification of the Berthelot hypothesis by Neumann is:

$$\gamma_{SL} = \gamma_S + \gamma_L - 2(\gamma_S \cdot \gamma_L)^{\frac{1}{2}}\left\{1 - \beta_2(\gamma_L - \gamma_S)^2\right\} \tag{2.35}$$

The coefficients β_1 = 0.0001247 and β_2 = 0.0001057 have been determined experimentally.

iii. Girifalco and Good model: Girifalco and Good attempted to re-formulate the equation of state. They introduced the parameter Φ, characterizing the interfacial energy as:

$$\gamma_{SL} = \gamma_s + \gamma_L - 2\Phi(\gamma_S \cdot \gamma_L)^{\frac{1}{2}} \tag{2.36}$$

In the case of an interfacial system, in both of which interactions of the same type occur, Φ = 1, was assumed.

This model is the earliest combining rule and the most used in manufacturing. The combining rule is an equation that tells more about the interfacial tension across the interface in terms of

the original substance-vapour surface tensions of the materials forming the interface. The combining rule equation is related to Young's equation with the formula:

$$(1+Cos\theta)\gamma_{LV} = 2\sqrt{(\gamma_{SV}\cdot\gamma_{LV})} - \pi \qquad (2.37)$$

π is the vapour pressure (≈ 0)

2.1.3b Based on Surface Tension components Approach

i. **Fowkes (1967):** was a pioneer of this approach. He assumed that the surface free energy of a solid (and of a liquid) is a sum of independent components of surface tension associated with specific interactions.

$$\gamma_S = \gamma_S^d + \gamma_S^p + \gamma_S^h + \gamma_S^i + \gamma_S^{ab} + \gamma_S^o \qquad (2.38)$$

Where: $\gamma_S^d, \gamma_S^p, \gamma_S^h, \gamma_S^i, \gamma_S^{ab} and \gamma_S^o$ are the dispersion, polar, hydrogen (related to hydrogen bonds), induction and acid-based components respectively, while γ_S^o refers to the remaining interaction.

In surface free energy determination based on partitioned surface tension into independent components, the methods used by Fowkes, Owens-Wendt, van Oss-Chaudhury-Good and Zisman models stem from the modified Young's equation of state, $\gamma_S = \gamma_{SV} + \gamma_L Cos\theta$ (for notational compactness, $\gamma_S = \gamma_{SV}$ and $\gamma_L = \gamma_{LV}$.

ii. **The van oss-Chaudhury-Good (vo-C-G) method:** is one of the interesting achievements in the studies of the surface free energy of polymeric materials. Taking into account that the component γ^{AB} being equal to $2\left(\gamma^+ + \gamma^-\right)^{0.5}$ and combining the Dupre equation:

$$W_{SL} = \gamma_S + \gamma_L - \gamma_{SL} \qquad (2.39)$$

Where: W_{SL} is as earlier defined. From the Antonew equation, $\gamma_{SL} = \gamma_L - \gamma_S$

They obtained the free energy of adhesion, using the surface tension component approach, written as:

$$\Delta F^{adh} = \gamma_{PS}^{LW} - \gamma_{PL}^{LW} - \gamma_{SL}^{LW} + \gamma_{PS}^{SR} - \gamma_{PL}^{SR} - \gamma_{SL}^{SR} \tag{2.40}$$

Or by grouping the interactions of the different components

$$\Delta F^{adh} = \Delta F^{LW} + \Delta F^{SR} \tag{2.41}$$

The superscript, SR is interchangeable with the superscript AB seen below.

To calculate the total particle-liquid and particle-solid interfacial tensions as required in the free energy of adhesion, the vo-C-G equation becomes:

$$\gamma_S^{total} = \gamma_S^{LW} \text{ and } \gamma_L^{total} = \gamma_L^{LW} \tag{2.42}$$

For situations where the matrix material is purely dispersive, equation (2.39) reduces to:

$$\Delta F^{adh} = \Delta F^{LW} \tag{2.41}$$

From the above equation (2.41), vo-C-G were able to deduce the total free energy of adhesion given by the dispersion interactions, from the Lifshitz theory considerations as:

$$\Delta F_{132}^{adh} = \left[\frac{-A_{132}}{12\pi L^2}\right] \tag{2.42}$$

Where: A is a Hamaker constant of the system.

iii. Isrealachvili (1972): introduced a cut-off distance parameter d_0 which represents the closest distance that two surfaces can approach. The parameter d_0 eliminates the divergence inherent in the Lifshitz theory. Hence, his free energy of adhesion, using the concept of d_0 was given by:

$$\Delta F_{132}^{adh} = \left[\frac{-A_{132}}{12\pi d_0^2}\right] \tag{2.43}$$

iv. **Hough and White (1980):** established that the value of 1.6 x 10^{-10}metres for d_0 gave satisfactory estimates of surface tension of liquid alkanes. Judged from equation (2.43), if the Hamaker constant was known for particle-liquid-solid system, then they recorded that it was possible to estimate the total dispersion (van der Waals interaction) and predict particle behavior at the solidification front for a system.

2.1.4 Lifshitz Relation to Hamaker Equation

The Hamaker's approach considered molecular properties, hence it is regarded as a microscopic approach and thus, it had its limitations by not taking into account the screening effects of molecules. This perceived limitations by Lifshitz and co-worker Dzyaloshinskii (1961) led them to develop an alternative derivation of the van der Waals forces between solid bodies. Considering the interaction between solid particles on the basis of their macroscopic properties, the Hamaker coefficient was expressed in terms of bulk material properties as:

$$A_{132} = \frac{3}{4}\pi\hbar\int_0^\infty \left[\frac{\varepsilon_1(i\zeta)-\varepsilon_3(i\zeta)}{\varepsilon_1(i\zeta)+\varepsilon_3(i\zeta)}\right]\left[\frac{\varepsilon_2(i\zeta)-\varepsilon_3(i\zeta)}{\varepsilon_2(i\zeta)+\varepsilon_3(i\zeta)}\right]d\zeta \tag{2.44}$$

Where: ε_j is the dielectric constant of material j along the imaginary frequency axis $(i\zeta)$ and it is the Plank's constant divided by 2π . This equation is rather complex and would be difficult to use hence, several approximations have been given. But using the Liftshitz approach for van der Waals interaction (in condensed media), Chaudhury (2005) experimentally demonstrated that dispersion(London), induction(Debye) and dipole (Keesom) contributions to the Lifshitz-van der Waals or (polar) components of the surface tension γ^{LW} are additional.

$$\gamma^{LW} = \gamma^L + \gamma^D + \gamma^K \tag{2.45}$$

It follows that on a macroscopic level, the three types of Van der Waals interactions; (Keesom, Debye and London) can be treated together as the total of polar or Lifshitz-Van der Waals (LW) interaction. Hence, the interfacial tension γ_{12} between two different materials 1 and 2 is one of the important concepts in colloidal and surface science as it leads directly to a quantitative expression for the free energy of inter-particle or inter-molecular interaction in condensed phase system. The interfacial tensions between two reasonably immiscible liquids

can be measured directly but the interfacial tensions between solids and liquids and between solids and solids cannot be determined directly. It thus becomes important to deduce these interfacial tensions, γ_{12} via the surface tension γ_1 and γ_2 of the interacting solid material 1 and liquid material 2.

The interfacial tension between a solid and a liquid (if only dispersion interaction forces are available between the two condensed phase materials of the solid and the liquid) as demonstrated experimentally by Good, Grifalco and Fowkes is given by:

$$\gamma_{12}^{LW} = \left(\gamma_1^{LW} - \gamma_2^{LW}\right)^2 \tag{2.46}$$

Or

$$\boldsymbol{\gamma}_{12}^{\mathbf{LW}} = \boldsymbol{\gamma}_1^{(\mathbf{LW})^2} + \boldsymbol{\gamma}_2^{(\mathbf{LW})^2} - 2\boldsymbol{\gamma}_1^{\mathbf{LW}}\boldsymbol{\gamma}_2^{\mathbf{LW}} \tag{2.47}$$

Equation (2.47) is referred to as Good-Grifalco-Fowkes combining rule. But, the surface tension γ_i (i.e. the surface free energy per unit area of a liquid in vacuum) is equal to one half of the free energy of cohesion (ΔG_{ii}) and opposite in sign; that is

$$\gamma_i = -\frac{1}{2}\Delta G_{ii} \tag{2.48}$$

Therefore, the polar component of the free energy of cohesion of material 1 is:

$$\Delta G_{ii}^{LW} = -2\gamma_1^{LW} \tag{2.49}$$

Hence, the free energy of interaction between materials 1 and 2 in vacuum is related to the surface tension by the Dupre equation:

$$\Delta G_{12}^{LW} = \gamma_{12}^{LW} - \gamma_1^{LW} - \gamma_2^{LW} \tag{2.50}$$

$$= \boldsymbol{\gamma}_1^{\mathbf{LW}} + \boldsymbol{\gamma}_2^{\mathbf{LW}} - 2\sqrt{\left(\boldsymbol{\gamma}_1^{\mathbf{LW}} + \boldsymbol{\gamma}_2^{\mathbf{LW}}\right)} - \boldsymbol{\gamma}_1^{\mathbf{LW}} - \boldsymbol{\gamma}_2^{\mathbf{LW}}$$

Therefore,

$$\Delta \mathbf{G}_{12}^{\mathbf{LW}} = -2\sqrt{\boldsymbol{\gamma}_1^{\mathbf{LW}} + \boldsymbol{\gamma}_2^{\mathbf{LW}}} \tag{2.51}$$

Since the Lifshitz-van der Waals forces are universal and always available at the surface, the equation (2.51) is stating that the atoms at an interface are pulled by those in the neighboring phase. It is also suggesting that the energy of interaction is negative, that is interaction energy between two purely polar condensed phases is always attractive. Similarly, the interaction energy between molecules or particles of material 1 immersed in a liquid 2 is:

$$\Delta G_{121}^{LW} = -2\gamma_{12}^{LW} \tag{2.52}$$

Therefore, two different particles 1 and 2 immersed in a liquid 3 are related to the interfacial tensions by:

$$\Delta G_{132}^{LW} = \gamma_{12}^{LW} - \gamma_{13}^{LW} - \gamma_{23}^{LW} \tag{2.53}$$

Using equations (2.46) and (2.50) to expand the interfacial surface tensions in equation (2.53) gives:

$$\Delta G_{132}^{LW} = -2\gamma_3^{LW} - 2\sqrt{\left(\gamma_1^{LW} \cdot \gamma_2^{LW}\right)} + 2\sqrt{\left(\gamma_1^{LW} \cdot \gamma_3^{LW}\right)} + 2\sqrt{\left(\gamma_2^{LW} \cdot \gamma_3^{LW}\right)} \tag{2.54}$$

From equation (2.51) it follows from equation (2.54) that;

$$\Delta G_{132}^{LW} = \Delta G_{33}^{LW} + \Delta G_{12}^{LW} - \Delta G_{13}^{LW} - \Delta G_{23}^{LW} \tag{2.55}$$

This is the Hamaker coefficient combining rule obtained through a purely surface thermodynamic treatment provided:

i. The geometric mean combining rule (2.46) holds for LW interactions.
ii. The equilibrium distance, r has the same value for all types of ΔG interactions.
iii. The constancy of r for LW interactions of all materials is as confirmed by van oss (1975).

2.1.5 Relationship between the Hamaker Coefficient and the Free Energy of Adhesion, ΔF_{132}^{adh}.

The Hamaker coefficient has been established, and representatively quoted in this work as A_{132} and the free energy of adhesion as ΔF^{adh}. Hence, for all given combinations, it is possible to express ΔF^{adh} in terms of van der Waals energies. For example, for two flat-flat plate geometry:

$$\Delta F_{12}^{adh}(d_1) = \left[\frac{-A_{12}}{12\pi d_1^2}\right] \tag{2.56}$$

Similarly,

$$\Delta F_{12}^{adh}(d_0) = \left[\frac{-A_{12}}{12\pi d_0^2}\right] \tag{2.57}$$

By extension (for three flat-flat-flat plane geometry):

$$\Delta F_{132}^{adh}(d_0) = \left[\frac{-A_{132}}{12\pi d_0^2}\right] \tag{2.58}$$

$d_1 \rightarrow$ a vacuum separation gap or distance

$d_0 \rightarrow$ a liquid separation gap or distance

on the basis of these results and in line with van oss et. al. (1979), the bulk van der Waals interaction term A_{132} is referred to as the Hamaker coefficient rather than the Hamaker constant. It is only in the case of a material interacting with itself through a vacuum that the Hamaker coefficient, A_{11} is a constant, with its own specific equilibrium interfacial separation distance. In establishing this relationship, Visser (1981) made the following deductions:

i. The use of the term 'Hamaker constant' is limited and should be replaced by 'Hamaker coefficient'.

ii. The occurrence of van der Waals repulsion for component systems can experimentally be demonstrated as well as theoretically.

iii. Interfacial separation distance between solid bodies vary depending on the materials involved, in particular, immersion of a system in a liquid can alter the equilibrium position between the adherents

iv. Surface tension data are the most useful tool to predict conditions for three-component systems to be repulsive leading to phase separation.

2.2 Theoretical Frameworks

This covers presentations of every applicable theory, including the name of theorists and the year of establishments.

2.2.1 Experimental Proof of Separation or Repulsion Forces.

This is the core interest behind the repulsion between particles in interaction. The following sub-sections relate to the concepts earlier reviewed.

2.2.2 Hamaker Approach to Separation of Particles Interacting in a Liquid

Particles interacting in liquid may be identical or different. According to the Hamaker approach, the dispersion interaction of two identical atoms or molecules or particles, i separated by an infinitesimally short distance (in vacuum) can be expressed as:

$$A_{ii} = \pi^2 q_1^2 \beta_{ii} \tag{2.59}$$

Where: A_{ii} → Hamaker constant, q_1→ number of atoms per unit volume,

β_{ii}→ London-van der Waals constant = $-3\hbar\nu\alpha^2/4(4\pi\varepsilon_0)^2$.

Therefore, the work of cohesion resulting from London dispersion forces is given as:

$$W_{(r)London} = -\frac{\beta_{ii}}{r^6} \tag{2.60}$$

Where: r is the distance between the atoms, i.

Using the macroscopic approximation, the total dispersion energy for two semi-infinite flat parallel bodies (of material i), separated by a distance, r (in air or in vacuum), becomes (for r greater than a few atomic diameters):

$$W_{(r)London} = -\frac{A_{ii}}{12\pi r^2} \tag{2.61}$$

Where: A_{ii} is the Hamaker constant for material, i.

Hence, the Hamaker pair-wise summation procedure can be used to calculate the combined Hamaker constant of two macroscopic identical particles interacting in a third medium. For two atoms of the same material, 1 in medium 3 (e.g. two individual clay particles in an aqueous suspension) the combining rule of thumb is:

$$A_{ij} = \sqrt{A_{ii} \cdot A_{ij}} \tag{2.62}$$

Then for combined Hamaker coefficient:

$$A_{131} = \left(\sqrt{A_{11}} - \sqrt{A_{33}}\right)^2 \tag{2.63}$$

Or

$$A_{131} = \left(A_{11} + A_{33} - 2A_{13}\right) \tag{2.64}$$

Where: A_{11} and A_{33} are referred to as the Hamaker constants of the solid and the medium respectively, in vacuum. The convention here is that the first and the third character in the triplet subscript identify the two particles which are interacting through a liquid medium, identified by the second character. Equation (2.59) suggests that the Hamaker constant A_{131} is always positive or zero.

According to the Berthelot's principle, the dispersion combined interaction constant between dissimilar molecules of different materials can be estimated as the geometric mean of the interaction constants of individual materials. Thus, the extended interaction of two different atoms i and j becomes:

$$B_{ij} = \sqrt{\beta_{ii} \cdot \beta_{jj}} \tag{2.65}$$

It likewise follows then that the combined Hamaker constant for two different particles is given by:

$$A_{ij} = \sqrt{A_{ii} \cdot A_{jj}} \tag{2.66}$$

This is known as the geometric combining rule, and is widely used for calculating dispersion energies of interaction between dissimilar materials. Hence, for the combined Hamaker

coefficient for two different particles (1 & 2) in medium 3, the Hamaker coefficient combining rule is given as:

$$A_{132} = A_{12} + A_{33} - A_{13} - A_{23} \tag{2.67}$$

Or

$$A_{132} = \left(\sqrt{A_{11}} - \sqrt{A_{33}}\right)\left(\sqrt{A_{22}} - \sqrt{A_{33}}\right) \tag{2.68}$$

Therefore, for two different materials, the combined Hamaker coefficient, A_{132} of equation (2.67) can be negative when;

$$A_{11} > A_{33} > A_{22} \tag{2.69}$$

$$A_{11} < A_{33} < A_{22} \tag{2.70}$$

Under this condition, the dispersion interaction energy becomes repulsive, i.e. $W_{(r)London} > 0$. The London dispersion interaction between two particles (identical or different) in vacuum is always attractive. In other words, when two different materials 1 and 2 interact immersed in liquid 3, $A_{11} \neq A_{22}$ and the conditions of (2.69) and (2.70) prevail, a net repulsion occurs.

Padday (1969) demonstrated the applicability of the Hamaker approach to n-alkanes by calculating the theoretical values of surface tension (γ_{ii}) of various n-alkanes using the following equations:

$$W_{ii} = 2\gamma_{ii} = \frac{A_{ii}}{12\pi r_{ii}^2} \tag{2.71}$$

Where: W_{ii} is work of cohesion resulting from London dispersion forces

r_{ii} is separation distance between two atoms in bulk.

The Hamaker's approach may not be entirely accurate because of many body effect (Horn, 1990). It may not be applicable to some colloidal system, since like the classical DLVO theory, it ignores the existence of hydrophobic interaction between particles of hydrophobic materials (Yildirim et. al., 2002).

2.2.3 The Thermodynamic Approach to Particle-Particle Interaction

The proponents to this idea are:

a. **Van der Waals (1873)**. He used the derivations of an ideal gas law to explain the Hamaker constants. An ideal gas law is stated as:

$$PV = RT \tag{2.13}$$

The kinetic energy of the molecules which strike a container wall is less than that of the bulk molecules. This phenomenon was explained with the fact that the surface molecules are attracted by the bulk molecules even when the molecules have no permanent dipoles. It follows that molecules can attract each other by some kind of cohesion force (van de Waals, 1873). These forces have come to be known as van der Waals forces. Hence, van der Waals introduced the following modifications to an ideal gas law of equation (2.13) to obtain the van der Waals' equation for a real gas as:

$$\left[P + \frac{a}{v^2}\right](V - b) = RT \tag{2.14}$$

Where, **a** is constant, **b** is a factor that depends on the actual volume (Okeke et al., 2008). The correction term to the pressure (**a/v^2**) indicates that the kinetic energy of the molecules which strike the container wall is less than that of the bulk molecules.

b. **London (1930)**. After the development of the theory of quantum mechanics, London quantified the van der Waals modification for molecules, without a dipole and so molecular attraction forces began to be known as London/van der Waals forces. London stated that the mutual attraction energy, V_A of two molecules (in vacuum) can be given by the relation:

$$V_A = \frac{-3}{4} h\nu_0 \left[\frac{\alpha^2}{H^6}\right] = -\left[\frac{\beta_{11}}{H^6}\right] \tag{2.72}$$

Where:

h → the Plank's constant

ν_0 → a characteristic frequency of a molecule

$\alpha \rightarrow$ the polarizability of a molecule

H → separation distance between molecules

c. Hamaker (1937). Hamaker made an essential step in 1937 (seven years) after London's quantification of the van der Waal's modification of an ideal gas law on the mutual attraction of two molecules. He deduced that assemblies of molecules (as in a solid body) must attract other assemblies. The interaction energy of attraction can then be obtained by the summation of all the interaction energies of all molecules present. He added that this would result in a van der Waal's pressure, P_{vdw} of attraction between two semi-infinite solid bodies at a separation distance, d (in vacuum). He then first established his model for P_{vdw} as:

$$P_{vdw} = \left[\frac{A_{11}}{6\pi d^3}\right] \tag{2.73}$$

Then, Hamaker in studying the force of attraction between a spherical semi-infinite body of radius R, at a minimum separation distance, d secondly established his model for a van der Waal's force of attraction as:

$$F_{vdw} = -\left[\frac{A_{11}R}{6d^2}\right] \tag{2.74}$$

Where: A_{11} is the Hamaker constant which is the non-geometrical contribution to the force of attraction (based on molecular properties only). Quantitatively,

$$A_{11} = \pi^2 q_1^2 \beta_{11} \tag{2.17}$$

Where: q_1 is the number of atoms per cm^3, β_{11} is the London-van der Waal's constant for an interaction between two identical molecules. Using obtained approximated values for β from the ionization potential of the molecules of interest, the Hamaker constant can be calculated. Therefore, a corresponding van der Waal's force between any two condensed bodies or particles of given geometry can be calculated provided their separation distance is numerically fixed. For combination of two different materials 1 and 2,

$$\beta_{12} \approx \sqrt{\beta_{11} \cdot \beta_{22}} \tag{2.18}$$

Hence, the Hamaker's constant for two different particles 1 & 2 is:

$$A_{12} = \sqrt{A_{11} \cdot A_{22}} \tag{2.77}$$

For a combination of three materials/particles when the gap between 1 and 2 is filled with a medium 3 (as with the case of this research study where 3 is a medium of herbal extracts in serum) the Hamaker's constants gives rise to the Hamaker coefficients and for identical particles 1 & 1 with medium 3 interwoven, the combined Hamaker coefficient is given as:

$$A_{131} = A_{11} + A_{33} - 2A_{13} = \left(\sqrt{A_{11}} - \sqrt{A_{33}}\right) \tag{2.78}$$

For un-identical particles 1 & 2 within medium 3 in-between, the combined Hamaker coefficient is given as:

$$A_{132} = A_{12} + A_{33} - A_{13} - A_{23} = \left(\sqrt{A_{11}} - \sqrt{A_{33}}\right)\left(\sqrt{A_{12}} - \sqrt{A_{33}}\right) \tag{2.79}$$

Equation (2.79) shows that, for a three-component system involving three different materials: 1(uninfected lymphocyte particle), 2 (HIV infected lympho. particle) and 3 (herbal extract particle in serum), A_{132} can become negative. This mathematically is when $A_{132} < 0$, or when $\sqrt{A_{11}}$ is greater than $\sqrt{A_{33}}$ and $\sqrt{A_{22}}$ is less than $\sqrt{A_{33}}$ or when $\sqrt{A_{11}} < \sqrt{A_{33}} < \sqrt{A_{22}}$

This Hamaker's approach to the interaction between condensed bodies from molecular properties is otherwise a 'microscopic' approach regarded as an 'over simplification' with its limitations. This is due to its neglect of the 'screening effect' of the molecules which are on the surface of two interacting bodies with respect to the underlying molecules in the bulk.

d. Lifshitz et. al., (1961). The limitations of Hamaker's approach led them to develop an alternative derivation of the modified van der Waal's forces of attraction between solid bodies or particles. He postulated that on the basis of 'macroscopic' properties, interaction between solids would consider the 'screening and even other effects' in their calculations. He then modified the equation for the Hamaker constant to be:

$$A_{132} = \frac{3}{4}\pi\hbar\int_0^{\infty} \left[\frac{\varepsilon_1(i\zeta)-\varepsilon_3(i\zeta)}{\varepsilon_1(i\zeta)+\varepsilon_3(i\zeta)}\right]\left[\frac{\varepsilon_2(i\zeta)-\varepsilon_3(i\zeta)}{\varepsilon_2(i\zeta)+\varepsilon_3(i\zeta)}\right]d\zeta \quad (2.44)$$

Where: $\varepsilon_j(i\zeta)$ is the dielectric constant of material j along the imaginary frequency axis ($i\zeta$) which can be obtained from the imaginary part $\varepsilon_1''(\omega)$ of the dielectric constant $\varepsilon_1(\omega)$.

e. Krupp (1967). A further deduction for a case of proper choice of materials for which the Lifshitz-Hamaker constant will be negative was investigated by Krupp and his co-workers. He developed a computer program that used optical data of the materials for calculating negative values for hypothetical combinations of materials. He opined that hypothetical combinations consist of systems in which the individual Lifshitz-Hamaker constants obey the equ.(2.80):

$$\left[\frac{A_{132}}{d_0^2}\right] = \left[A_{12} - A_{13} - A_{23} + \frac{A_{33}}{d_1^2}\right] \quad (2.80)$$

Where: d_0 → Equilibrium separation distance filled with a liquid medium

d_1 → Equilibrium separation distance in vacuum

This implies that in the macroscopic theory of van der Waals forces, there are situations when the van der Waals forces of three different materials can be negative. This concept of negative van der Waals was actually obtainable. Krupp demonstrated the 'physical' meaning of equation (2.80) by showing that the factor, ln [$\varepsilon(i\zeta) - 1/ \varepsilon(i\zeta) + 1$] is a function of ($i\zeta$)-the frequency axis, ε being the dielectric constant.

f. Langbein (1969) has shown that, as a consequence of the 'screening effect' in the interaction between two flat plates at a separation distance d, the predominant contribution to the interaction by van der Waal's forces comes from those parts of the interacting bodies, which are in a layer of a thickness equal to the separation distance d, between the two plates.

g. Ninham and Parsegian (1970); **Isralachvili (1972)**; **Nir et al. (1972)** and **Visser (1975)** all further approximated the Lifshitz-Hamaker equation (2.44).

h. Omenyi (1978) established the thermodynamic free energy of adhesion of a particle P on a solid S in a liquid L at a separation distance, d_0 given by:

$$\Delta F_{PLS}^{Adh}(d_0) = \gamma_{PS} - \gamma_{PL} - \gamma_{SL} \tag{2.81}$$

Where: ΔF^{Adh} is the free energy of adhesion, integrated from infinity to the equilibrium separation distance d_0. γ_{PS}, γ_{PL} γ_{SL} are the interfacial free energy between particle, solid and liquid as the case may be.

For interactions between individual components, similar equations can also be written as;

$$\Delta F_{PS}^{Adh} = \gamma_{PS} - \gamma_{PV} - \gamma_{SV} \tag{2.82a}$$

$$\Delta F_{SL}^{Adh}(d_1) = \gamma_{SL} - \gamma_{SV} - \gamma_{LV} \tag{2.82b}$$

$$\Delta F_{PL}^{Adh}(d_1) = \gamma_{PL} - \gamma_{PV} - \gamma_{LV} \tag{2.82c}$$

For a liquid, the force of cohesion which is the interaction with itself is as described by:

$$\Delta F_{11}^{Coh}(d_1) = -2\gamma_{LV} \tag{2.83}$$

ΔF^{Adh} can be determined by various approaches apart from the surface free energy approach. It is the classical Hamaker work of 1937 that is most appropriate.

i. Visser (1981) demonstrated most of the establishments in simple pictorials. On the discovery that the kinetic energy of molecules which strike a container wall is less than that of the bulk molecules by van der Waal in 1873, he depicted as shown in figure 2.1:

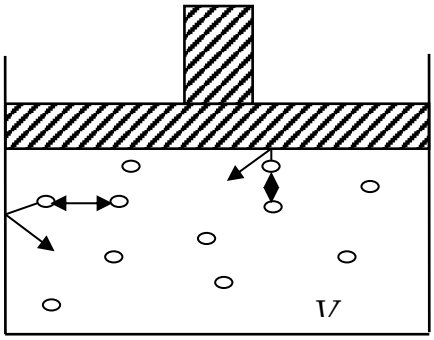

Figure 2.1: Attraction of surface molecules by bulk molecules in a container of volume, V (Visser, 1981)

On the statement of London about the mutual attraction energy of two molecules in a vacuum, he depicted as shown in figure 2.2:

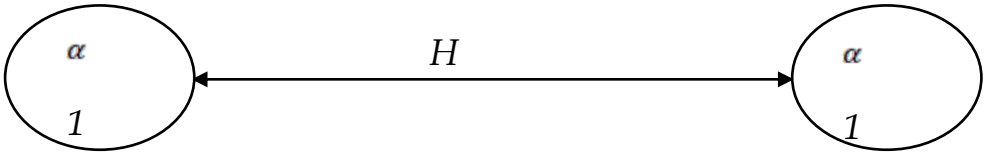

Figure 2.2: Interaction of two identical molecules of a material 1 with polarizability, α and separation distance, H

On the mutual attraction of two molecules as in a solid body in a vacuum, Visser depicted as shown in figure 2.3:

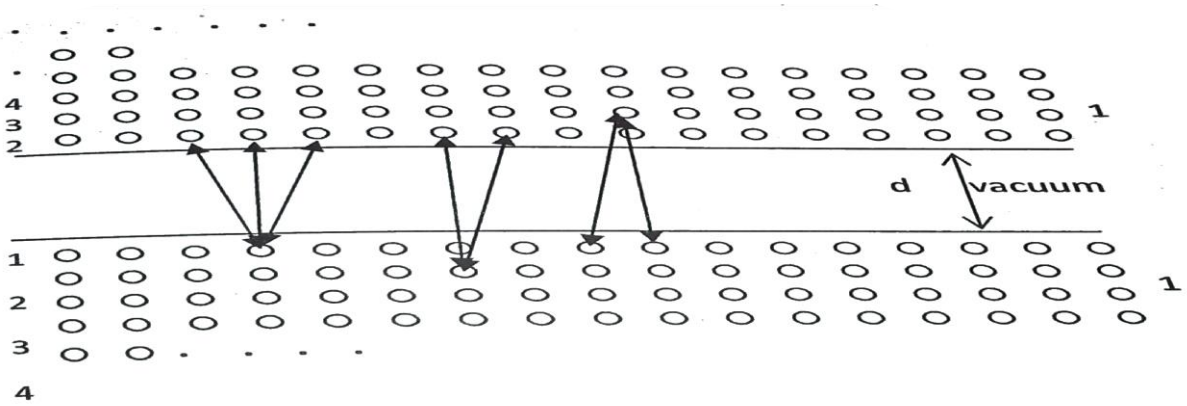

Figure 2.3: Interaction of two semi-infinite solid bodies 1 at a separation, d in vacuum (Visser, 1981).

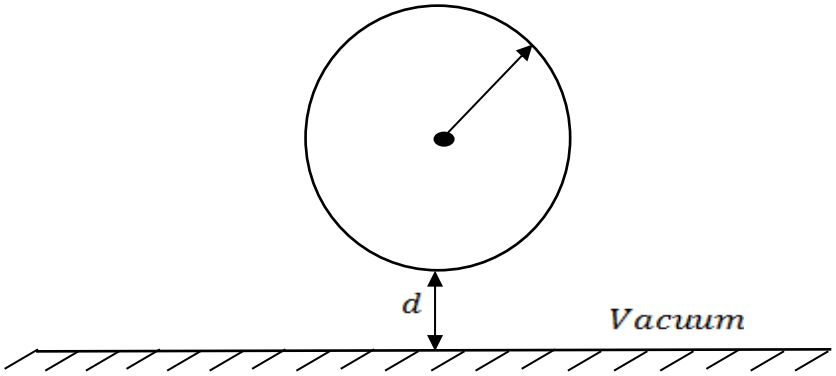

Figure 2.4: Interaction of a sphere of radius, R at a separation, d from a solid surface of the same material, 1 in vacuum (Visser, 1981)

On the hypothetical combinations of material for a negative Lifshitz-Hamaker constant, Visser developed a table as shown below:

Table 2.2: Combination of materials for which negative Lifshitz-van der Waal's constant A_{132} are found (Visser, 1981)

System	A_{132}/Ev
Si/Al_2O_3	− 0.19
Ge/Cds/Polystyrene	− 0.28
Cu/MgO/KCl	− 0.17
Au/Si/KCl	− 0.81
Au/Polystyrene/H_2O	− 0.14

2.2.4 Polar or Lewis Acid-Base Interactions

The interactions between HIV and blood cell treated with herbal extracts naturally involve water (a polar agent), chemical active principles or extracts (acids and bases), proteins, etc., which are hydrophobic in nature. It appeared to be the distinction between all the three polar electrodynamics' forces that impeded progress in the search for a true polar surface interaction. Chaudhury (2005) showed that the three polar electrodynamics' forces are simply additional and should be treated as a single entity. It became necessary to examine the nature of polar (Lewis Acid-Base) properties of surfaces and electrodynamics' apolar (Lifshitz-van der Waals') properties.

Significant advances have been made in the thermodynamic treatment and interpretation of interfacial tensions between solid-liquid interacting surfaces. It has now become formal that in aqueous media (especially for solid surfaces which are rich in oxygen such as silicate materials), the principal polar interaction is the hydrogen bonding involving donors and acceptors. This type of interaction according to Lewis can be attributed to occurring between a Bromated acid (hydrogen donors) and a bromated base (hydrogen acceptors). The polar interaction accounts for the dual nature of such interactions. Polar surface interactions are not restricted to hydrogen bonding but extend to include all electrons donating and accepting phenomena. This is what is encompassed in the more general acid-base paradigm of Lewis.

Every interaction is considered to have the polar (Lewis Acid-Base) and apolar (Lifshitz-van der Waals') components. These two polar and apolar components of the surface tension are additional.

$$\Delta G = \Delta G^{AB} + \Delta G^{LW} \tag{2.84}$$

Where: ΔG^{AB} is the free energy due to Lewis Acid-Base interactions ΔG^{LW} is the free energy due to Lifshitz-van der Waals' interactions. Re-writing equ. (2.84):

$$\Delta G_{ii} = -2\gamma_i \tag{2.85}$$

In general it then follows that

$$\gamma_i^{total} = \gamma_i^{AB} + \gamma_i^{LW} \tag{2.86}$$

Where: γ_i^{AB} and γ_i^{LW} refer to the polar (acid-base) and the apolar (Lifshitz-van der Waals') components of surface tension of material i respectively.

For the purpose of this research, the Dupre's equation for three condensed media 1, 2, and 3 of which at least one must be a liquid 3 (herbal extract in serum), the change in interaction energy was considered as given by:

$$\Delta G_{132} = \gamma_{12} - \gamma_{13} - \gamma_{23} \tag{2.87}$$

Expanding this in terms of AB and LW components yields;

$$\Delta G_{132} = 2\left(\sqrt{\gamma_1^{LW}}\cdot\sqrt{\gamma_3^{LW}}+\sqrt{\gamma_2^{LW}}\cdot\sqrt{\gamma_3^{LW}}-\sqrt{\gamma_1^{LW}}\cdot\sqrt{\gamma_2^{LW}}-\sqrt{\gamma_3^{LW}}+\sqrt{\gamma_3^{\varphi}}+\sqrt{\gamma_1^{\theta}}+\sqrt{\gamma_2^{\theta}}-\sqrt{\gamma_3^{\theta}}\right)$$
$$+\sqrt{\gamma_3^{\theta}}\left(\sqrt{\gamma_1^{\varphi}}+\sqrt{\gamma_2^{\varphi}}-\sqrt{\gamma_3^{\varphi}}\right)-\sqrt{\gamma_1^{\varphi}}\cdot\sqrt{\gamma_2^{\theta}}\cdot\sqrt{\gamma_1^{\theta}}-\sqrt{\gamma_2^{\varphi}} \quad (2.88)$$

Where: γ^{φ} is the acid component of surface tension; γ^{Θ} is the base component of surface tension.

Similarly, the interaction energy between two identical particles 1 and 1 immersed in liquid 3 is given by:

$$\Delta G_{131} = -2\sqrt{\gamma_{13}} = 2\left(\sqrt{\gamma_1^{LW}}-\sqrt{\gamma_3^{LW}}\right)^2 - 4\left(\sqrt{\gamma_1^{\varphi}\cdot\gamma_3^{\theta}}-\sqrt{\gamma_2^{\varphi}\cdot\gamma_3^{\theta}}-\sqrt{\gamma_1^{\varphi}}\cdot\sqrt{\gamma_3^{\theta}}-\sqrt{\gamma_3^{\varphi}}+\sqrt{\gamma_1^{\varphi}}\right) \quad (2.89)$$

Similarly also, the interaction energy between two different particles 1 and 2 immersed in liquid 3 all in a vacuum is given by:

$$\Delta G_{132} = -2\left(\sqrt{\gamma_1^{LW}\cdot\gamma_2^{LW}}+\sqrt{\gamma_1^{\varphi}\cdot\gamma_2^{\theta}}+\sqrt{\gamma_2^{\varphi}\cdot\gamma_1^{\theta}}\right) \quad (2.90)$$

Looking at equation (2.90), the sign of the interaction energy between any two particles (in vacuum) is always negative (meaning there is no attraction between them and cannot be zero because γ^{LW} for all particles is finite and positive). When in aqueous system, low energy substances interact with each other, γ_{13} is positive and ΔG_{132} being negative implies an attraction. The opposite is true for high surface energy substances. The sign would determine whether the interaction (adsorption) between herbal extract substances and blood cells is thermodynamically possible. A negative ΔG_{132} would indicate a feasible adsorption reaction and vice versa. The magnitude of the negative ΔG_{132} would be an indication of the strength of the adsorption interaction-the larger the value, the stronger the interaction is adjudged.

2.3 Empirical Reviews

Empirical review of technical literatures, in line with the earlier stated objectives are made.

2.3.1 Review of Key Thermodynamic Interactions between Particles

Certain considerations are basic for particles separation or repulsion during any interaction of particles. Hence, an experiment for an evidence of repulsion forces would definitely precede any study to show the roles of repulsive forces in particles' interaction system.

2.3.2 Thermodynamic Considerations on Particles Separation

Recalling an earlier work using experimental rig with Teflon, Polystyrene, Nylon, Acetyl particles (in biphenyl), Silicone glass and Naphthalene matrices as test specimens, based on table 2.1, Omenyi et al. (1981) stated conditions between actual and theoretical observations about free energies. They established that, thermodynamically a net change in free energy ΔF_{NET} that is greater than zero, is a condition for particle rejection, i.e. separation.

$\Delta F_{NET} > 0$. But if the net change in free energy, ΔF_{NET} is less than zero, a condition for particle engulfment or attraction or adhesion exists. $\Delta F_{NET} < 0$ from the process of engulfment of a sphere particle, b by particle, c of unit surface areas given in equation as:

$$\Delta F_{NET} = \Delta F_b + \Delta F_c \tag{2.91}$$

Consider the pictorial below of a particle embedded in a liquid matrix by a solid.

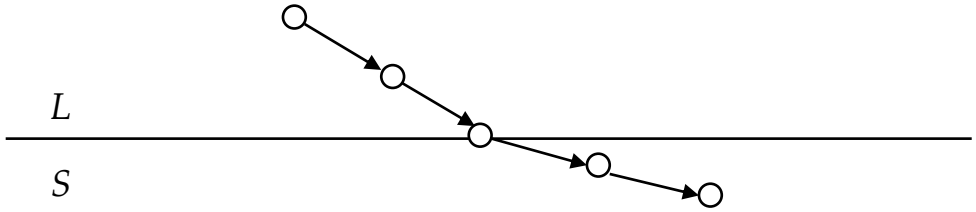

Figure 2.5: Sketch of Thermodynamic engulfment of a particle P embedded in a liquid matrix L by a solid S.

The free energy of engulfment of the particle by the solid phase reduces to

$$\Delta F_{NET} = \gamma_{PS} - \gamma_{PL} \tag{2.92}$$

The free energy of adhesion of the particle (originally suspended in the liquid medium) to the solid-liquid interface is given as:

$$\Delta F^{Adh} = \gamma_{PS} - \gamma_{PL} - \gamma_{SL} \tag{2.93}$$

Where: γ_{ij} is the interfacial free energy.

In conclusion, adhesion is expected when the free energy change is negative. If it is positive, repulsion is predicted. Therefore, for a situation at which there is particles rejection, the particles remain at the advancing solid-liquid interface. However, with increasing rates of solidification, a 'viscous drag force' is generated which opposes the thermodynamic repulsive

force. In other words, when the viscous drag force becomes equal to the repulsive force, engulfment occurs. When the value of equation (2.92) or (2.93) is negative, adhesion occurs. But if positive, repulsion or separation occurs.

In terms of Hamaker coefficient, A_{132}, the two equations for separation and engulfment are predictive models. This conclusion was made based on an electron microscopy.

Omenyi (1978), Visser (1968), Neumann et al. (1979), van oss et al. (1983) in Omenyi et al. (1980) nine varieties of particles were studied in a Naphthalene matrix and both thermodynamic and theoretical (van der Waals') predictions were compared with the electron microscopic observations as shown on the table 2.3.

Table 2.3: Theoretical Thermodynamic Predictions and Actual microscopic observations in Naphthalene matrix (Omenyi et al., 1980)

System	$A_{PLS}\times10^{14}$(MJ)	ΔF^{Adh} (MJ/m^2)	Observation
Acetyl	−2.10	+1.68	Rejection
Nylon-6	−2.05	+2.26	Rejection
Nylon-6,6	−1.85	+2.10	Rejection
Nylon-12	−1.30	+1.67	Rejection
Nylon-6,10	−0.75	+1.22	Rejection
Nylon-6,12	+0.20	+0.45	Rejection
Polystyrene	+1.26	−0.39	Engulfment
Teflon	+4.25	−2.78	Engulfment
Silicone glass	+5.23	−3.57	Engulfment

In the table 2.3, the effective Hamaker coefficient A_{132} was determined from the surface tensions of liquid and solid Naphthalene and of particle materials (all at the melting point of Naphthalene) using the model of equ. (2.23):

$$A_{132} = -12d_0^2\left(\gamma_{PS} - \gamma_{PL} - \gamma_{SL}\right) \tag{2.23}$$

Where: d_0 = 1.82A. It was to be noted that the predictions were borne out of experimental observations, with the partial exception of Nylon-6, 12. A comparison with theoretical predictions and actual visual observations of phase separations (of polymer mixture solutions) in table 2.4, indicates that a solution of two or more different polymers (in a single solvent)

separate into two homogeneous phases when the entropy of mixing is small and there is a slight positive enthalpy of mixing, thus giving rise to positive Gibbs free energy of mixing.

Table 2.4: Theoretical Thermodynamic predictions and Visual observations of phase separation of Polymer mixture solutions (Omenyi, 1978) as abridged.

System	Obser-vation	$A_{132}x10^{14}$(MJ)	System	Obser-vation	$A_{132}x10^{14}$(MJ)
PMMA/MEK/CLA	NS	+7.51	PS/CBZ/PMMA	S	−0.09
PMMA/THF/CLA	NS	+4.83	PIB/CBZ/PVC	S	−0.67
PS/MEK/PMMA	NS	+3.79	PIB/TLN/PS	S	−1.27
PVC/THF/PMMA	NS	+2.57	PIB/CTC/PS	S	−1.53
PIB/CBZ/PPL	NS	+2.17	PIB/DCBZ/PMMA	S	−1.98
PIB/DCBZ/PS	NS	+1.88	PIB/THF/PMMA	S	−3.48
PS/BNZ/PMMA	NS	+1.12	PIB/BNZ/PMMA	S	−3.49
PS/CHXN/PVDF	NS	+0.66	PIB/THF/CLA	S	−3.76
CLA/THF/PS	NS	+0.21	PS/DCBZ/PMMA	S	−0.37

The complete table for table 2.4 studied thirty-one different polymer pairs comprising of ten different polymers and seven different solvents, (Omenyi, 1978) and (van oss et al., 1979). The combined A_{132} values were calculated and found to range from ($+7.51x10^{-14}$MJ to $-3.76x10^{-14}$MJ) as shown. Most known studies were based on the determination of the enthalpy of mixing with the Flory-Huggins formulation of the combinational entropy (Flory, 1953).

Generally speaking, particles of similar material have a tendency for mutual attraction, whereas particles of different materials tend towards mutual repulsion (in liquids) under certain circumstances (Omenyi, 1978). It becomes reasonable to extend this rule found for the properties of suspended particles to biomaterials like blood, HIV and herbal extract particles. The attraction or repulsion between any two particles can be explained in terms of the London-van der Waals interaction energy. As discussed earlier, it is the sign of the resulting interaction energy that suggest repulsion of particles (phase separation) or attraction (phase mixing). In conclusion, techniques for determining surface free energies of particulate materials have been advanced. Such techniques include particle exclusion technique, suspension stability studies and phase separation. Can HIV suppression be achieved through surface thermodynamics

approach (Surface Energetic Study)? This is the question asked by (Omenyi, 2006) that this research is hoped to proffer a unique answer.

2.3.3 Experimental Evidence for van der Waals' Repulsion

The particle engulfment or repulsion measurements at solidification fronts of van oss et al. (1979) and his phase separation studies of polymer solutions were the first experiments to demonstrate systematically that, van der Waals' repulsion had to be accepted as a genuine phenomenon in colloidal chemistry. But before this time, Fowkes (1967) had predicted that under certain conditions, the system of PTFE/Glycerol/Iron oxide is repulsive on the basis of surface tension data of the materials involved. Wittmann et. al. (1971) indicated that the extremely low Hamaker constant for quartz could give rise to negative values for a large number of combinations with other materials when water was acting as the third medium. (Schulz & Cichos,1972) published the first values of Hamaker constants having a negative sign for the system of air bubbles on a quartz surface in water; A_{132} was recorded to be $-1.1x10^{-13}$erg ($-1.1x10^{-20}$Joules).

Sonntag et al. (1972) also gave experimental evidence for negative Hamaker constants for the system of Oil/Water/Organic solvent (decane, benzene and Xylene). Churaev (1974) confirmed the work of Wittmann et al. (1971) in particular, for combinations with air. Kruglyakov (1974) used the procedure of Ninham and Parsegian (1970)-a simplification of Lifshitz theory, to calculate negative values for an n-hexane film on water to be $-2.18x10^{-14}$erg ($-2.18x10^{-21}$Joules) and for an n-hexane film on water to be $-0.23x10^{-14}$erg ($-0.23x10^{-21}$Joules). Deryagin et al. (1972) calculated A_{132} for a system of Air/Tetradecane/Quartz to be $-0.76x10^{-13}$erg ($-0.76x10^{-20}$Joules). This was in accordance with experiments regarding been reviewed

Lately, Visser (1981) predicted that under certain conditions, the van der Waals' forces could be repulsive when he saw (Fowkes, 1967) work as earlier referenced. Smith et al. (1983) conducted some special flocculation studies on mixtures of PTFE and graphite particles in water. On the basis of their surface tension data of 18.6, 110 and 72.8 respectively, a negative value for A_{132} could be predicted. It was discovered that no mutual flocculation could be detected whereas from the point of view of collision between the particles, there was no selective flocculation. Thus, the PTFE and graphite particles repel each other.

2.3.4 Repulsive van der Waal's Interaction Role in Separation of Particles

It has already been reviewed in this literature that conditions could arise when the sign of the van der Waals interaction energy between two different unchanged bodies, surrounded by a liquid might be negative. This implies that such particles would repel each other. This phenomenon is implicit in Hamaker's classical paper on van der Waals-London interactions study. Believing probably that the van der Waals-London theory was somehow erroneous, Hamaker (1947) wrote as earlier stated that:

if two particles are embedded in a fluid and the London-van der Waals' force between particles and fluid is greater than between the particles themselves, it might be thought that the resultant action will be repulsive rather than attraction.

Recall that Fowkes (1967) demonstrated the existence of such repulsive interaction with poly-(Tetrafluoroethylene)-Glycol-Iron oxide. Visser (1972) in a review on Hamaker constants stated explicitly "when two materials are immersed in a liquid medium and the interactions of each of those materials with that of the liquid medium is larger than the interaction between these materials themselves, spontaneous separation can occur due to dispersion forces only". Omenyi et al. (1982) on the dissociation of antigen-antibody bonds of the van der Waals type, and on the elution of protein by hydrophobic chromatography columns of van oss et al. (1979), gave results of both studies which confirmed the validity of the van der Waals theory and the entire practicality of the experimental procedures of van oss et al. (1978). They actually showed theoretically and experimentally that the sign of the net van der Waals interaction between two different solid bodies or between two different dissolved macromolecules in liquid often is negative (i.e. they repel one another even if they are electrically neutral and even when they are immersed in polar liquids).

Therefore, the new capability to change the attraction between different (even neutral) solids submerged in liquids, and/or dissolved macromolecules into repulsion have considerable implications for a variety of novel as well as traditional separation methods. The theories as has been introduced earlier are basically the same. The assumption here for simplicity is that interaction between two different solids (or dissolved) bodies 1 and 2 in a liquid 3 may be represented as an interaction between semi-infinite slabs. Considering the Hamaker expression for free energy for interaction:

$$\Delta F(d) = \left[\frac{-A_{132}}{12\pi d^2} \right] \tag{2.94}$$

Assuming a minimum separation distance d_0 and that equation 2.94 is still valid for such a small separation distance, the Hamaker coefficient can be expressed as:

$$A_{132} = 12\pi d_0^2 \cdot \Delta F(d_0) \tag{2.95}$$

Once the free energy of adhesion between two bodies is evaluated, the combined Hamaker coefficient A_{132} for the interaction between two different bodies in a liquid can be calculated from equation (2.95).

The free energy of adhesion is given by:

$$\Delta F_{132}^{Adh} = \gamma_{12} - \gamma_{13} - \gamma_{23} \tag{2.96}$$

The values of γ_{23}, γ_{13}, and γ_{12} can be obtained using the equation of state approach. Alternatively, A_{132} can be determined by:

$$A_{132} = A_{12} + A_{33} - A_{13} - A_{23} \tag{2.97}$$

For this approach; A_{23}, A_{13} and A_{12} are obtained from the general rule:

$$A_{ij} = 12\pi d_0^2 \cdot \Delta F_{ij}(d_0) \tag{2.98}$$

And A_{33} can be derived from the free energy of cohesion:

$$\Delta F_{ij}^{Coh} = -2\gamma_{iv} \tag{2.99}$$

The γ_{3V} for the liquid 3 can be measured using the Wilhelmy method (Padday, 1969). A positive value of A_{132} implies that the net van der Waals interaction between particles 1 and 2 immersed in liquid 3 is attractive, while a negative value means that the net van der Waals forces is repulsive. However, according to Omenyi et al. (1982), if the absolute value of A_{132} becomes closer to zero than $\approx \pm 3.5 \times 10^{-15}$ergs ($3.5 \times 10^{-22}$Joules), an exact prediction of attraction or repulsion based on whether A_{132} is positive or negative may no longer be reliable. This then would call for different separation method(s).

2.3.5 Medical and Ethno-medical Literatures

2.3.5A Medical

The idea of medicine is especially about the preservation of health and the treatment of disease. Hence, medicine has been defined as the healing art or the science of the preservation of health and of treating disease for the purpose of cure. Therefore, considering the statements for this research problem, the review of medical literatures would be on substances that possesses or reputed to possess curative or remedial properties. All medicines contain active principles, agents, ingredients, chemicals or compounds that determine their properties.

Having advanced from the age when death and disease were regarded by humans as not being natural phenomena; the use of charms and talisman are still prevalent in modern times. There is no doubt that infectious diseases caused by different viral pathogens, particularly chronic and emerging viruses represent a growing worldwide anxiety in human health as well as in veterinary field, since viruses can be inactivated by only a few numbers of prophylactic and therapeutic agents (Vanden et al., 1986 in: Okeke et. al., 2005).

a. Drug Interactions and Management of Disease with Synthetic Drugs

In an overview of antiretroviral and drug interactions, the pharmacokinetics interactions among drugs used in HIV therapy are often 'multi-factorial', involving altered drug absorption, p-glycoprotein modulation, CYP450 induction or inhibition, changes in renal elimination and fluctuations in intracellular drug concentration (Pistelli, 2001). Drug interactions associated with HIV medications can be broadly classified into two: pharmacokinetics and pharmacodynamics. Looking at what happens to a drug inside the body (pharmacokinetics), their absorption, metabolism (processing), distribution to tissues and elimination are of research interest. Pharmacokinetics of antiretroviral drugs may be significantly altered in HIV positive patients with hepatitis B or C, and such impairment may be more pronounced in those with more advanced liver problem. However, avoiding and managing interactions has become an increasing important part of HIV medicine because of the effects of PI metabolism, NNRTI and NRTI processes.

The management of a disease is of two major approaches. One is carrying out a surgery to gain access into a living body in order to treat any disorder or ailment. The other approach is prescribing drugs which are orally taken or applied externally to provide cure. Depending on

the later nature of the disease, this research dwells on the later approach with a view to establishing a thermodynamic criterion for the efficacy of selected drugs for the treatment of the HIV disease. Admittedly, the very first savior against a disease is a drug. A drug may be 100% chemically synthesized like all known synthetic drugs, or 100% physically extracted as crude. This is to say that, the management of any viral disease can be done using either an antiviral synthetic (antiretroviral therapy) drug or an antiviral herbal extract (integrative therapy).

Before 1987, antiretroviral (ARV) drugs have not been developed and treatment of the HIV consisted of treating the complications from the immunodeficiency. The first HIV/AIDS medicine also known as antiretroviral drug/therapy was actually developed and licensed in 1987 (Warnke et. al., 2007). Stefano et al. (2012) described the development of antiretroviral therapy as a unique advancement in the history of medicine.

The very first ARVs were deoxynucleoside reverse transcriptase inhibitors (NRTIs) and the first was Azidothymidine (AZT) also known as Zidovudine (ZDV). Three other NRTIs were approved for use in HIV infection: Zalcitabine (ddC), Didanosine (ddI) and Stavudine (d4T) (Furman et al., 1986). (Skowron et. al., 1993) pointed out that single NRTI therapy was not as effective as desired considering its side effects and toxicities, and that this led to other intolerable diseases that claimed lives. However, Connor et. al. (1994) discovered a most important result obtained with the initial use of NRTIs which was the demonstration that the treatment of HIV-infected pregnant women with Zidovudine substantially decreased HIV transmission to their newborn. Presently, antiretroviral therapy to prevent mother-to-child transmission is based on triple drug combinations as the global standard, but single-double drug treatment was also used initially and represented an important proof of concept.

When Zidovudine was administered with Dalcitabine or Didanosine, the impact in terms of CD4 count increased and survival was better but tolerability remained poor. An unfortunate effect of the NRTIs is that the drugs also inhibit cellular DNA polymerase-a and mitochondrial polymerase-1 which are dose-dependent. A step forward occurred when the cytidine analogue: Lamivudine (3TC) was associated with the rapid development of resistance; Lamivudine was synergistic with many of the other nucleosides including Zidovudine and was relatively well tolerated. In addition to combining Lamivudine with Zidovudine, it was also given successfully with Stavudine. However, none of the dual nucleoside combinations when administered

without a third drug could effectively control HIV infection. The next advance in HIV therapeutics came with the development of non-nucleoside reverse transcriptase inhibitors (NNRTIs) and protease inhibitors (PIs). Nevirapine (NVP), the first NNRTI to be approved in 1996 has had a long-lived history and is still in use in many parts of the world (Darbyshire, 1995). Other PIs available are Ritonavir and Indinavir. Indinavir which was approved in 1996 substantially changed the treatment landscape, ushering in the highly active antiretroviral therapy (HAART) era.

Gulick et al. (2000) established that a combination of Indinavir, Zidovudine and Lamivudine (a triple combination) had sustainable HIV suppression. During the Vancouver AIDS conference in 1996, the successful impact of triple combination therapy was reported by Ani (2015). With the advent of HAART-triple combination therapy containing PIs, the HIV/AIDS was turned into a chronic manageable condition. Although HAART provides durable control of virus replication in most patients, it is not devoid of side effects, some of which surface in populations on long-term treatment. The emergence of multidrug resistance and transmission of drug-resistance HIV strains, limits the clinical efficacy of current therapy. Further simplification of treatment and identification of more effective drug combinations are really needed to improve patient compliance and adherence. Fixed-Dose Combination (FDC) has done a lot well in improving adherence. It is the combination of complex regimes into simpler formulas, for instance, two pills containing two or three medications each can be taken twice daily (Department of Health & Human Services, 2012).

The management of HIV/AIDS normally includes the use of multiple antiretroviral drugs in an attempt to control HIV infection. Progress in antiretroviral therapy has been characterized by the availability of the relatively safe antiretroviral drugs of the old class (NRTIs, NNRTIs and PIs). Newer classes of antiretroviral drugs are the entry/attachment inhibitors (EIs) and the integrase inhibitors (IIs) otherwise called the CCR5 inhibitors. Dejesus et al. (2009) supported that different regimes are currently available and are mainly composed of a nucleoside/nucleotide dual ‘backbone’ and a third drug that can be chosen among four different classes: NNRTI, PI, II or CCR5 inhibitors.

b. Factors that Predict the Speed of the Disease Progression

One factor predicting how fast a patient develops AIDS after being infected with HIV is the viral set-point. The viral set-point is the viral load established within a few weeks to months after infection after the initial burst of virus replication has subsided. The viral set-point is thought to remain steady for an indefinite period of time if the infection is not treated with antiretroviral drugs. The viral load and CD4 are markers of HIV disease progression and the following have been found to responsible for variations in CD4 counts:

i. Injuries and burns
ii. Exposure to opiates
iii. Drug interactions
iv. Hemophilia condition
v. Normal pregnancy
vi. Malnutrition
vii. Psychological stress and social isolation
viii. Over-exercising
ix. Other infections

c. Human Immunodeficiency Virus (HIV) and the Anatomy of the Virus

A virus is a small infectious agent that can only replicate inside a living cell or another organism. An HIV virus particle is spherical and has a diameter of about 1/10,000 mm. Like other viruses, HIV does not have a cell wall or a nucleus. Viruses can infect all types of life forms-humans, animals, plants and micro-organisms, including bacteria and algae. They are found in almost every ecosystem on earth, and they are the most abundant type of biological entity. Viruses have actually been described as "organisms at the edge of life" because they carry genetic material, reproduce and evolve through natural selection, but they lack cell structure, which is generally needed to be considered living. Hence, HIV is equally considered a particle. The scary thing about contracting a virus is that antibiotics do not work. Vaccines are also unpredictable, and viruses including those that cause AIDS and viral hepatitis, evade these vaccine-induced immune responses and result in chronic infections.

HIV belongs to a group of retroviruses called lentiviruses. The genome of retroviruses is made of ribonucleic acid (RNA), and each virus has two 'single chains' of RNA. For replication, the virus needs a host cell, and the RNA must first be transcribed into deoxyribonucleic acid (DNA), which is done with the enzyme, reverse transcriptase. The human immunodeficiency virus is the virus that potentially causes AIDS (acquired immune deficiency syndrome). HIV primarily attacks the immune defense system, making the patient extremely vulnerable to opportunistic infections, which are infections that occur in people who have weakened immune system.

HIV primarily infects and destroys immune cells with the CD4 receptor protein on their cell surfaces (also called CD4-positive or CD4+ T-cells). Healthy individuals have a CD4 cell count between 600 and 1,200 cells per microliter of blood. HIV patients have less than 600 CD4 cells per microliter of blood. Patients progress to AIDS when/if their CD4 cell count drop to lower than 200 cells per microliter of blood. The most common type of HIV worldwide is called HIV-1 with subtypes A through H and O. Since 1981, when the first case of AIDS was reported in the United States, the disease has become a global pandemic, causing an estimated 65 million infections and 25 million deaths worldwide.

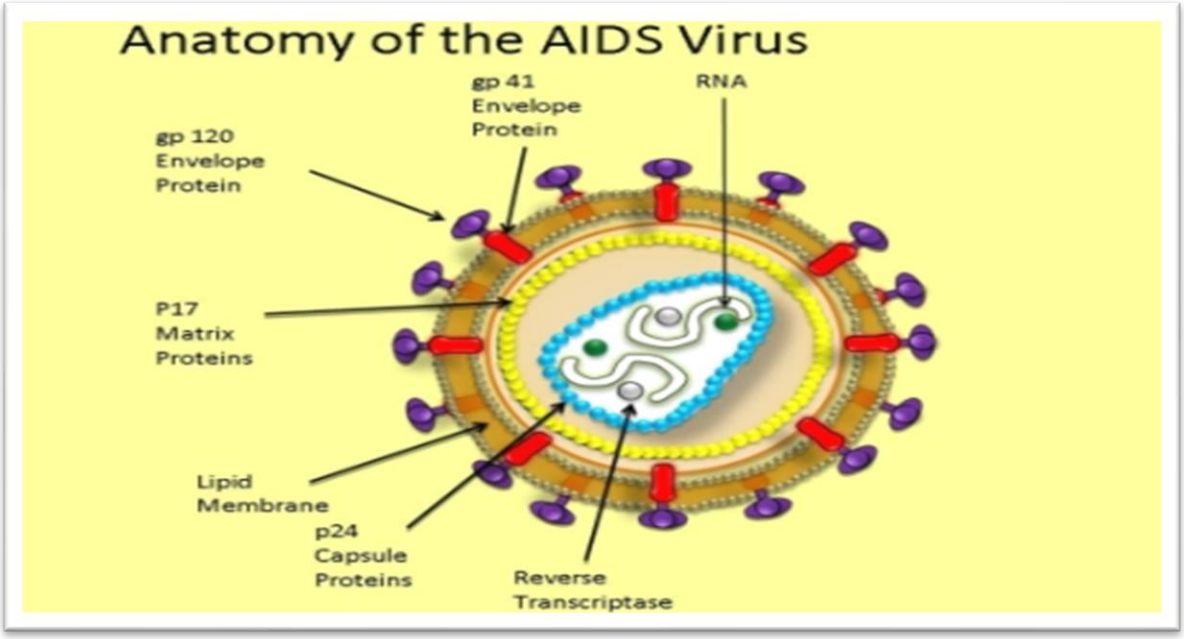

Plate 2.1: The HIV Structure/Anatomy (http://HIVstructure/anatomy Browsed 10/04/2019)

The viral envelope – this is the outer coat of the virus, consisting of two layers of lipids; different proteins are embedded in the viral envelope, forming 'spikes' consisting of the outer glycoprotein (gp) 120 and the trans-membrane gp41. The lipid membrane is borrowed from the host cell during the budding process (formation of new particles). The gp120 is needed to attach to the host cell, and gp41 is critical for the fusion process.

The viral core – this contains the viral capsule protein p24 which surrounds two single strands of HIV-RNA and the enzymes needed for HIV replication, such as reverse transcriptase, protease, ribonuclease and integrase. Out of the nine virus genes, there are three, namely gag, pol and env, which contain the information needed to make structural proteins for new virus particles. The HIV matrix protein (consisting of the p17 protein), lie between the envelope and the core.

d. The HIV model of Attachment of the Virus to a host Cell

HIV uses the CD4 molecule to attach to T cells; the CD4 molecule is expressed at the cell surface of a subset of T cells (T-helper cells) but also on monocytes, macrophages, dendritic cells, and microglia. However, monocytes, for example, have 10 times fewer CD4 receptors than the CD4 T cells (T-helper cells).

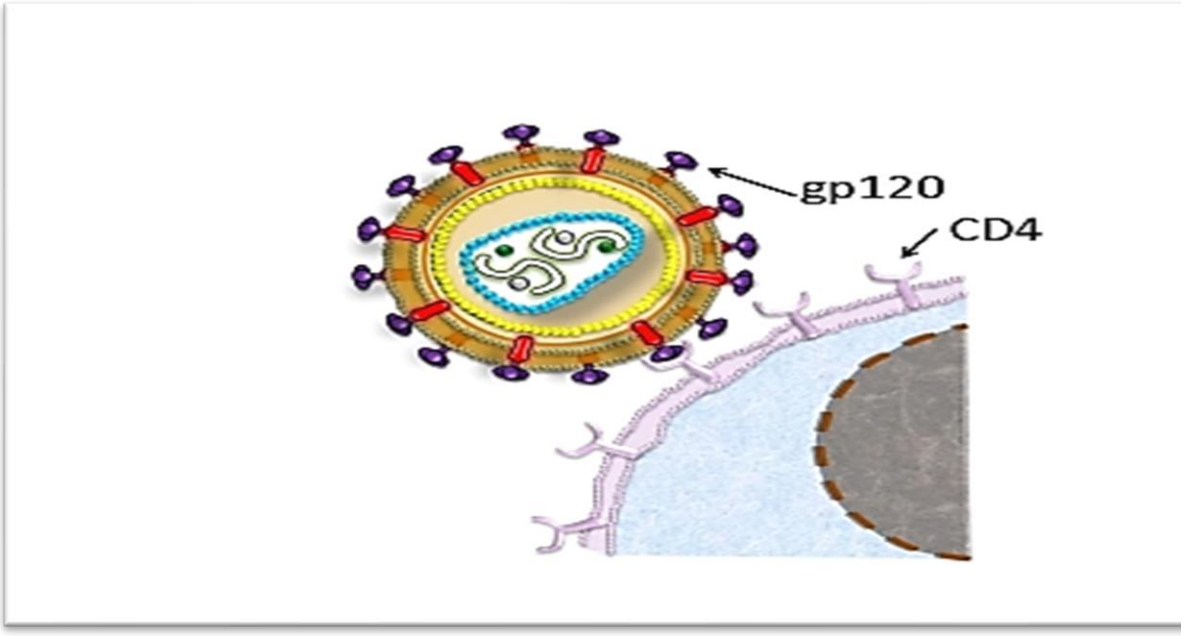

Plate 2.2: HIV attachment to a host cell (http://HIVattachmentmechanism Browsed 10/04/2019)

One or more of the virus's gp120 molecules bind tightly to CD4 molecule(s) on the cell's surface. The binding of gp120 to CD4 results in a conformational change in the gp120 molecule. This conformational change allows gp120 to bind to a second molecule on the cell surface, known as the HIV co-receptor. The two major co-receptors for HIV-1 are CCR5 and CXCR4. After the binding of the virus to the host cell, the fusion (attachment due to attraction) under the influence of the viral gp41 molecule.

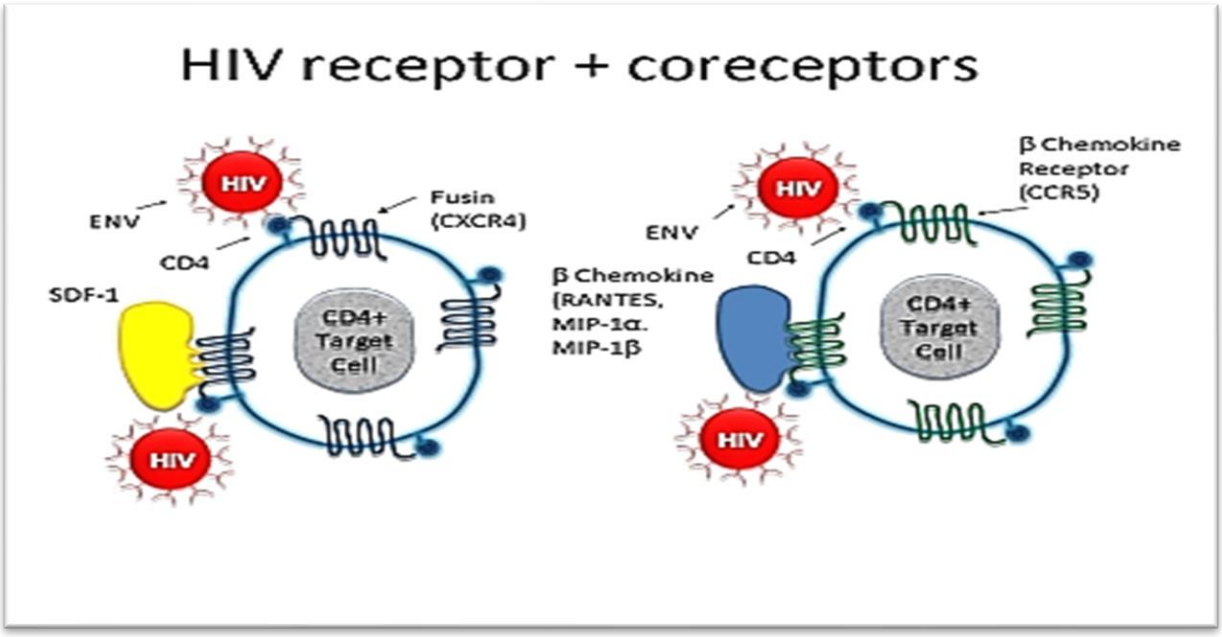

Plate 2.3: HIV receptor and co-receptor (https://www.nature.com/articles/38564a0 Browsed 10/04/2019)

e. Classes of ARV drugs and Guidelines for use

There are several classes of drugs, which are usually used in combination, to treat HIV infection. The use of these drugs in combination is termed ARTs or Anti-Retroviral Therapy (ART), combination anti-retroviral therapy (cART) or highly active anti-retroviral therapy (HAART). ARV drugs are broadly classified by the phase of the retrovirus life-cycle that the drug inhibits. The following cycles have been identified:

1. **Entry Inhibitor (or Fusion Inhibitor)** – interferes with binding, fusion and entry of HIV to the host cell by blocking one of several targets. This is the hope of this research. Drugs already developed for this aim are Maraviroc and Enfuvirtide. But to prevent fusion of the virus with the host membrane, Fuzeon (T20) has been used (Bai, 2013). There nas been new advances in Hepatitis C virus (HCV) treatment with entry inhibitors (Xi-Jang et al., 2016).

2. **Reverse Transcriptase Inhibitors (Nucleoside and Nucleotide/Nonnucleoside Reverse Transcriptase Inhibitors) (NRTIs, NRTIs/NNRTIS)** – nucleoside and nucleotide analogues inhibit reverse transcription. Examples of NRTIs include deoxythymidine, Zidovudine, Stavudine, Didanosine, Zalcitabine, Lamivudine,

Abacavir, Tenofovir and Emtricitabine (Kalyan, 2013). Non-nucleosides inhibit reverse transcriptase by binding to an allosteric site of the enzyme acting as a non-competitive inhibitor of reverse transcriptase. Examples of NNRTIs are Nevirapine, Delavirdine, Efavirenz and Rilpivirine (Kalyan, 2013).

3. **Integrase Inhibitors (IIs)** – inhibit the enzyme integrase which is responsible for integration of viral DNA into the DNA of the infected cell. Examples of IIs are Raltegravir and Elvitegravir (Peter, 2013).

4. **Protease Inhibitors (PTs)** – block the viral protease enzyme necessary to produce mature virons upon budding from the host membrane. Particularly, these drugs prevent the cleavage of gag and gag/pol precursor proteins (Wensing, 2010). Examples of PIs are Lopinavir, Indinavir, Nelfinavir, Amprenavir and Rifonavir.

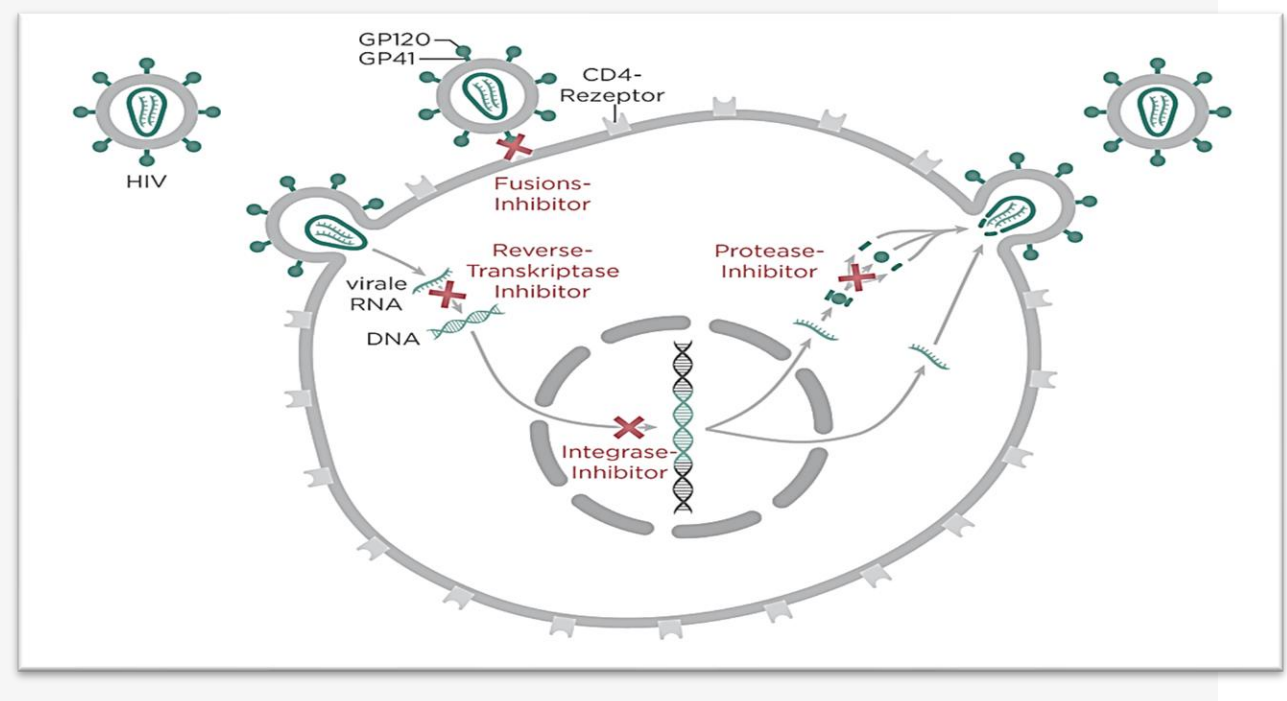

Plate 2.4: Schematic description of the mechanism of the four classes of currently available antiviral drugs against the HIV. (https://en.m.wikipedia.org/wiki/Management_of_HIV/AIDS Browsed 10/04/2019)

Table 2.5: Some fixed-Dose Combination with their company names (US dept of health and human services, as modified in 2016)

Brand Name	Drug Names (INN)	Date of FDA Approval	Company
Combivir	lamivudine + zidovudine	September 26, 1997	GlaxoSmithKline
Kaletra	lopinavir + ritonavir	September 15, 2000	Abbott Laboratories
Trizivir	abacavir + lamivudine + zidovudine	November 15, 2000	GlaxoSmithKline
Epzicom (in USA) Kivexa (in Europe and Russia)	abacavir + lamivudine	August 2, 2004	GlaxoSmithKline
Truvada	tenofovir disoproxil fumarate + emtricitabine	August 2, 2004	Gilead Sciences
Atripla	emtricitabine + tenofovir disoproxil fumarate + efavirenz	July 12, 2006	Gilead Sciences and Bristol-Myers Squibb
Complera (in USA) Eviplera (in Europe and Russia)	emtricitabine + rilpivirine + tenofovir disoproxil fumarate	August 10, 2011	Gilead Sciences and Janssen Therapeutics (formerly Tibotec)

Stribild	elvitegravir + cobicistat + emtricitabine + tenofovir disoproxil fumarate	August 27, 2012	Gilead Sciences
Triumeq	abacavir + dolutegravir + lamivudine	August 22, 2014	ViiV Healthcare
Evotaz	atazanavir + cobicistat	January 29, 2015	Bristol-Myers Squibb
Prezcobix	darunavir + cobicistat	January 29, 2015	Janssen Therapeutics
Dutrebis	lamivudine + raltegravir	February 6, 2015	Merck & Co.
Genvoya	elvitegravir + cobicistat + emtricitabine + tenofovir alafenamide fumarate	November 5, 2015	Gilead Sciences
Descovy	emtricitabine + tenofovir alafenamide fumarate	April 4, 2016	Gilead Sciences

Guidelines for the Use of Antiretroviral Agents in HIV-1-Infected Adults and Adolescents as published by Clinical Guidelines Portal (as adapted by the author. Last updated: July 14, 2016; last reviewed: July 14, 2016).

In general, treatment guidelines include:

- The initiation of antiretroviral therapy (timing-early treatment)

- The regimens to be involved; HAART and FDC (two or more ART drugs collected from different classes into a single pill) with respect to first and second-line regimens available

-The salvage regimens to be used (combination of drugs that will probably work even against viruses that are partly drug resistant).

2.3.5B Ethno-medicals: Management of HIV with Antiviral Herbal Extracts (Integrative therapy)

This is medicinal plants research also known as 'Ethnomedicine'. According to an estimate of world health organization (WHO), herbal medicine covers the health needs of up to 80% of the world's population, especially in the rural areas of developing countries according to Robinson and Zhang (2011). In Ghana, Mali, Nigeria and Zambia, the first line treatment for 60% of children with malaria is the use of herbal medicine. In San Francisco, London and South Africa, 70% of people living with HIV/AIDS use traditional medicine, LAD Williams (2006). As at 2003, the annual global market for herbal medicine stood at over US $60 billion (WHO, 2003). The global herbal supplements and remedies market is forecast to reach $107 billion by the year 2017, spurred by growing aging population and increasing consumer awareness about general health and wellbeing, according to a new report from Global Industry Analysts. Antiviral herbs inhibit the development of viruses. They can be used to treat infections without caution because they are harmless and typically cause no or few side effects. Many antiviral herbs boost the immune system, which allows the body to attack viral pathogens. This can even be better than attacking specific pathogen, which antiviral drugs are designed to do, because pathogens mutate over time and become less susceptible to treatment. Undoubtedly, the plant kingdom still holds many species of plants containing substances of medicinal value which are yet to be discovered; large numbers of plants are constantly being screened for their possible bioactivity.

The universal role of plants in the treatment of disease is exemplified by their employment in all major aspects of medicine. There is a great wealth of knowledge concerning the medicinal and other properties of plants that is transmitted from generation to generation by traditional societies. The use of single pure compounds, like the ARTs synthetic drugs mentioned above, are not without limitations, and in recent years there has been an immense revival in interest in the herbal system of medicine which rely heavily on plant sources. Medicinal plants are rich source of bioactive phytochemicals or bio nutrients. The major classes of phytochemicals with disease-preventing functions are dietary, fiber, antioxidants, anticancer, detoxifying agents, immunity-potentiating agents and neuro-pharmacological agents (Mamta et al., 2013). Medicinal plants contain some organic compounds which produce definite physiological action on the human body and these bioactive substances include tannins, alkaloids, carbohydrates, terpenoids, steroids and flavonoids, Edoga et. al., (2005) in: Mann (1978). In fact, plants and its derived compounds are typically appropriate as antiviral candidates for many reasons:

i. They have a long history of use as medications against different diseases including infectious diseases.

ii. Plants produce a large number of phytochemical substances to adapt themselves to environmental stresses including invasion by microorganisms (those substances include: Indoles, Phytosterols, Polysaccharides, Alkaloids, Tannins, Glucans, Phenolics, etc.)

iii. Plants are natural, that is why they may cause less damage to host cells infected by viruses, than do pharmaceutical antivirals (Dixon, 2001 in: Guo et. al., 2006).

In wide-ranging dietary, phytochemicals are naturally present in fruits, vegetables, legumes, whole grains, nuts, seeds, fungi, herbs and spices. Phytochemical compounds accumulate in different parts of the plant, such as in the roots, stems, flowers, fruits or seeds. These compounds are known as secondary plant metabolites and have biological properties such as anti-oxidant activity, anti-microbial effect, modulation of detoxification enzymes, stimulation of the immune system, decrease of platelet aggregation and modulation of hormone metabolism and anti-cancer property. There are more than thousand known and many unknown phytochemicals. It is well-known that plants produce these chemicals to protect themselves, but recent researches have demonstrated that many phytochemicals can also protect humans against diseases.

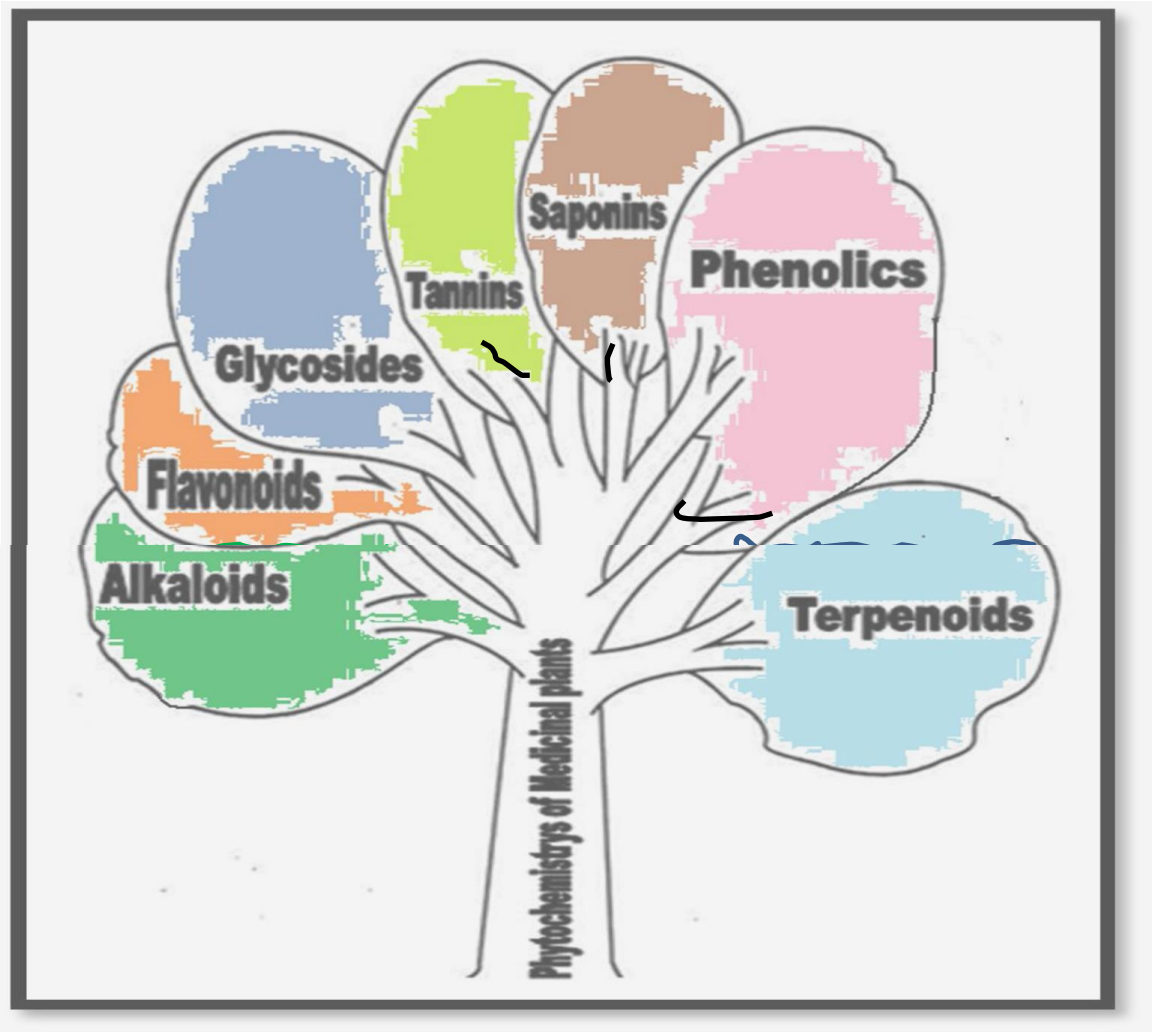

Plate 2.5: A sketch of Phytochemicals in a Plant

After centuries of empirical use of herbal preparation, the first isolation of active principles alkaloids such as morphine, strychnine, quinine and so on was in about the early 19th century. This marked the new era in the use of medicinal plants and the beginning of modern medicinal plants research. Emphasis shifted away from plant derived drugs with the tremendous development of synthetic pharmaceutical chemistry and microbial fermentation after 1945. With the development of chemical science, pharmacognosy physicians began to extract chemical products from medicinal plants. Phytomedicine almost went into extinction during the first half of the 21st century due to the use of the 'more powerful and potent synthetic drugs'.

Although investigations of the antiviral potential of various promising plants was difficult in the past, in the last four decades, scientific strategies for the in vitro evaluation of plant natural extract products with biological activity have progressed, based on the development of highly

automated antiviral bioassay screening colorimetric quantification of the proliferating cell cultures. Tea (Camellia sinensis) extract exhibited a marked antiviral activity against rotavirus and enterovirus in-vitro (Mukoyama et al., 1991). Moreover, the US Food and Drug Administration has approved a topical ointment Veregen® (Sinecatechins 15%) for the treatment of external genital and perianal warts caused by human papillomavirus (HPV). The active ingredient is a mixture of catechins extract from green tea that possesses an immunomodulation and antiviral activities (Gross et al., 2007 in U.S. FDA 2008). In the recent years, green tea crude extract and various derived catechins (EGCG, ECG and EGC) have demonstrated antiviral activities against various influenza virus strains (Song et al., 2005). Similarly, pomegranate (Punica granatum) components blocked interaction between HIV-1 viral envelope glycoproteins with cell receptors and inhibited in vitro infection, this being attributed to high level of polyphenolic compounds in pomegranate fruits (Neurath et al., 2004).

Recently, it was found that pomegranate components are directly virucidal for influenza viruses and also act at the intracellular level to inhibit influenza virus replication (Haidari et al., 2009). On the other hand, although it has been previously reported that Quercus species extracts are rich in polyphenolic compounds such as proanthocyanidins, tannins and acylated flavonoid glycosides (Zhentian et al., 1999 in: Meng et al., 2001 in: Hideyuki et al., 2002). This is suggested to be the cause of the reported antibacterial activity shown by the extracts of Quercus ilex leaves (Gulluce et al., 2004) and Quercus ilex bark (Berahou et al., 2007). However, information including antiviral activities of Mangifera indica and Garcinia kola have been reported in Joseph (2011) and that of Azadirachta indica has been reported (Mohammad et al., 2013). Part of the aim of this work is to evaluate in a thermodynamic way the in-vitro antiviral potential of Mangifera indica (leaf), Garcinia kola (seed) and Azadirachta indica (leaf) extracts in comparison to five antiretroviral synthetic drugs of known properties against the human immunodeficiency virus as one of the most harmful pathogens in human medicine. However, because of the numerous side effects of these drugs, the value of medicinal plants is being rediscovered as some of them have proved to be as effective as synthetic medicines with fewer or no side effects and contraindications. This is what this research tends to achieve by comparing the thermodynamic efficacy of some herbal extracts in treating HIV with synthetic ARTs whose efficacies have been confirmed thermodynamically. Hence, the essence of a thermodynamic verification of a drug's potency is to identify those active phytochemicals that inhibit particle (HIV) entry into a cell.

The Garcinia kola belongs to a family of tropical plants known as Guttifera (Plowden, 1972). It is commonly called "Aki-ilu" in Igbo, "Namiji goro" in Hausa and "Orogbo" in Yoruba lands of Nigeria. The seed is an edible nut generally known as "Bitter kola" in Nigeria. The Garcinia kola (Heckel) seed is a masticatory, used in traditional hospitality, cultural and social ceremonies. The seeds are used to prevent or relieve colic, cure head or chest colds and relieve cough (Iwu, 1993). The seed also has anti-inflammatory, antimicrobial, antidiabetic and antiviral according to Iwu (1986), as well as antiulcer properties (Ibironke, et al., 1997). Phytochemical and biochemical studies of Garcinia kola have shown the presence of sterols, terpenoids, flavonoids, glycosides, pseudotannins, saponin, proteins and starch (Igboko, 1983 in: Braide, 1989). Kolaviron (a mixture of three biflavonoids GB-1, GB-2 and Kolaflavanone, KF) has been isolated from fresh seeds of an indigenous plant (Iwu, 1985 in: Nwankwo, 2011). Kolaviron possesses a variety of anticancer activities including antioxidant, anti-genotoxic, and so on. For the fact that there are anti-HIV terpenoids and flavonoids, the Garcinia kola is believed to have anti-HIV activity and the extent of this activity is hoped to be established in this research. The phyto-chemical assay showed that Tannin (0.347%), Sapoium (0.680%), Phytic acid (0.550%), Phenol (0.163%), Sterol (0.093%), Flavonoid (2.130%), Alkaloid (0.433%) (Mazi et al., 2013).

Azadirachta indica is a tree in the mahogany plant family of Meliaceae. There are about two species in the genus of Azadirachta. It is popularly known as Neem or locally called Dogonyaro in Nigeria. The Neem leaves and all other parts of the plant are used medicinally for different diseases. The evaluation of antioxidant activity of crude extract with GC-MS analysis reveals that the neem contains hydrocarbons, phenolic compounds, terpenoids, alkaloids and glycosides (Mohammad, et al., 2013). Anti-HIV phenols are Lignin and Caffeic acid derivatives (Chicoric, Rosmarinic and Lithospermic acid). Anti-HIV terpenoids includes; 2-acetoxyalphitdic acid, 3-acetoxyalphitdic acid, Betulin, Betulinic acid, 3,4- Secodammarane triterpenoid and Dammarenolic acid and so on (Mohammad, et al., 2013). The neem leaves also contains 1.03% phenol, 5.33% Lavonoid and 1.83% Tannin (Garima, et al., 2014).

The genus Mangifera indica belongs to the plant family of Anacardiaceae and there are about 40 species distributed in tropical and sub-tropical parts of Africa, South East Asia and Latin America. It is popularly known as Mango. The mango leaf as well as the fruit, immature fruit, root, bark, seed (kernel), resin and flower are the parts used medicinally (Nikhal et al.,2010). The thirst-relieving pulp of the pericarp promotes blood circulation, while the fruit rind acts as

a tonic. The immature fruit, when sliced and dried is efficacious in Septicemia. The leaves are steeped to produce a tea with cooling effect. The liquid is used also as a bath to treat fever and cold. The bark is considered to be diuretic, astringent hemostatic and anti-rheumatic when used in hot local baths and hot dressing. The Mangifera Indica contains alkaloids and glycosides which are of great importance pharmacologically (Maduagu et al., 1990 in Ross and Brain, 1977). Mangifera Indica also contains Mangiferin (a glucosylxanthone), Nwankwo (2011) and hopefully many other phytochemicals already identified and characterized or yet to be discovered. Mangiferin has been obtained as the yellow principle from leaves of the mango tree (Scheline, 1978 in Nwankwo, 2011). Mangiferin has been shown to have antitumor and immunomodulatory activity against Ascitic fibrosarcoma in Swiss mice, as well as antagonizing in vitro cytopathic effect of HIV (Guha et al., 1996 in Nwankwo O.J., 2011). It has been demonstrated to have antiviral activity against herpes simplex virus type 2 in vitro (Zheng and Lu, 1990 in Nwankwo, 2011). It has also been found to induce extensive in vitro proliferation of marine and thymocytes at the doses of 5-40 μ g/ml as well as activating the Splenocytes of tumor hosts at early and late stages of tumor growth (Chattopadhyay et al., 1987). According to Chattopadhyay et al. (1987), there are considerable increases in concentration of Mangiferin in plants during incidences of injury and infection with pathogenic micro-organism. The later property, added to the pronounced metal chelating properties of mangiferin, and their observed protection of mice treated with mangiferin against P-338, L-1210, S-180, fibrosarcoma and ehrlich ascites tumor, suggested that mangiferin may be a potential immune-modulatory agent.

The Alkaloids (Quinoline types) are the main anti-HIV Phytochemicals in records. Alkaloids are basic in character for virtually all herbal bioactive extracts. It has been estimated that over five thousand comprising all structural types exist in nature, and their class is a naturally-occurring organic substance that shows a wide range of structures (Hess, 1981). Suffice it to say that, it is the Quinoline alkaloids that have been verified to have interactions with the HIV and as such described as anti-HIV alkaloids just like anti-Hepatitis B (HBV) and anti-Herpes Simplex virus (HSV) alkaloids. Some of the various groups of compounds present in anti-HIV class of alkaloids are: Quinolone-2-, Quinolone-4-, Furoquinolines, Quinine (Cinchona), Camptotheca, Isoquinoline, Lycorine, Homolycorine, 2-o-acetyllycorine, Trisphaeridine, Haemanthamine, Pavine, and so on. The Camptothecins have attained yet another pharmacological milestone for possessing anti-HIV activity. Camptothecin (10-hydroxy-CPT

and 7-hydroxymethyl-CPT) have been evaluated in vitro, for their therapeutic index against HIV-1 (IIIB), in the C8 166 cell line, and against strain HIV-1 (KM0 18), clinical isolates in peripheral blood monocytes (Li et al., 2009). The antiviral parameters assayed for in Li et al. (2009) included: inhibition of viral cell-to-cell transmission, inhibition of reverse transcriptase, protease or integrase in cell-free systems and selective killing of chronically infected cells after three days of incubation while 7-hydroxymethyl-CPT showed the most potent anti-HIV activity. The leaf of mangifera indica Linn, per 100g of its powder contains: Alkaloid 0.84mg, Flavonoid 11.24mg, Phenol 0.09mg, Saponins 3.22mg and Tannin 0.45mg (Donatus, et. al.: 2008).

a. Solid Surface Thermodynamics of Blood Cells and Thromboresistance of Biomaterials

The applicability of thermodynamics to thrombus formation induced by biomaterial implants was carried out by Neumann et. al. (1975) with special interest on the attachment and subsequent adhesion of platelets to various substrates. The introduction of thermodynamic or at least quasi-thermodynamic quantities to this subject, from the earlier qualitative concepts of 'hydrophilic' and 'hydrophobic' surfaces was done by Lyman et. al. (1965) in (Baier et. al., 1972). Their works applied the critical surface tension of wetting and a surface free energy quantity, γ_{So} (solid surface tension against a vacuum). They correlated these parameters empirically with factors relevant to thrombogenesis like clotting time, platelet adhesion, extent and type of thrombus formation.

The conventional γ_c values of polymer, particularly those measured by Zisman et. al. (1952) agree closely with the γ_{SV} obtained from the equation of state. Lyman et al. (1965) found empirical correlation between γ_c (obtained before protein adsorption) to bare polymer surface, and clotting time as well as platelet adsorption. Baier and Bull (1972) found a correlation between γ_c and thrombus formation (clotting). The conventional γ_c values of polymers, particularly those measured by Zisman et al. (1952) agree closely with the γ_{SV} obtained from the equation of state. This development admits the correlation as relevant while the conclusions drawn from contact angle data of carbon or adsorbed protein layers are somewhat unclear. Figure 2.10 shows a theoretical correlation between platelet adhesion and surface tension of the

solid platelet. A biomaterial of a higher surface tension of about 75ergs/cm^2 (7.5 x 10^{-2}J/m^2) might absorb protein to a smaller extent than that of a surface tension of say, 60ergs/cm^2 (6.0 x 10^{-2}J/m^2) and hence, will effectively have a smaller resultant surface tension than the later.

b. Surface Thermodynamics and Adhesion of Platelets (to a homogeneous solid surface)

A homogeneous surface is a surface that is of the same composition or character all through. A plane surface glass slide is an ideal homogeneous solid surface. Recall that contact angle is a quantitative measure of the wetting of a solid by a liquid. They set up an experiment to study the adhesion or attachment of a platelet P, originally suspended in a liquid L to a smooth and homogeneous solid glass surface/substrate S, figure 2.6.

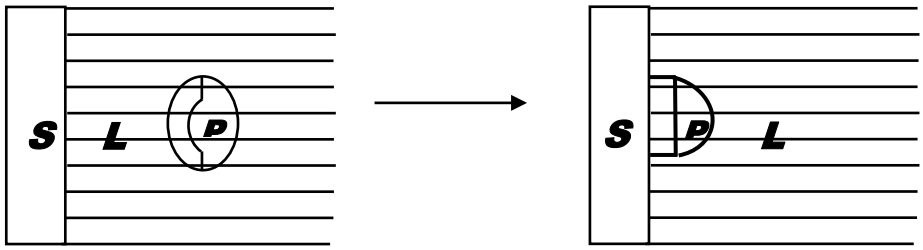

State1: *Suspended platelet* ***State2:*** *Adhering platelet*

Figure 2.6: Process of Platelet Adhesion to a surface (Neumann et al., 1975).

The platelet was adsorbed out of a suspension in saline onto the surface. This was different from a real-life complicated scenario where the surfaces of biomaterials (blood, herbal extracts, etc.) are actually rough and heterogeneous. This process generated a new platelet-substrate PS interface thus eliminating the natural platelet-liquid PL and substrate-liquid SL interfaces. Hence, the work done per unit area in generating and eliminating the various interfaces is the interfacial tension γ_{PS}, γ_{PL} or γ_{SL}. Therefore, the overall work done per unit area of platelet adhesion/attachment is given by the change in the Helmholtz free energy of adhesion, ΔF^{adh}.

$$\Delta F^{adh} = \gamma_{PS} - \gamma_{PL} - \gamma_{SL} \qquad (2.21)$$

A negative value of ΔF^{adh} indicates that platelet-substrate contact resulted to an adhesion. A positive value would invariably indicate that platelet-substrate contact resulted to repulsion. This is significant and central to this research on surface energetic study. Neumann et. al. (1975) finally gave an explicit expression for γ_{SL} as:

$$\gamma_{SL} = \left[\frac{\left\{ (\gamma_{SV})^{\frac{1}{2}} - (\gamma_{LV})^{\frac{1}{2}} \right\}^2}{1 - 0.015(\gamma_{SV}\gamma_{LV})^{\frac{1}{2}}} \right] \tag{2.32}$$

According to Omenyi et. al. (1980), they reviewed and recorded that the solid-liquid interfacial tensions can be expressed in terms of the solid-vapour and liquid-vapour interfacial tensions as:

$$\gamma_{SL} = \mathrm{f}(\gamma_{SV}, \gamma_{LV}) \tag{2.100}$$

But from the Young's equation, Neumann went further to recall that:

$$\gamma_{SV} - \gamma_{\mathrm{SL}} = \gamma_{\mathrm{LV}} Cos\theta_Y \tag{2.101}$$

By substituting equation (2.33) in equation (2.98) and making $Cos\theta_Y$ the subject of the relation:

$$\gamma_{SL} = \left[\frac{(0.015\gamma_{SV} - 2.00)(\gamma_{SV}\gamma_{LV})^{\frac{1}{2}} + \gamma_{LV}}{\gamma_{LV}\left\{0.015(\gamma_{SV}\gamma_{LV})^{\frac{1}{2}} - 1\right\}} \right] \tag{2.102}$$

The parameters of θ_Y, γ_{SV} and γ_{LV} are important in the investigation of biological systems where the intervening medium (drug in blood serum) that contact with a substrate particle (HIV) results in changes of the substrate, since the liquid medium is not water or an isotonic saline.

From a single pair of ($\gamma_{\mathrm{LV}}, Cos\theta_Y$) data, γ_{SV} can be calculated using equation (2.102). The value of the corresponding γ_{SL} can be obtained from Young's equation (2.101). Alternatively, γ_{SL} can be calculated from equation (2.20) that makes use of contact angle data on platelets (where the index P replaces S in equation (2.100 to 2.102). Similarly, the interfacial tension between platelet and substrate can be calculated from equation (2.32) (by replacing γ_{LV} with γ_{PV}). Using equation (2.20), the ΔF^{adh} value can be obtained from contact angles and the liquid surface tension γ_{LV}.

This thermodynamic approach has been applied to in vitro phagocytosis of various bacteria of human neutrophils. Phagocytosis would occur when the free energy changes and all the interactions involved in adhesion are negative. It follows that, since the theory of surface

energetic has been applied to a biological process involving cellular adhesion, it is likely that it can be applied to platelet adhesion (Neumann et al., 1975).

c. Liquid Surface Tension of Blood Cells and Proteins

Van der Scheer and Smolders (1978) showed that interfacial tensions have been shown to play vital roles in phenomena as diverse as the critical closing and opening of vessels in the micro-circulation, cell adhesion, protein adsorption, antigen-antibody interactions and phagocytosis. The deductions from their extensive studies were summarized as follows:

i. Surface tension of biological cells and proteins are relatively high as then are hydrophilic in nature.

ii. Surface tension of biological cells and proteins (biomaterials) can be measured by a variety of techniques; and results obtained from the different techniques are always in good agreement.

iii. The interpretations of surface tension experiments with biomaterials show that surface tension governs cell adhesion, protein adsorption, stability of suspension and phagocytosis.

Neumann et al. (1983) established the fact that the role of surface properties in various biological processes is verifiable by various techniques as shown in table 2.7:

Table 2.6: Surface Tension of Biological Entities (in ergs/cm^2)T = 22˚C((Neumann et al., 1983))

System	Contact Angle from Equation of State	Engulfment			Adhe-sion	Detach-Ment	Suspending Stability
		Advan-cing Solidi-fication	Phagocytic Ingestion				
			Granu-locyts	Platelets			
Granulocytes(Human)	69.1	69.3	-	-	69.0	69.0	-
Lymphocytes(Human)	70.1	70.6	-	-	-	-	-
Erythrocytes(Human)	-	64.9	-	-	-	-	64.3

Horse	-	65.1	-	-	-	-	65.4
Chicken	-	64.8	-	-	-	-	65.2
Turkey	-	65.1	-	-	-	-	65.7
Canine	-	63.9	-	-	-	-	64.4
Platelets(Porcine)	67.2	-	-	67.9	-	-	-
Bacteria-E. Coli	69.7	-	69.6	69.3	69.6	-	-
-S. Aureus	69.1	-	68.7	68.8	69.3	-	-
-S. Epidermidis	67.1	-	66.9	67.3	66.0	-	-
-L. Monocytogenes	66.3	-	66.1	-	65.6	-	-
Proteins-B. Serum Albumin	70.2	-	-	-	-	-	-
-H. Serum Albumin	70.3	-	-	-	70.2	-	-
-H. Immunoglobulin G.	67.3	-	-	-	67.7	-	-
-H. Immunoglobulin M.	69.4	-	-	-	71.0	-	-
-H. a_2 Macroglobulin	71.0	-	-	-	71.0	-	-
-H. Transferrin	66.8	-	-	-	-	-	-

*(B=Bovine; H=Human)

Table 2.7: Comparison of Surface Tension Data of Biological Cells obtained from some Techniques (Omenyi et al., 1982)

Material	Surface Tension at Maximum DMSO concentration γ_{iv} (ergs/cm^2)		Combined Hamaker Coefficient A_{131} (x 10^{-15} ergs)
	Droplet Sedimentation	Freezing Front	
Chicken	65.2	65.1	5.08
Turkey	65.7	65.4	4.35
Canine	64.4	64.2	6.38
Horse	65.4	64.5	4.78
Human	64.3	64.1	6.55

(* collected at 25°C) *DMSO=Dimethyl Sulfur (II) oxide.

d. Surface Thermodynamics and Adhesion of Platelets (in the presence of proteins) to a non-homogeneous surface

A non-homogeneous surface is rough, heterogeneous or irregular (naturally occurring). Platelets are more readily absorbed at the blood-gas interface and in large numbers than on most biomaterials. The number of platelets adhering to a biomaterial could therefore be more a function of the number of surface imperfections than a function of the surface thermodynamic properties of the biomaterial says (Neumann et. al., 1975). From their studies about platelet, the following deductions can be made:

i. A thermodynamic analysis of platelets (from a suspension in saline) attachment onto a smooth and homogeneous solid surface can be done theoretically and experimentally. The thermodynamic analysis shows that the relative magnitude of the surface tension of the platelets and the liquid in which they are suspended are of critical importance.

ii. A decrease in platelet adhesion results when the surface tension of the liquid is greater than the surface tension of the platelets while an increase in platelet adhesion is as a result of the surface tension of the liquid being less than that of the platelets, with increasing γ_{SV}.

iii. The presence of plasma proteins in biomaterials introduces considerable difficulties. The reason lies in the fact that the presence of proteins could cause complications in the surface tension of platelets i.e. adsorption of proteins could affect γ_{PV}.

iv. The roughness of biomaterials induces considerable difficulties to platelet adhesion by means of stabilization of gas pockets. This difficulty arises from nucleation or entrapment of gas or air bubbles.

Therefore, after a biomaterial like herbal extract is brought in contact with blood, a layer of solid protein rapidly builds up on the surface. This in consequence changes the surface tension γ_{SV} of solid platelet (Vroman and Adams, 1967). Values for the high and low energy patches on the solid surface could be obtained from the contact angle experiment. However, equation (2.20) would no longer represent the free energy of platelet adhesion if the surfaces are rough, with lateral dimensions of rigors or crevices.

e. Blood-HIV Interaction

Alderman (1988) suggested that the depletion of CD4+ lymphocytes might activate some homeostatic mechanism that would increase their production. This assumption was on the basis that homeostatic mechanism increases the production of both CD4+ and CD8+ lymphocytes and do not discriminate between the two T-cells subpopulation. Bragardo et al. (1997) showed that HIV-1 glycoprotein120 induced CD4+ association with several molecules on the surface of CD4+ lymphocytes. One of the molecules was CD38, which was involved in lymphocyte/endothelium interactions. They therefore examined the possibility of glycoprotein120 binding, altering the CD4+ T-cell interaction with vascular endothelium in vitro and in vivo. They confirmed that glycoprotein120 induces CD4 association with CD38 in peripheral blood CD4+ T-cells.

Hart (1997) showed that dendritic cells-unique leukocytes population, control the primary response of blood. Shortman (2002) studied the mouse and human dendritic cell subtypes. Abbas et al. (2003) studied the role of monocytes in both innate and adaptive immune function. Wu and Kewal-Ramani (2006) studied dendritic-cell interaction with HIV infection and viral dissemination. Meyer (2007) worked on the impact of HIV on cell survival and antiviral activity of plasmacytoid dendritic cell. Martinson et al. (2007) studied the dendritic cells from HIV-1 infected individual and less response to toll-like receptor (TLR) ligands. Triboulet et al. (2007) showed that HIV-1 is capable of suppressing some inhibitory miRNA which may reflect on evolutionary interaction of HIV-1 and host factors. Wang (2009) studied the role of naturally occurring anti-HIV micro-RNA (miRNA) in suppressing HIV-1 replication in peripheral blood monocytes. Zeng (2009) showed that HIV-Tat encourages the survival of monocytes in situations where they would normally be cleared.

Hraba and Dolezal (2009) presented a mathematical model of CD4+ lymphocyte dynamics in HIV infection. The model incorporated a feedback mechanism regulating the production of T-lymphocyte and simulated the dynamics of CD8+ lymphocytes, whose production was assumed to be closely linked to that of CD4+ cells. Hence, because CD4+ lymphocytes count are a good prognostic indicator of HIV infection, the model was used to simulate such therapeutic interactions as chemotherapy and active and passive immunization. The model was also used to simulate the therapeutic administration of anti-CD8 antibodies; this intervention being assumed to activate T-cell production by activating a feedback mechanism blocked by the

number of CD8+ lymphocytes present in HIV-infected persons. This model concentrated on CD4+ lymphocytes because the depletion of the T-cell subpopulation and the parallel decrease in the helper activity of T-lymphocytes seem to be major immune system defect caused by HIV infection. The model was purely on maintenance of T-cell population in HIV infection.

f. Surface Thermodynamics Approach to HIV-Blood Interaction

The electrostatic repulsion and van der Waals attraction mechanisms can be used to establish the role of surface thermodynamics in various biological processes (Achebe, 2010). In his work, Achebe (2010) declared that a solution to HIV can be found by thermodynamically modelling the interaction between HIV and blood. His experimental method for investigation involved blood samples from twenty HIV-infected and uninfected persons to measure their absorbance and CD4 counts. He then used the Hamaker Coefficient approach as a thermodynamic tool to determine the interaction processes by computations in the Lifshitz formula using MATLAB software tool to solve the ensuing mathematics. In his research, the absolute combined Hamaker coefficient, A_{132abs} for infected HIV blood samples was calculated as 0.2587×10^{-21}Joules (i.e. 0.2587×10^{-14} erg). The positive sign of the value implies net positive van der Waals forces indicating an attraction between the HIV virus and the lymphocytes which confirms infection. But his lower value of $A_{131abs} = 0.1026 \times 10^{-21}$Joules obtained for the uninfected blood samples is an indicator that a zero or even negative absolute combined Hamaker coefficient is attainable. Achebe (2010) then developed a mathematical model for the HIV-blood interaction mechanism from the principle of particle-particle interaction. He proposed a solution to HIV infection by finding a way to render the A_{132abs} negative. A mathematical derivation for $A_{33} \geq 0.9763 \times 10^{-2}$ Joules which satisfies this condition foe negative A_{132abs} was used in his study. It was finally suggested that the condition of the stated A_{33} above, would be achieved by administering possible additive(s) in the form of drugs to the serum as the intervening medium. It was based on this premise that (Ani, 2015) confirmed the effectiveness of five (5) antiretroviral HAART drugs by obtaining A_{132abs} values ranging from -0.03998×10^{-21} Joules to -0.05844×10^{-21} Joules. Hence, this research is aimed at establishing A_{132abs} values for herbal extract drugs which can compare with those used by (Ani, 2015).

g. Potency of Herbals using Medical Approach

The trend of this research is following the most recent efforts by:

Chukwuneke (2015) who investigated the nature of interaction between mycobacterium Tuberculosis (M-TB), macrophage and HIV particles. He confirmed that the positive value of the absolute combined Hamaker coefficient which entails net positive van der Waals forces, demonstrates attraction between M-TB and the macrophage. But in the presence of HIV, the interaction energy is reduced and the negative value of the absolute combined Hamaker coefficient indicates that the repulsion of M-TB is realistic.

Ani (2015) verified the efficacy of five antiretroviral pharmaceutical drugs against the HIV particle using the Hamaker concepts of the surface energetics. The negative values of the absolute combined Hamaker coefficient for infected blood-drug interactions he recorded, implies repulsion or blocking of the invading virus by the drug-coated lymphocyte thus, confirming (Chukwuneke, 2015). The positive values of the absolute combined Hamaker coefficient for uninfected blood-drug interactions as he recorded implies attraction or coating of a lymphocyte particle by a drug particle.

Therefore, the power of effecting functional cure is the potency of the antiretroviral drugs that have been quantitatively and qualitatively verified thermodynamically by (Ani, 2015). Hence, as an empirical novel research and, considering the scope within relevant literatures, the potencies of the research herbal extracts are what have been established using the thermodynamic criterion, under the prevalent set conditions of environment, biomaterials' quantities and qualities.

2.4 Summary of Literature Review

The van der Waals' phenomenon of attraction and repulsion is widely referenced based on its merits. It is on the basis of this idea in line with the Hamaker coefficient concept for surface thermodynamic interactions that Neumann & Omenyi (1981) established experimentally the interaction mechanism of bio-particles, Achebe (2010) quantified mathematically the HIV-blood interactions, Ani (2015) studied and deduced the efficacy of known synthetic pharmaceutical antiretroviral drugs on HIV infected and uninfected blood samples, and Chukwuneke (2015) established experimentally the nature of interactions between mycobacterium tuberculosis-Human sputum.

The study of literature has shown that there has been no attempt made to predict antiviral herbal extract drugs treatment relative success by determining the resistance to natural surface free

energy of an ‘invading virus’ which can be measured by UV absorbance for a measure of thermodynamic efficacy. This thus, forms the knowledge gap that is filled by this research. This will be implemented through thermodynamic investigation of the potency of selected antiviral herbal crude extracts as drugs for HIV management in comparison to standard antiretroviral synthetic drugs whose potencies have been verified. This investigation is based on negative values of the Hamaker coefficient for the interactions which indicate repulsion between drug-coated lymphocytes and the virus as a thermodynamic proof of efficacy.

CHAPTER THREE
MATERIALS AND METHODS

3.1 Materials

The three herbal drug materials investigated are *Garcinia* kola commonly called (Akilu*), *Azaradichta indica* (Dogonyaro*) and *Mangifera indica* (Mango*) (see Plates 3.1 – 3.3).

Plate 3.1: Garcinia kola tree with pods containing seeds

Plate 3.2: Azadirachta Indica tree

Plate 3.3: Mangifera Indica tree

* Common names in Nigeria – West Africa

3.2 Equipment and Tools

The laboratory equipment and tools employed for the purpose of experiments are:

3.2.1 Equipment

i. VICTORIA Grain Mill, High Hopper, Ref: 600009. MECANICOS UNIDOS, SA.
ii. S. METTLER digital balance.
iii. OHAUS® Pioneer™ digital weighing balance.
iv. Rotary evaporator
v. Refrigerator
vi. Cytoflowmetre – CF PARTEC counter II. No.: 110473322
vii. KJMR – II Blood Roll Mixer
viii. Ultraviolet Visible MetaSpecAE1405031Pro Spectrophotometer. Wavelength range: 200-1000nm.
ix. BUCK M910 Gas Chromatography (with FID)
x. RESTEK 15 meter MXT-1 Column (15m x 250µm x 0.15µm)

3.2.2 Tools

i. Sieve plate. No.7 Ø 0.1mm
ii. Absorbent cotton
iii. Beakers 2000ml capacity
iv. Conical flasks 500ml
v. Wattmann No.1 filter paper (125mm dia., Cat No. 1001 125)
vi. Spatulas
vii. 5ml test-tubes (with EDTA), syringes, hand gloves, masking tape
viii. Micro-pipettes (700µl)
ix. 25.4 x 76.2 x 1.2mm microscope slides (@ least 800 pieces)
x. Microsoft Excel software 2018 updated version
xi. SPSS software Version 22

3.3 Sourcing and Processing of Research Materials

3.3.1 Drug Materials

Fresh leaves of the Mangifera indica and the Azadirachta indica were collected from Amachara village of Afikpo-North L.G.A. of Ebonyi State, and the seeds of Garcinia kola were collected

from its plant at Ubahu village of Okigwe L.G.A of Imo State. The plant materials were air dried at room temperature for fourteen (14) days, ground and sieved into fine powders. The smooth powders were stored in air-tight glass wares and kept away from direct sunlight and ambient condition until they were used.

Plate 3.4a: Garcinia kola seed

Plate 3.4b: Garcinia kola seed powder

Plate 3.5: Azadirachta Indica leaves powder

Plate 3.6: Mangifera Indica leaves powder

Plate 3.7: Garcinia kola, Azadirachta indica and Mangifera indica powder samples for blending

Plate 3.8: (a) Efavirenz (b) Efavirenz, Lamivudine, Tenofovir combination therapy

Efavirenz (Efv) is of 600mg (ESTIVA-600) and Efavirenz, Lamivudine, Tenofovir (ELT) combination is of 600mg/300mg/300mg disoproxil fumarate, all manufactured by HETERO LABS Ltd. India.

3.3.2 Blood Materials

Ten HIV infected blood samples were collected from volunteers who have been on antiretroviral drugs, under an ethical clearance by relevant authorizing office at Chukwuemeka Odumegwu Ojukwu Teaching Hospital, Awka Anambra State, Nigeria. A certified medical

laboratory scientist guided and collected blood samples of HIV uninfected and infected blood samples from volunteers-including the researcher.

3.3.3 Other Materials

i. Ethanol AR (JHD ® M = 32.04, M.P = -98^{o}C)

ii. Potassium hydroxide

iii. Anhydrous sodium sulfate

iv. Pyridine

v. hexane

vi. Sterile water

3.4 Phytochemical Profiling/Characterization of Herbal Drugs used

3.4.1 Extraction of Phytochemicals

The methods involved washing, shade drying and mechanical powdering of at least 500g of each plant material. Herbal powders were first obtained by macerating 1g each of the dried herbal drug samples (weighed with S. METTLER digital balance) into a test tube and 15 ml ethanol and 10 ml of 50% w/v Potassium hydroxide was added. The test tube containing the each macerated quantities, in 25 mls of ethanol-potassium hydroxide solution, was allowed to interact in a water bath for 60 minutes. After the interaction or reaction time, the reaction product contained in the test tube was transferred to a separator funnel. The tube was washed successfully with 20 ml of ethanol, 10 ml of cold water, 10 ml of hot water and 3 ml of hexane, which was then transferred to the funnel. The extract for each herbal material of: Garcinia kola (GK), Azadirachta Indica (AI) and a mixture of: GK+ AI + Mangifera Indica (MI) abbreviated GAM, was washed three times with 10% v/v ethanol aqueous solution. The solutions as dried with anhydrous sodium sulfate were also allowed open for a complete evaporation of ethanol. The samples were solubilized in 1000µl of Pyridine of which 200µl were each transferred to a vial for analysis. However, the results of GK, AI and MI phytochemicals present in each herbal extract are as tabulated in table 4.43 curtsey of Springboard Research Laboratories, Awka Anambra state. Phytochemicals were determined by the ratio between the area and mass of internal standard and the area of the identified phytochemicals. The concentration of different phytochemicals were expressed in µg/g.

3.4.2 Identification of Functional Groups (FT-IR Analysis)

The Fourier Transform Infrared (FT-IR) spectra was used to identify the functional groups which are pointers to the active phytochemicals present in the herbal drugs and to be sure that there are no cancer causing elements. The application of infrared radiation (IR) to a bio-sample is to reveal its phytochemical composition and structure of its molecule by measuring the level of absorbance of the infrared light at various wavenumbers (which are inverses of wavelengths). The IR spectrum helps to determine the functional groups present in a material substance. The x-axis or horizontal axis represents the infrared spectrum, which plots the intensity (transmittance) of infrared spectra. The peaks are also regarded as the absorbance bands and they correspond to the various vibrations of the sample's atoms when they are exposed to the infrared region of the electromagnetic spectrum. The y-axis or the vertical axis represents the amount of infrared transmitted by the material being tested. The IR spectrum can be distinguished into four regions: the first region ranges from 2500 to 4000 cm^{-1}, the peak corresponding to the absorption caused by the N-H, C-H and O-H single bond atomic structures. The second region is characterized with peaks in the range of 2000 to 2500 cm^{-1} and are typical of triple bond atoms. The third region has peaks ranging from 1500 to 2000 cm^{-1} and are peculiar to double bond atoms such as C = O, C = N, and C = C. The fourth region is also called Fingerprint region of the IR spectrum and it contains number of absorption peaks that account for a large variety of other single bond atoms.

The analysis of active components was performed on a BUCK M910 Gas Chromatography (GC) equipped with a Flame Ionization Detector (FID). A RESTEK 15 meter MXT-1 column (15 m x 250 µm x 0.15µm) was used. The injector temperature was 280^0C with split less injection of 2µl of sample and a linear velocity of 30 cms^{-1}. Helium 5.0 pa. was the carrier gas with a flow rate of 40 ml/min. the oven initially operated at 200^0C was heated up to 330^0C at a rate of 3^0C per minute and it was maintained at this temperature for 5 minutes. The detector was operated at 320^0C.

3.5 Preparation of Drug Sample solutions with Sterile Water

GK, AI and GAM, are represented as Drug1, Drug2 and Drug3 respectively while Efv and ELT are represented as Drug4 and Drug5.

3.5.1 Slides preparation of Herbal Extract Drugs in H_2O

A glass slide was placed on a balance and its weight recorded as S, in mg. Weighed slide was retained on the balance. The calculation (S + 790) mg was recorded as T, in milligrams. Using a spatula, a quantity of drug1 powder was taken and added onto slide on balance until the balance reads T mg. The spatula was cleaned up. The slide with drug1 was then emptied into a conical flask. Using a syringe, 1ml of sterile water was taken and added into the conical flask containing 790mg of drug1 powder shook well and seen to dissolve into a solution.

Using a pipette, few drops of the drug1 solution were drawn and holding a clean slide at 45^o to the horizontal and allowing only one drop of solution from the pipette to drop on the slide and immediately a clean spatula was used to smear the drop gently and evenly along the length of the slide. The spatula was immediately cleaned up again. Slide1 (S1) of drug1 (D1) i.e. S1D1 was prepared as such and kept to dry in a dust-free laboratory room temperature.

The procedure was repeated and using a syringe 2, 3, 4 and 5 mls of sterile water were added to the same 790 mg of drug 1 to prepare: S2D1, S3D1, S4D1 and S5D1. A total of 15 slides were prepared for drugs1, 2 and 3 in, 1 to 5 milliliters of sterile water.

3.5.2 Slides preparation of Antiretroviral (Synthetic) Drugs 4 & 5 in H_2O

One (1) tablet each of drug4 and drug5 were crushed separately into powder and put into different conical flasks. Using a syringe, 1ml of sterile water was added into the conical flask containing 600mg of drug4 powder and the mixture was seen to dissolve into a solution.

Using a pipette, few drops of the drug4 and drug5 solutions were drawn and holding a clean slide at 45^o to the horizontal and allowing only one drop of solution from the pipette to drop on the slide, and immediately a clean spatula was used to smear the drop gently and evenly along the length of the slide. S17 to S20 of drug4 and 5, and all kept to dry in a dust-free laboratory room temperature.

3.6 Blood Samples Collection

Instruments: syringes, 5ml test tubes (with EDTA), refrigerator

A. 5ml each of Infected HIV Blood Samples (IBS) of 10 persons

B. 5ml each of Uninfected HIV Blood Samples (UBS) of 10 persons

NB: All blood samples by being inside EDTA test tubes were automatically treated with anti-coagulants and were stored in a refrigerator ready for use.

3.7 Serial Dilution of Drug Samples

790mg of drug1 powder was put into a labeled test tube and was added 10ml of sterile water, shook, to make first solution in an ambient laboratory room temperature. Using a fresh pipette, 1ml of first solution, was put in a labeled test tube containing 9ml of sterile water, shook to make second serial solution. Using another fresh pipette, 1ml of second solution was put in a labeled test tube containing 9ml of sterile water, shook, to make third serially diluted solution drug 1. The steps were repeated with 970mg of drug2 to make a third serially diluted solution of drug 2.Repeatedly, with a combined 2800mg of drug3, crushed 600mg of drug 4 and crushed 1200mg of drug5 and put in a labeled test tube, the third serially diluted solutions of all drug materials were prepared and ready to be used for blood inoculation.

3.8 Drugs Interactions with Blood Samples (in-vitro experiment) and slides preparation

A. Uninfected Blood component Samples$_{1\text{-}10}$ with Drugs$_{1\text{-}5.}$

Each of UBS$_{1\text{-}10}$ (Uninfected Blood Sample 1 to 10) was shared into 5, of 0.8ml each and 0.16ml $\cong$ 0.2ml of third serial solution of drug$_{1\text{-}5}$ was added in each blood sample. Incubation was allowed for 24 hours and separation with a centrifuge machine was done. The separated serum blood component was smeared on 10 slides (USe$_{1\text{-}10}$), separated WBC (White Blood Cell) were smeared on 10 slides of UW$_{1\text{-}10}$ (Uninfected White 1 to 10), separated RBC (Red Blood Cell) were smeared on 10 slides of UR$_{1\text{-}10}$ (Uninfected Red 1 to 10) and a well shook mixture of Whole Blood (WB) were smeared on 10 slides of UWb$_{1\text{-}10}$ (Uninfected Wholeblood) using the method stated earlier.

Therefore, for 10 UBS interacted with 0.8ml of each of the 5 drug samples, on: (25.4 x 76.2 x 1.2mm microscope slides; for UV Spec.), a total of 200 slides were prepared.

B. Uninfected Blood component samples 1-10, without Drugs

After separation with a centrifuge machine, there were smeared serum on 10 slides (USe_{1-10}), smeared WBC on 10 slides (UW_{1-10}), smeared RBC on 10 slides (UR_{1-10}) and smeared Whole Blood (Wb) on 10 slides (UWB_{1-10}).

Where: USe_{1-10}, UW_{1-10}, UR_{1-10} and UWB_{1-10} → Uninfected: Serum $Slide_{1-10}$, White blood $Slide_{1-10}$, Red blood $Slide_{1-10}$ and Whole blood $Slides_{1-10}$ respectively.

Therefore, for 10 UBS without drug samples, on: (25.4 x 76.2 x 1.2mm microscope slides) for, four (4) blood components, a total of 40 slides were prepared.

The same process as in A or B was repeated and for 10 infected blood samples interacted with 0.8ml of each of the 5 drug samples, on: (25.4 x76.2 x1.2mm microscope slides). A total of 200 slides were prepared. For 10 infected blood samples interacted without drugs, a total of 40 slides were prepared.

Finally, a grand total of 505 slides were prepared for spectroscopy experiment. 25 slides (for drug samples in sterile water), 80 slides (for blood samples without drugs) and 400 slides (for blood samples with drugs).

3.9 UV Spectroscopy

All 505 slides were meticulously placed under the digital UV visibleMetaspecAE1405031Pro spectrophotometer and light absorbance values were measured. All experimental processes were carefully carried out to ensure reliability of all data collected. The selected samples of herbal plants and antiretroviral drugs were preserved at ambient temperatures. To prevent collected blood samples from getting lysed (spoilt) due to their susceptibility to bacterial and thermal attacks, adequate refrigeration with solar power technology was employed at the laboratory.

Plate 3.9: Ultraviolet Visible MetaSpecAE1405031Pro Spectrophotometer, Wavelength range: 200-1000nm.

3.10 Computation methods

It has been stated earlier that the task is aimed at establishing the Combined Hamaker Coefficient using the Lifshitz model equation in terms of the bulk material properties of ε (dielectric constant of a solvent with regard to its capability to dissolve ionized solutes) and n (refractive index of glass) using the obtained absorbance values. On the basis of the Hamaker theory, the following empirical laws have relationships to the deductions for the Hamaker constant:

the Boyle's law, the Charles' law, the General Gas Equation, the Ideal Gas Equation and the van der Waals' equation for real gases, all contributed to the Hamaker equation for: semi-infinite solids in vacuum ($F_{vdw} = -\frac{A_{11}}{6\pi d^3}$) , and a sphere and semi-infinite plate

($F_{vdw} = -\frac{A_{11}R}{6d^2}$).

Where: $F_{vdw} \Rightarrow$ van der Waal's force of attraction, $A_{11} \Rightarrow$ Hamaker constant (subscript refers to material 1; for this research, uninfected Lymphocyte ideal molecules). This particular constant is a non-geometrical contribution to the force of attraction based on molecular properties only, $R \Rightarrow$ radius of an ideal sphere of molecule, $d^2 \Rightarrow$ minimum separation distance between ideal molecules.

Due to the limitation of not taking into account by Hamaker, the screening effects of molecules (which are effects between a molecule and an underlying molecule i.e., effects on molecular properties), Lifshitz derived an alternative to Hamaker constant (now in terms of bulk material properties).

The following models then were directly used, with several approximate equations, in the computations of thermodynamic expressions that are related to the establishment of the energy values of bio-material particles that would change the thermodynamic interaction that favors repulsion according to the van der Waals' forces:

3.10.1 The Hamaker Constant model (in terms of real part of refractive index of a plane glass slide, n_1)

The model equation is:

$$A_{ii} or A_{jj} or A_{kk} = 2.5\left[\frac{n_1^2 - 1}{n_1^2 + 1}\right]^2 \tag{3.1}$$

But in terms of dielectric constant, ε_{10}:

$$A_{ii} or A_{jj} or A_{kk} = 2.5\left[\frac{\varepsilon_{10} - 1}{\varepsilon_{10} + 1}\right]^2 \tag{3.2}$$

In this report, the former equation (3.1) for Hamaker constant is employed for any material particle i, another different particle **j** and another particle **k**

Where:

i $\Rightarrow$ Material 1 (Uninfected lymphocyte), **j** $\Rightarrow$ material 2 (Infected lymphocyte: HIV), **k** $\Rightarrow$ material 3 (Infected serum): 3 would equally stand for (Uninfected serum) in subsequent definitions. All particles can be interacted with and without drugs. n$\Rightarrow$ refractive index of a polymer at zero frequency-a bulk material property of any material 1 or 2 or 3 as the case may be.

$$n_1 = \left[\frac{1 - R_1^{0.5}}{1 + R_1^{0.5}}\right] \tag{3.3}$$

Where:

$$\mathbf{R}_1 = (1 - a_1 - \mathbf{T}_1) \qquad (3.4)$$

Where: a_1 or $\bar{a}_1 \Rightarrow$ absorbance of sample 1 (which were measured with a digital spectrophotometer, $\mathbf{R} \Rightarrow$ reflectance and $\mathbf{T} \Rightarrow$ transmittance

$$T_1 = Exp^{-\bar{a}1} \qquad (3.5)$$

3.10.2 Hamaker Constant values for Drugs$_{1\text{-}5}$ in 1-5mls of sterile water.

By backward substitutions in equations (3.5), (3.4) and (3.3) into equation (3.1), thermodynamic parameters are computed using the Microsoft Excel 2018 software version and shown on the tables of appendixes F to J. The absolute Hamaker constant values for all drug samples dissolved in sterile water are presented on the table.

3.10.3 Hamaker Constant values for Uninfected Components$_{1\text{-}4}$ of Blood samples$_{1\text{-}10}$ (without drugs).

$$A_{11} = 2.5\left[\frac{n_1^2 - 1}{n_1^2 + 1}\right]^2 \quad ; \quad A_{22} = 2.5\left[\frac{\mathbf{n}_2^2 - 1}{\mathbf{n}_2^2 + 1}\right]^2 \quad ; \quad A_{33} = 2.5\left[\frac{\mathbf{n}_3^2 - 1}{\mathbf{n}_3^2 + 1}\right]^2$$

The following definitions of thermodynamic parameters for calculations of the Hamaker constants (using experimentally obtained absorbance values) were made:

A_{11}: D^- (Hamaker constant for Uninfected lymphocyte (UNf.Lymphos.) particles (without drugs). See Tables G1-G4 of appendix G.

A_{11}: D^+ (Hamaker constant for UNf.Lymphos. particles with drugs$_{1\text{-}5}$). See Tables I1-I8 of appendix I.

A_{33}: D^- (Hamaker constant for Uninfected serum (US) particles without drugs). See Tables G1-G4 of appendix G.

A_{33}: D^+ (Hamaker constant for US particles with drugs$_{1\text{-}5}$). See Tables G1-G4 of appendixG.

A_{22}: D^- (Hamaker constant for INfected lymphocyte (INf. Lymphos.) particles without drugs). See Tables H1-H4 of appendix H.

A_{22}: D^+ (Hamaker constant for INf. Lymphos. particles with drugs$_{1\text{-}5}$).

See Tables J1-J20 of appendix J.

A_{33}: D^- (Hamaker constant for INfected serum(IS) particles without drugs).

See H1-H4 of appendix H.

A_{33}: D^+ (Hamaker constant for IS particles with drugs$_{1\text{-}5}$). See H1-H4 of appendix H.

3.11 Combined Hamaker constant model (in terms of Hamaker constants)

The trio of A_{ij}, A_{ik} and A_{jk} were addressed properly with respect to the connotations of $_{i}$, $_{j}$ and $_{k}$. (Hamaker, 1937)

$$A_{ij} = \sqrt{A_{ii} A_{jj}} \qquad 3.6$$

$$A_{ik} = \sqrt{A_{ii}} A_{jj} \qquad 3.7$$

$$A_{jk} = \sqrt{A_{jj} A_{kk}} \qquad 3.8$$

Where:

i, j, k represent materials 1, 2 & 3 respectively.

$$A_{12} = \sqrt{A_{11} A_{22}} \qquad 3.9$$

$$A_{13} = \sqrt{A_{11} A_{33}} \qquad 3.10$$

$$A_{23} = \sqrt{A_{22} A_{33}} \qquad 3.11$$

3.11.1 Combined Hamaker Constant values for Infected Components$_{1\text{-}4}$ of Blood samples$_{1\text{-}10}$ without drugs.

Using appropriate substitutions in relevant model of equs. (3.9) to (3.11), US meaning Uninfected Serum and IS meaning Infected Serum, the following definitions that yielded results for all combined Hamaker constants were made as referred to in the various appendices:

A_{12}: D^- (Combined Hamaker Constant values ($A_{12abs.}$) for UNf.Lymphos.-INf.Lymphos. interacting system (without drugs). See Table K1 of appendix K.

A_{12}: D^+ (Combined Hamaker Constant values ($A_{12abs.}$) for UNf.Lymphos.-INf.Lymphos interacting system (with $drugs_{1\text{-}5}$). See Table K2 of appendix K.

A_{13}: IS D^- (Combined Hamaker Constant values ($A_{13abs.}$) for UNf.Lymphos.-IS interacting system (without drugs). See Table L2 of appendix L.

A_{13}: IS D^+ (Combined Hamaker Constant values ($A_{13abs.}$) for UNf.Lymphos.-IS interacting system (with $drugs_{1\text{-}5}$. See Table L2 of appendix L.

A_{23}: IS D^- (Combined Hamaker Constant values ($A_{23abs.}$) for INf.Lymphos.-IS interacting system (without drugs). See Table L3 of appendix L.

A_{23}: IS D^+ (Combined Hamaker Constant values ($A_{23abs.}$) for INf.Lymphos.-IS interacting system (with $drugs_{1\text{-}5}$). See Table L4 of appendix L.

A_{13}: US D^- (Combined Hamaker Constant values ($A_{13abs.}$) for UNf.Lymphos.-US interacting system (without drugs). See Table M1 of appendix M.

A_{13}: US D^+ (Combined Hamaker Constant values ($A_{13abs.}$) for UNf.Lymphos.-US interacting system (with $drugs_{1\text{-}5}$). See Table M2 of appendix M.

A_{23}: US D^- (Combined Hamaker Constant values ($A_{23abs.}$) for INf.Lymphos.-US interacting system (without drugs). See Table M3 of appendix M.

A_{23}: US D^+(Combined Hamaker Constant values ($A_{23abs.}$) for INf.Lymphos.-US interacting system (with $drugs_{1\text{-}5}$). See Table M4 of appendix M

3.12 Hamaker Coefficient model (in terms of Combined Hamaker constants)

The Lifshitz derivation of an alternative to Hamaker coefficient (Lifshitz et. al., 1961); in terms of bulk material properties, is:

$$\mathbf{A}_{132} = \frac{3}{4}\pi\hbar\int_0^{\infty}\left[\frac{\boldsymbol{\varepsilon}_1(\mathbf{i}\zeta)-\boldsymbol{\varepsilon}_3(\mathbf{i}\zeta)}{\boldsymbol{\varepsilon}_1(\mathbf{i}\zeta)+\boldsymbol{\varepsilon}_3(\mathbf{i}\zeta)}\right]\left[\frac{\boldsymbol{\varepsilon}_2(\mathbf{i}\zeta)-\boldsymbol{\varepsilon}_3(\mathbf{i}\zeta)}{\boldsymbol{\varepsilon}_2(\mathbf{i}\zeta)+\boldsymbol{\varepsilon}_3(\mathbf{i}\zeta)}\right]\mathbf{d}\zeta \qquad (3.12)$$

Where:

$\hbar \Rightarrow$ Lifshitz correction factor (dimensionless), $\varepsilon_{1,2or3}(i\zeta) \Rightarrow$ dielectric constant of material 1, 2 or 3 along the imaginary i, Zeta potential ζ frequency axis, $d\zeta \Rightarrow$ a small differential of the Zeta potential.

It is the Hamaker constants, combined constants and their average and absolute values, of all interacting systems, that are sort, for the determination of the Absolute Combined Hamaker Coefficients of all the interacting systems.

The thermodynamic prediction method of criteria are:

1. If the positive values of $A_{131abs.}$ (UNf.Lymphos.-US-UNf.Lymphos.) i.e., HIV- interaction is greater than the positive values of $A_{232abs.}$ (INf.Lymphos.- IS-INf.Lymphos.) i.e., HIV+ then, the drugs concerned attract the lymphocytes which facilitates the binding or surface coating of the lymphocytes.

2. The lesser in value of the positive values of $A_{131abs.}$ (UNf.Lymphos.-US-UNf.Lymphos.) i.e., HIV- ,the strongest binding or attractive van der Waals forces which will give the lymphocytes the most effective surface coating the drugs concerned will possess.

3. If $A_{132abs.}$ (UNf.Lymphos.-IS/US-INf.Lymphos.) i.e., HIV+ is negative, then the drugs concerned have coated the lymphocytes with increased surface free energy potential which encourages van der Waals repulsion and as such are effective antiviral drugs for HIV treatment.

4. If $A_{132abs.}$ (UNf.Lymphos.-IS/US-INf.Lymphos.) i.e., HIV+ is near zero or zero, then the drugs concerned have coated the lymphocytes with increased surface free energy potential which encourages van der Waals attraction and as such are effective antiviral drugs for HIV treatment.

Therefore, the three identities for Hamaker coefficients $A_{ikjabs.}$, $A_{ikiabs.}$and $A_{ijkabs.}$ could as well be addressed properly with respect to the connotations of: i , j and k. (Hamaker, 1937)

$$A_{ikj} = \left(\sqrt{A_{ii}} - \sqrt{A_{kk}}\right)\left(\sqrt{A_{jj}} - \sqrt{A_{kk}}\right) \quad (3.13)$$

$$A_{iki} = \left(\sqrt{A_{ii}} - \sqrt{A_{kk}}\right) \quad (3.14)$$

$$A_{jkj} = A_{jj} + A_{kk} - 2A_{jk} \quad (3.15)$$

Where: i, j, k represents materials 1, 2, 3 respectively.

$$A_{132} = \left(\sqrt{A_{11}} - \sqrt{A_{33}}\right)\left(\sqrt{A_{22}} - \sqrt{A_{33}}\right) \quad (3.16)$$

$$A_{131} = \left(\sqrt{A_{11}} - \sqrt{A_{33}}\right) \quad (3.17)$$

$$A_{232} = A_{22} + A_{33} - 2A_{23} \quad (3.18)$$

3.12.1 Combined Hamaker Coefficient values ($A_{131abs.}$, A_{132abs} & $A_{232abs.}$) For UNf.Lymphos.-IS-UNf.Lymphos. interacting system (without drugs) and (with drugs$_{1-5}$)

Employing the models of equs. 3.16 to 3.18, the following definitions for calculations were made:

$A_{131:\,IS}\ D^-$ (Combined Hamaker Coefficient values ($A_{131abs.}$) for UNf.Lymphos.-IS-UNf.Lymphos. interacting system (without drugs). See Table N1 of appendix N.

$A_{132:\,IS}\ D^-$ (Combined Hamaker Coefficient values ($A_{132abs.}$) for UNf.Lymphos.-IS-INf.Lymphos. interacting system (without drugs). See Table N2 of appendix N.

$A_{232:\,IS}\ D^-$ (Combined Hamaker Coefficient values ($A_{232abs.}$) for INf.Lymphos.-IS-INf.Lymphos. interacting system (without drugs). See Table N3 of appendix N.

$A_{131:\,IS}\ D^+$ (Combined Hamaker Constant values ($A_{131abs.}$) for UNf.Lymphos.-IS-UNf.Lymphos.interacting system (with drugs$_{1-5}$). See Table O1 of appendix O.

$A_{132:\,IS}\ D^+$ (Combined Hamaker Coefficient values ($A_{132abs.}$) for UNf.Lymphos.-IS-INf.Lymphos.interacting system (with drugs$_{1-5}$). See Table O2 of appendix.

$A_{232:\,IS}\ D^+$ (Combined Hamaker Coefficient values ($A_{232abs.}$) for INf.Lymphos.-IS-INf.Lymphos. interacting system (with drugs$_{1-5}$). See Table O3 of appendix O.

3.12.2 Combined Hamaker Coefficient values ($A_{131abs.}$, $A_{132abs.}$, & $A_{232abs.}$) for UNf.Lymphos.-US-INf.Lymphos. interacting system (without drugs) and (with drugs$_{1-5}$)

Equally, using the relevant models of equs. (4.16 to 4.18) the following definitions for calculations were made:

$A_{131:\,US}\,D^{-}$ (Combined Hamaker Coefficient values ($A_{131abs.}$) for UNf.Lymphos.-US-UNf.Lymphos. interacting system (without drugs). See Table P1 of appendix P.

$A_{132:\,US}\,D^{-}$ (Combined Hamaker Coefficient values ($A_{132abs.}$) for UNf.Lymphos.-US-INf.Lymphos. interacting system (without drugs). See Table P2 of appendix P.

$A_{232:\,US}\,D^{-}$ (Combined Hamaker Coefficient values ($A_{232abs.}$) for INf.Lymphos.-US-INf.Lymphos. interacting system (without drugs). See Table P3 of appendix P.

$A_{131:\,US}\,D^{+}$ (Combined Hamaker Coefficient values ($A_{131abs.}$) for UNf.Lymphos.-US-UNf.Lymphos. interacting system (with drugs$_{1-5}$). See Table Q1 of appendix Q.

$A_{132:\,US}\,D^{+}$ (Combined Hamaker Coefficient values ($A_{132abs.}$) for UNf.Lymphos.-US-INf.Lymphos. interacting system (with drugs$_{1-5}$). See Table Q2 of appendix Q.

$A_{232:\,US}\,D^{+}$ (Combined Hamaker Coefficient values ($A_{232abs.}$) for INf.Lymphos.-US-INf.Lymphos. interacting system (with drugs$_{1-5}$). See Table Q3 of appendix Q.

3.13 Deductions for the Absolute Combined Negative Hamaker coefficients.

There are logical relations that express the conditions for an Absolute Hamaker coefficient to become a negative numerical value (Hamaker, 1937). That is:

$$A_{132abs.} = \left(\sqrt{A_{11}} - \sqrt{A_{33}}\right)\left(\sqrt{A_{22}} - \sqrt{A_{33}}\right) \leq 0 \qquad (3.19)$$

This condition is calculated to hold true when:

$\sqrt{A_{11}} > \sqrt{A_{33}}$ and when, $\sqrt{A_{22}} < \sqrt{A_{33}}$ or when, $\sqrt{A_{11}} < \sqrt{A_{33}}$ or, when

$A_{11} < A_{33} < A_{22}$ and $A_{11} > A_{33} > A_{22}$.

Hence, the mean of all values of $A_{11abss.}$ and $A_{22abss.}$ are obtained and substituted in equation (3.19) to compute corresponding values for $A_{33abss.}$ at which $A_{132abs.}$ is equal to or less than zero. To compute values for corresponding $A_{33abs.}$ at which corresponding $A_{132abs.}$ are equal

to zero or less than zero (negative), the modification of the model of equation (3.20) holds as deduced below:

$$A_{132} = \left(\sqrt{A_{11}} - \sqrt{A_{33}}\right)\left(\sqrt{A_{22}} - \sqrt{A_{33}}\right) \tag{3.20}$$

Let $\sqrt{A_{11}} = x$, $\sqrt{A_{22}} = y$ and $\sqrt{A_{33}} = z$

For A_{132} to be equal to zero;

$$(x - z)(y - z) = 0 \tag{3.21}$$

$$xy - xz - zy + z^2 = 0 \tag{3.22}$$

Collecting like terms:

- $xz - zy + z^2 = -xy$ or $z^2 - z(x + y) = -xy$

Forming a quadratic equation in x,y& z:

$$Z^2 - z(x + y) + xy = 0 \tag{3.23}$$

By a way of simplification using the model of (4.24):

$$Z_{1,2} = \frac{-b \pm \sqrt{b^2 - 4ac}}{2a} \tag{3.24}$$

Where:

a = 1 , b = -(x+y) , **c** = xy

$$Z_{1,2} = \frac{-\left[-(x+y)\right] \pm \sqrt{\left[-(x+y)\right]^2 - 4xy}}{2 \times 1} \tag{3.25}$$

$$= \frac{(x+y) \pm \sqrt{(x+y)^2} - 2\sqrt{xy}}{2}$$

$$= \frac{(x+y) \pm (x+y) - 2\sqrt{xy}}{2}$$

Either

$$Z_1 = \frac{2(x+y) - 2\sqrt{xy}}{2} = (x+y) - \sqrt{xy} \tag{3.26}$$

or

$$Z_2 = \frac{-2\sqrt{xy}}{2} = -\sqrt{xy} \tag{3.27}$$

Re-writing equs. (3.26) & (3.27) in terms of $A_{11abs.}$, $A_{22abs.}$& $A_{33abs.}$:

$$\sqrt{A_{33}} = \left(\sqrt{A_{11}} + \sqrt{A_{22}}\right) - \sqrt{\sqrt{A_{11}}\sqrt{A_{22}}} = \sqrt{A_{11}} + \sqrt{A_{22}} - \left(\sqrt{A_{11}}\sqrt{A_{22}}\right)^{0.5} \tag{3.28}$$

Squaring both sides of equ. (3.28):

$$A_{33} = A_{11} + A_{22} - \left(\sqrt{A_{11}}\sqrt{A_{22}}\right) \tag{3.29}$$

But if:

$$\sqrt{A_{33}} = -\left(\sqrt{\sqrt{A_{11}}\sqrt{A_{22}}}\right) = -\left(\sqrt{A_{11}}\sqrt{A_{22}}\right)^{0.5} \tag{3.30}$$

Then, squaring both sides of the equ. 3.30in turn:

$$A_{33} = -\left(\sqrt{A_{11}}\sqrt{A_{22}}\right) \tag{4.31}$$

3.14 Computations & Deductions for the Surface Free Energy of Cohesion of the interacting systems (in terms of the Hamaker constants)

It has been established:

$$A_{ii,jj,kk} = -12\pi d_0^2 \Delta F_{ii,jj,kk}^{coh}\left(d_0\right) \tag{3.32}$$

and,

$$\Delta F_{ii,jj,kk}^{coh} = -2\gamma_{sv} \tag{3.33}$$

Where:

$A_{ii,jj,kk} \Rightarrow$ Combined Hamaker constant A_{11}, A_{22}, A_{33} of particles 1, 2, 3 interacting in a systems.

$d_0 \Rightarrow$ a minimum distance between the particles of $i, j, k \equiv 1.82$Å or 1.82nm or 1.82×10^{-9}m)

$\Delta F_{ij}^{coh} \Rightarrow$ Change in free energy of cohesion between dissimilar particles of i, j, k

$\gamma_{sv} \Rightarrow$ Interfacial surface free energy between liquid and vapour surfaces or, the liquid/vapour interfacial tension. Substituting equation 4.36 in 4.35:

$$A_{ii,jj,kk} = -12\pi d_0^2\left(-2\gamma_{sv}\right)$$

By simplifications:

$$A_{ii,jj,kk} = 24\pi d_0^2\gamma_{sv} \tag{3.34}$$

Therefore, for every A_{ii} , A_{jj} , A_{kk} , the solid/vapour interfacial surface tension or free energy is given by:

$$\gamma_{sv} = \frac{A_{ii,jj,kk}}{24\pi d_0^2} \tag{3.35}$$

where the four playing parameters are as earlier defined.

3.15 Computations & Deductions for the Surface Free Energy of Adhesion of the interacting systems

It has been established, for all given combinations that the Surface Free Energy of Adhesion can be expressed in terms of van der Waals energies using for instance an ideal flat plate geometry as:

$$A_{ij}^{adh}\left(d_1\right) = -\left[\frac{A_{ij}}{12\pi d_1^2}\right] \tag{3.36}$$

That is:

$$A_{12}^{adh}\left(d_1\right) = -\left[\frac{A_{12}}{12\pi d_1^2}\right] \tag{3.37}$$

Similarly, a gap in vacuum (the equilibrium separation distance, d_1) is filled with a liquid, a new equilibrium separation distance, d_0 is expected. Hence, for i, j particles within an intervening medium k :

$$\Delta F_{ikj,iki,jkj}^{adh}\left(d_0\right) = -\left[\frac{A_{ikj,iki,jkj}}{12\pi d_0^2}\right] \tag{3.38}$$

That is:

$$A_{132,131,232}^{adh}\left(d_0\right) = -\left[\frac{A_{132,131,232}}{12\pi d_0^2}\right] \tag{3.39}$$

Where:

$A_{ikj,iki,jkj} \Rightarrow$ Combined Hamaker coefficients A_{132}, A_{131} or A_{232} of interacting systems.

$d_0 \Rightarrow$ a minimum distance between any one, two or both particles of ii, jj with the liquid medium, kk in between.($d_0 \equiv 1.82$Å or 1.82nm or 1.82×10^{-9}m)

$\Delta F^{adh.}_{ikj.iki.jkj} \Rightarrow$ Change in free energy of adhesion between any one, two or both particles of ii, jj with the liquid medium, kk in between.

3.16 Statistical Analysis of Variance (ANOVA)

The combined Hamaker coefficient values being mean of the samples were compared using the two-way ANOVA at 0.05 level of significance.

Table 3.1: Expected summary for ANOVA results

Hamaker parameter variable	Control: D0	D1	D2	D3	D4	D5	$LSD_{0.05}$
A_{132} HIV+	$^{+}_{-}\mathbf{a}^{x}_{y}$	$^{+}_{-}\mathbf{b}^{x}_{y}$	$^{+}_{-}\mathbf{c}^{x}_{y}$	$^{+}_{-}\mathbf{d}^{x}_{y}$	$^{+}_{-}\mathbf{e}^{x}_{y}$	$^{+}_{-}\mathbf{f}^{x}_{y}$	-
A_{131} HIV-	$^{+}_{-}\mathbf{g}^{x}_{y}$	$^{+}_{-}\mathbf{h}^{x}_{y}$	$^{+}_{-}\mathbf{i}^{x}_{y}$	$^{+}_{-}\mathbf{j}^{x}_{y}$	$^{+}_{-}\mathbf{k}^{x}_{y}$	$^{+}_{-}\mathbf{l}^{x}_{y}$	-
A_{232} HIV+	$^{+}_{-}\mathbf{m}^{x}_{y}$	$^{+}_{-}\mathbf{n}^{x}_{y}$	$^{+}_{-}\mathbf{o}^{x}_{y}$	$^{+}_{-}\mathbf{p}^{x}_{y}$	$^{+}_{-}\mathbf{q}^{x}_{y}$	$^{+}_{-}\mathbf{r}^{x}_{y}$	-
$LSD_{0.05}$	-	-	-	-	-	-	

Where:

- $^{+}_{-}\mathbf{a-r}$ would indicate the combined Hamaker coefficients of A_{132}, A_{131} and A_{232}
- Superscript (x) would indicate significant difference among **Parameters** at 5% Level of Significance (i.e., Prob. Value, $P < 0.05$ significant value).
- Subscript (y) would indicate significant difference among **Levels** at 5% level of significance (i.e., Prob. Value, $P < 0.05$ significant value).
- Least Significant Difference at 5% level of significance is the calculated Standard Error multiplied by 1.96 constant factor
- Standard error is as calculated on the Multiple Comparisons tables (see Tables U1 to U9 of appendix U)

- 1.96 is for a degree of freedom (df, within groups, being greater than 30. See ANOVA Tables U1 to U9 of appendix U). Columns 2, 3, 4, 5, 6, 7 are the parameter levels = 6.

D0 $\Rightarrow$ Without drug

D1 $\Rightarrow$ With drug 1

D2 $\Rightarrow$ With drug 2

D3 $\Rightarrow$ With drug 3

D4 $\Rightarrow$ With drug 4

D5 $\Rightarrow$ With drug 5

CHAPTER FOUR
RESULTS AND DISCUSSION

4.1 Obtained Experimental Results

From the very first results that were collated (CD4+ count measurements with digital Cytoflowmetre), which were indications of the levels of healthiness of the persons, the light absorbance (ā) capacities, which are dimensionless quantities or described in terms of Absorbance Units (AU), of all blood samples which were measured with digital MetaSpecAE1405031*Pro* Spectrophotometer, over wavelengths (λ) as measured in nanometres (nm) ranging between 200 nm and1000 nm, all obtained values were used in relevant thermodynamic models to compute results.

4.1.1 CD4+ Counts of Uninfected and Infected blood samples used for experiments.

Table 4.1: CD4+ cells count of different blood samples collected

Blood sample Number #	HIV Negative Blood Samples. CD4 cells/mm^3	HIV Positive Blood Samples CD4 cells/mm^3
1	679	956
2	772	263
3	1880	376
4	1407	373
5	1502	32
6	834	790
7	1263	676
8	1371	930
9	1568	229
10	1029	439

NB: the CD4+ count for an average normal/healthy adult without HIV infection is between 460 to 1600cells/mm^3.

4.1.2 Drug samples in sterile water

Table 4.2: Summary of Peak absorbance (ā) values of drugs and corresponding Peak wavelength (λ) values of different antiviral drugs used in different milliliters of sterile H_2O.

Drug Abbrevs.		Peak ā and Peak λ for different drugs in different milliliters of sterile H_2O					Avg. values of
		1 ml	2 mls	3 mls	4 mls	5 mls	â and λ
D1	Ā	1.482	0.354	0.184	1.523	0.253	0.759
	Λ	330	320	320	320	320	322
D2	Ā	0.543	0.745	0.186	2.154	0.253	0.776
	Λ	320	320	320	320	320	320
D3	Ā	0.453	0.453	1.754	1.562	0.552	0.955
	Λ	320	320	320	350	320	326
D4	Ā	0.401	0.345	0.643	1.254	0.558	0.64
	Λ	320	440	320	320	320	344
D5	Ā	0.425	0.354	0.953	1.522	0.454	0.742
	Λ	440	320	320	320	320	344

Table 4.2 summarily shows the average peak absorbance, ā values of the antiviral drugs in water ranging from 0.6402AU to 0.9548AU and their corresponding wavelengths, λ between 320 and 344nm. These fell within the visible range of the UV radiation which is 300-600 nm. From the table, all the herbal drugs D3, D2 and D1 appeared to have the highest absorbance values between 322-326 nm. But at a higher wavelength, 344nm, D5 and D4 have lower absorbance in comparison. These are sure implications in drugs' efficacy as would be read later.

4.1.3 Experimental values of Absorbance for $Drugs_{1\text{-}5}$ samples in sterile water.

The experimental data of absorbance for the five (5) drug samples in 5 different mls of sterile water used in experiments, are seen on Tables A1-A5 of appendix A.

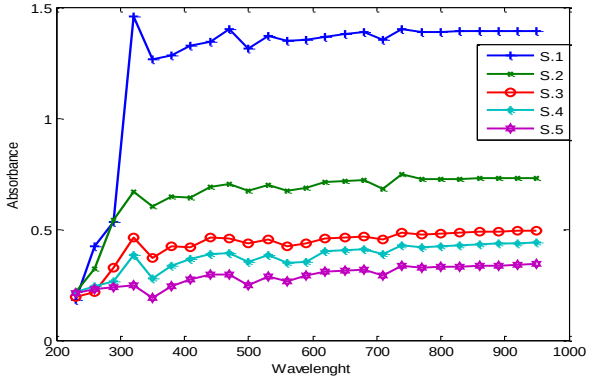

Fig.4.1: S1-S5 (D1-D5) in 1ml conc. of sterile water

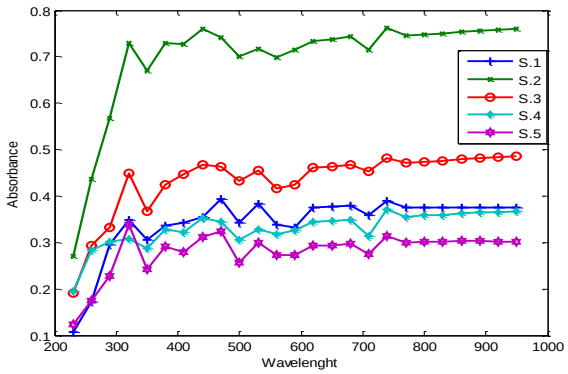

Fig.4.2: S1-S5 (D1-D5) in 2mls conc. of sterile water

In a higher concentration, a particular sample with a higher absorbance at any given wavelength, equally indicates a better resistance property in comparison to all other samples at the same wavelength. Therefore, within the visible range of the UV radiation, that is 300 – 600nm, samples with higher values of absorbance indicate their levels of resistance to radiation which shows how well they would resist penetration by radiations from other particles in their natural state of surface free energies.

Figures 4.1– 4.5 show the natural pattern for the experimental drug samples (antiviral herbal extract drugs samples S1, S2 and S3 with known antiretroviral drug samples S4 and S5) in 1ml – 5mls different concentrations of sterile water. All drug samples appear to peak at 320nm between 0.2AU and 1. 45AU absorbance values. Increase in wavelengths showed gradual stabilization of absorbance and then a constant absorbance between 800 – 950nm and this is well outside the visible range of radiation.

Figure 4.2 shows the natural pattern for the antiviral herbal extract drugs samples S1, S2 and S3 with known antiretroviral drug samples S4 and S5 in 2ml concentration of sterile water.
All drug samples appeared to peak at 320nm with absorbance values between 0.1AU and 0.76AU. Increase in wavelengths showed constant absorbance between 800 – 950nm.

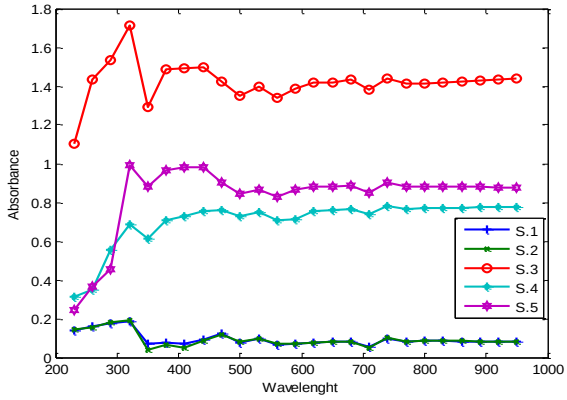

Fig.4.3: S1-S5 (D1-D5) in 3mls conc. of sterile water

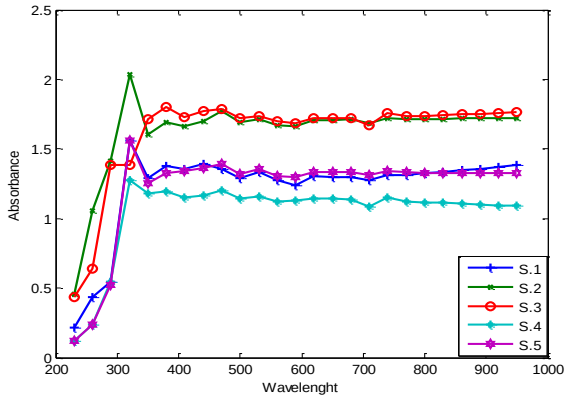

Fig.4.4: S1-S5 (D1-D5) in 4mls conc. of sterile water

Figure 4.3 shows the natural pattern for the antiviral herbal extract drugs samples S1, S2 and S3 with known antiretroviral drug samples S4 and S5 in 3ml concentration of water. The figure equally shows the natural pattern for the antiviral herbal extract drugs samples S1, S2 and S3 with known antiretroviral drug samples S4 and S5 in 3ml concentration of sterile water. All drug samples appear to peak at 320nm with absorbance values between 0.2AU and 1.7AU. Increase in wavelengths showed constant absorbance between 800 – 950nm.

Figure 4.4 shows the natural pattern for the antiviral herbal extract drugs samples S1, S2 and S3 with known antiretroviral drug samples S4 and S5 in 4ml concentration of water. Also, the natural pattern for the antiviral herbal extract drugs samples S1, S2 and S3 with known antiretroviral drug samples S4 and S5 in 4ml concentration of sterile water are shown. All drug samples appear to peak at 320nm with absorbance values between 0.2AU and 2.0AU. Increase in wavelengths showed constant absorbance between 800 – 950nm.

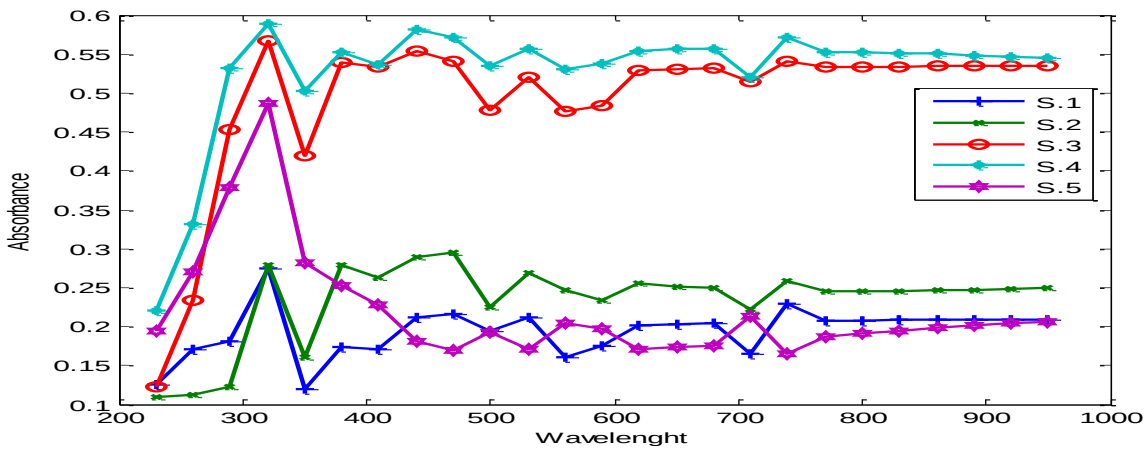

Fig.4.5: S1-S5 (D1-D5) in 5mls conc. of sterile water

Figure 4.5 shows the natural pattern for the antiviral herbal extract drugs samples S1, S2 and S3 with known antiretroviral drug samples S4 and S5 in 5ml concentration of water. The figure also shows the natural pattern for the antiviral herbal extract drugs samples S1, S2 and S3 with known antiretroviral drug samples S4 and S5 in 5ml concentration of sterile water. All drug samples appear to peak at 320nm with absorbance values between 0.2AU and 0.58AU. Increase in wavelengths showed constant absorbance between 800 – 950nm.

4.1.4 Infected Components$_{1\text{-}4}$ of Blood samples$_{1\text{-}10}$ with drugs$_{1\text{-}5}$

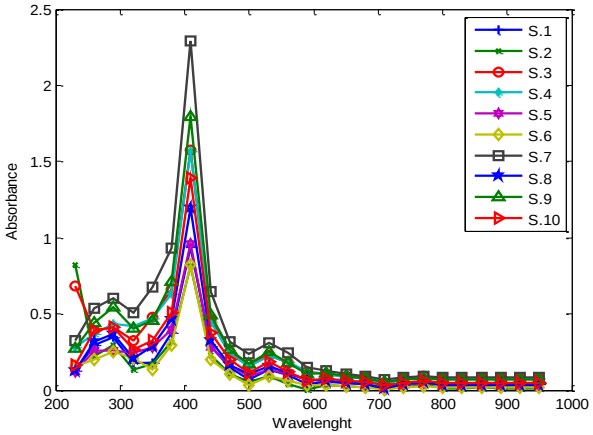

Fig.4.6: Absorbance, ā values versus Wavelength, λ values of infected SERUM blood samples (with drug 1).

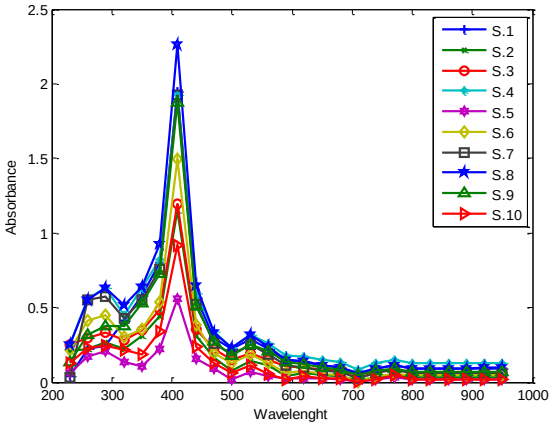

Fig.4.7: Absorbance, ā values versus Wavelength, λ values of infected WHITE blood samples (with drug 1).

Similarly, like the explanation under sub-sub-section 4.1.3, blood-drug interactions (for infected samples) which have been exposed to UV radiation test, show rise, peak and fall characteristics. As such, any blood sample with any particular drug, at any given wavelength, offers a quantifiable value of absorbance. The blood sample if infected with a certain virus like HIV, and is treated with a drug, will naturally offer resistance to the natural surface free energy of the invading virus. These degrees of absorbance are as shown in figures 4.6 – 4.25.

It then follows that, the higher the absorbance of any blood sample with any drug, the better the resistance of such components. It equally follows that, if a drug with a higher absorbance /resistance is used to treat a virus, the absorbance-wavelength plot would be like depicted herein (Ani, 2015). This probably indicates the level of resistance involved. So, within the visible UV radiation, the difference between the absorbance values of the blood-drug interaction and, the absorbance values of the drugs alone, gives the value for the level of

resistance of the blood-drug treated samples. The higher-absorbance better-resistance quantities are levels of potency or efficacy for different blood samples with different drugs at the same wavelength or constant intensity of UV visible radiation.

With drug 1 in figure 4.6, all infected serum blood samples with drug 1 appear to peak at 400nm with absorbance values between 0.2 and 2.30AU. Increase in wavelengths showed constant absorbance between 800 – 950nm.

In figure 4.8, all infected red blood samples with drug 1 appear to peak at 400nm with absorbance values between 0.2 and 2.30AU. Increase in wavelengths showed constant absorbance between 800 – 950nm.

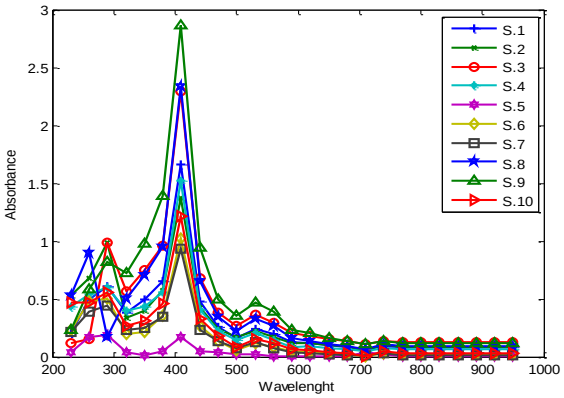

Fig.4.8: Absorbance, ā values versus Wavelength, λ values of infected RED blood samples (with drug 1).

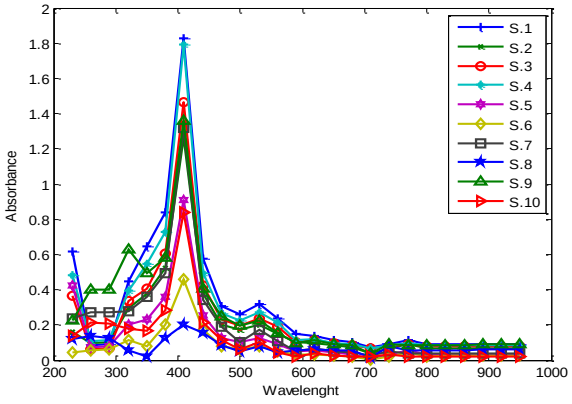

Fig.4.9: Absorbance, ā values versus Wavelength, λ values of infected WHOLE blood samples (with drug 1).

In figure 4.9, all infected whole blood samples with drug 1 appear to peak at 400nm with absorbance values between 0.02 and 2.80AU. Increase in wavelengths showed constant absorbance between 760 – 950nm.

In figure 4.10, all infected serum blood samples with drug 1 appear to peak at 400nm with absorbance values between 0.02 and 1.82AU. Increase in wavelengths showed constant absorbance between 770 – 950nm.

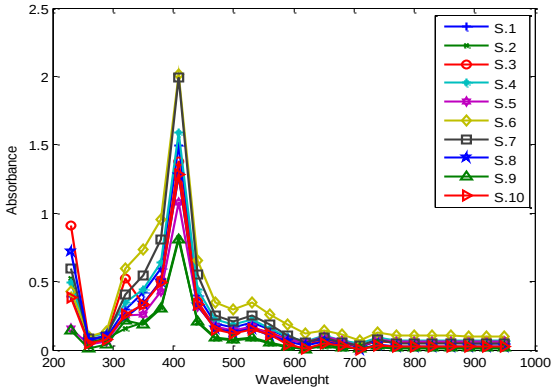

Fig.4.10: Absorbance, ā values versus Wavelength, λ values of infected SERUM blood samples (with drug 2).

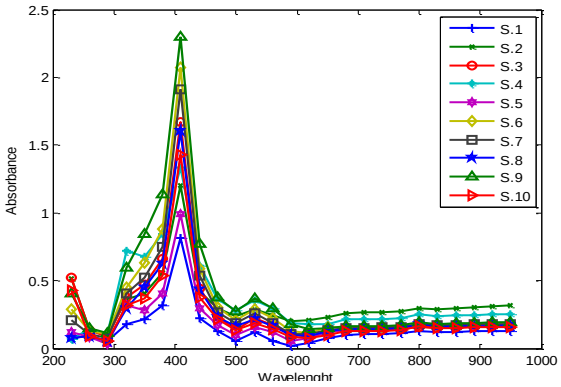

Fig.4.11: Absorbance, ā values versus Wavelength, λ values of infected WHITE blood samples (with drug 2).

With drug 2, in figure 4.10, all infected serum blood samples with drug 2 appear to peak at 400nm with absorbance values between 0.02 and 2.00AU. Increase in wavelengths showed constant absorbance between 740 – 950nm.

In figure 4.11, all infected white blood samples with drug 2 appear to peak at 400nm, with absorbance values between 0.02 and 2.42AU. Increase in wavelengths showed constant absorbance between 830 – 950nm.

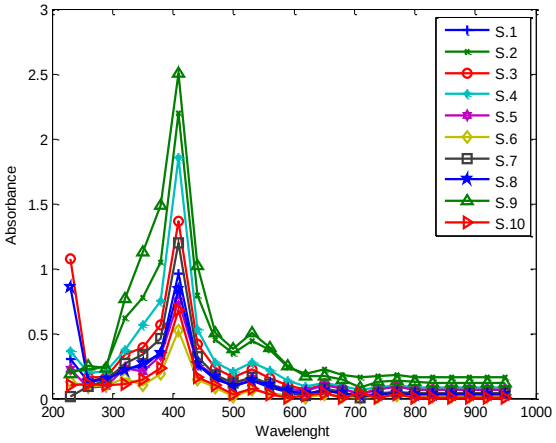

Fig.4.12: Absorbance, ā values versus Wavelength, λ values of infected RED blood samples (with drug 2).

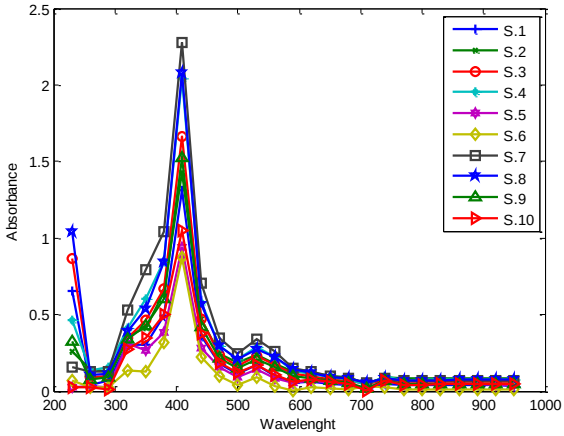

Fig.4.13: Absorbance, ā values versus Wavelength, λ values of infected WHOLE blood samples (with drug 2).

In figure 4.12, all infected red blood samples with drug 2 appear to peak at 400nm with absorbance values between 0.01 and 2.52AU. Increase in wavelengths showed constant absorbance between 800 – 950nm.

In figure 4.13, all infected whole blood samples with drug 2 appear to peak at 400nm with absorbance values between 0.01 and 2.31AU. Increase in wavelengths showed constant absorbance between 770 – 950nm.

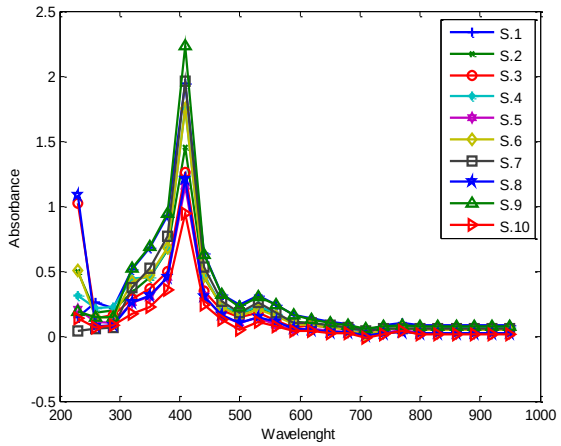

Fig.4.14: Absorbance, ā values versus Wavelength, λ values of infected SERUM blood samples (with drug 3).

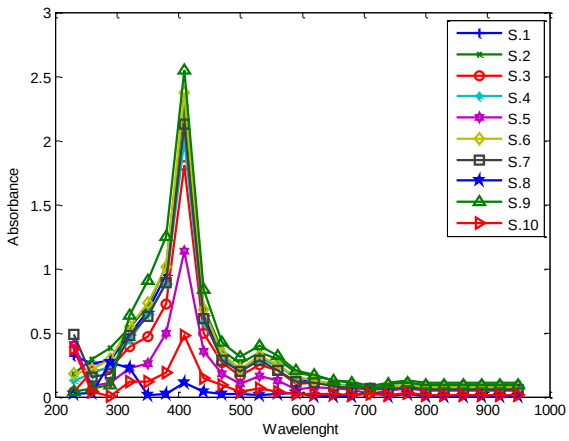

Fig.4.15: Absorbance, ā values versus Wavelength, λ values of infected WHITE blood samples (with drug 3).

With drug 3 in figure 4.14, all infected serum blood samples with drug 3 appear to peak at 400nm with absorbance values between 0.05 and 2.31AU. Increase in wavelengths showed constant absorbance between 800 – 950nm.

In figure 4.15, all infected white blood samples with drug 3 appear to peak at 400nm with absorbance values between 0.01 and 2.61Å. Increase in wavelengths showed constant absorbance between 800 – 950nm.

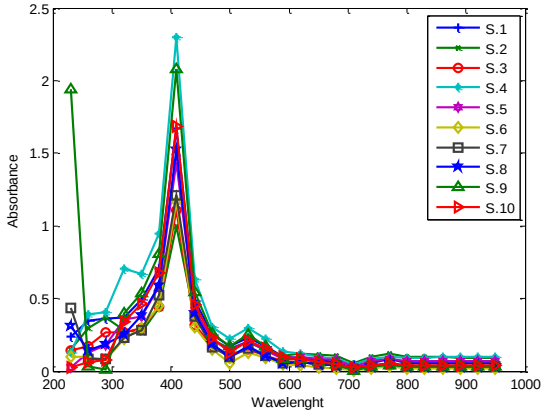

Fig.4.16: Absorbance, ā values versus Wavelength, λ values of infected RED blood samples (with drug 3).

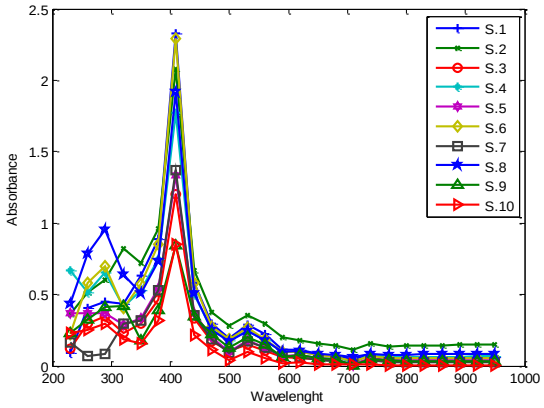

Fig.4.17: Absorbance, ā values versus Wavelength, λ values of infected WHOLE blood samples (with drug 3).

In figure 4.16, all infected red blood samples with drug 3 appear to peak at 400nm with absorbance values between 0.01 and 2.31AU. Increase in wavelengths showed constant absorbance between 800 – 950nm.

In figure 4.17, all infected whole blood samples with drug 3 appear to peak at 400nm with absorbance values between 0.1 and 2.31AU. Increase in wavelengths showed constant absorbance between 770 – 950nm.

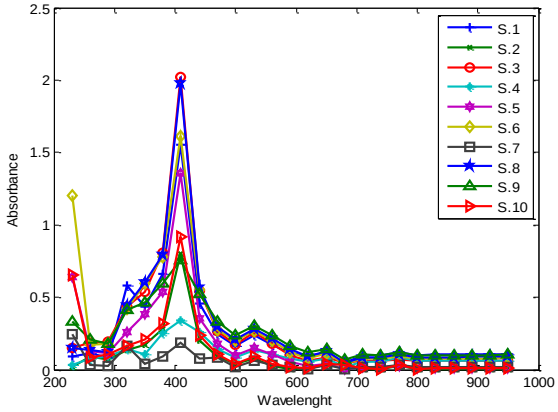

Fig.4.18: Absorbance, ā values versus Wavelength, λ values of infected SERUM blood samples (with drug 4).

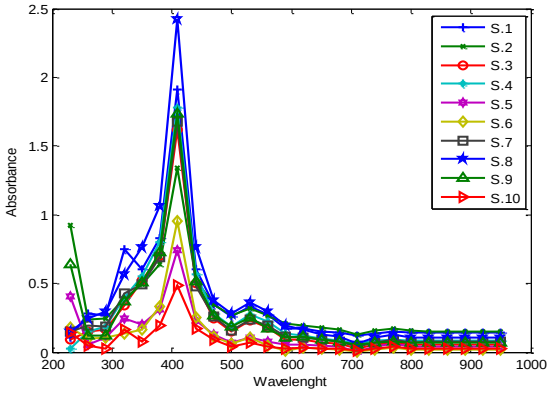

Fig.4.19: Absorbance, ā values versus Wavelength, λ values of infected WHITE blood samples (with drug 4).

With drug 4 in figure 4.18, all infected serum blood samples with drug 4 appear to peak at 400nm with absorbance values between 0.01 and 2.00AU. Increase in wavelengths showed constant absorbance between 800 – 950nm.

In figure 4.19, all infected white blood samples with drug 4 appear to peak at 400nm with absorbance values between 0.01 and 2.40AU. Increase in wavelengths showed constant absorbance between 800 – 950nm.

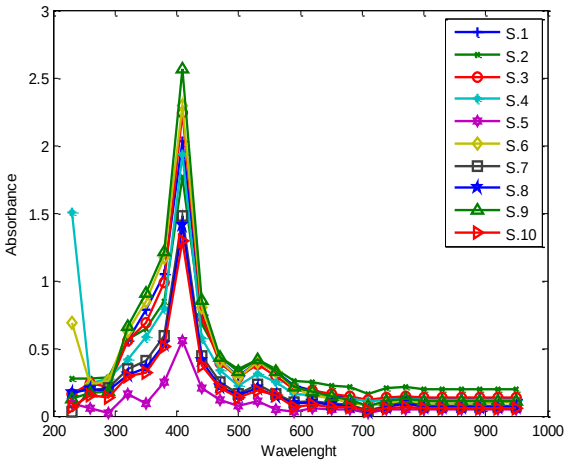

Fig.4.20: Absorbance, ā values versus Wavelength, λ values of infected RED blood samples (with drug 4).

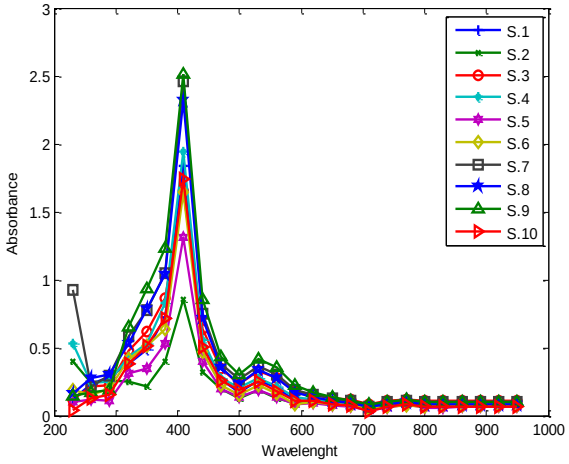

Fig.4.21: Absorbance, ā values versus Wavelength, λ values of infected WHOLE blood samples (with drug 4).

In figure 4.20, all infected red blood samples with drug 4 appear to peak at 400nm with absorbance values between 0.01 and 2.62AU. Increase in wavelengths showed constant absorbance between 730 – 950nm.

In figure 4.21, all infected whole blood samples with drug 4 appear to peak at 400nm with absorbance values between 0.1 and 2.5AU. Increase in wavelengths showed constant absorbance between 800 – 950nm.

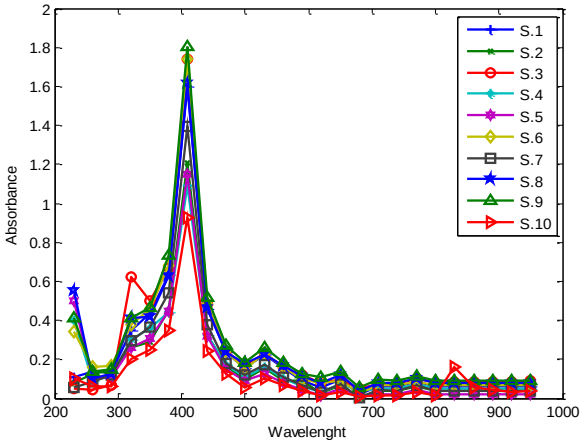

Fig.4.22: Absorbance, ā values versus Wavelength, λ values of infected SERUM blood samples (with drug 5).

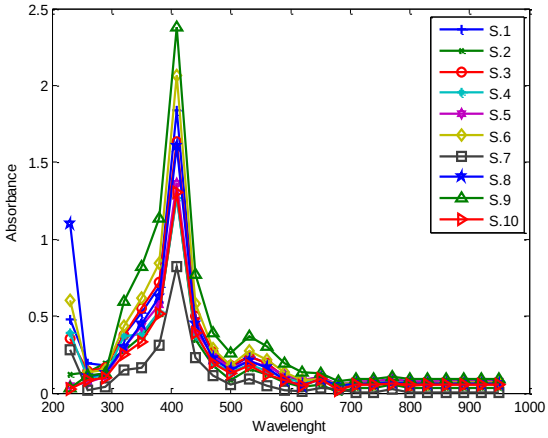

Fig.4.23: Absorbance, ā values versus Wavelength, λ values of infected WHITE blood samples (with drug 5).

With drug 5 in figure 4.22, all infected serum blood samples with drug 5 appear to peak at 400nm with absorbance values between 0.02 and 1.82AU. Increase in wavelengths showed constant absorbance between 800 – 950nm.

In figure 4.23, all infected white blood samples with drug 5 appear to peak at 400nm with absorbance values between 0.01 and 2.40AU. Increase in wavelengths showed constant absorbance between 700 – 950nm.

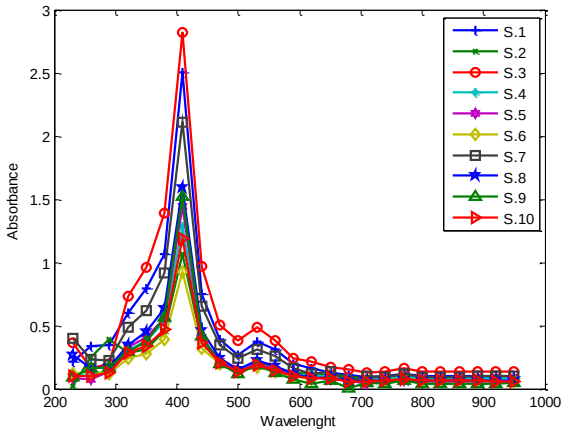

Fig.4.24: Absorbance, ā values versus Wavelength, λ values of infected RED blood samples (with drug 5).

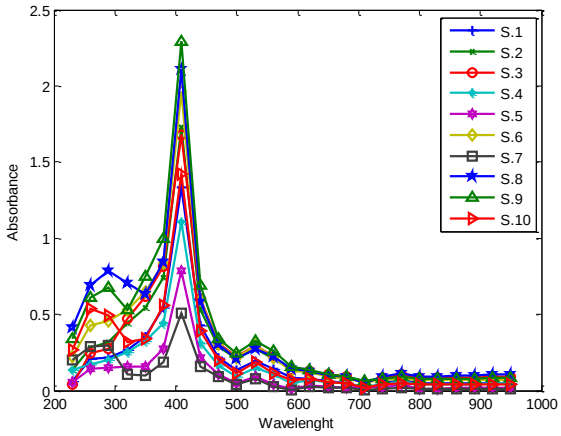

Fig.4.25: Absorbance, ā values versus Wavelength, λ values of infected WHOLE blood samples (with drug 5).

In figure 4.24, all infected red blood samples with drug 5 appear to peak at 400nm with absorbance values between 0.25 and 2.81AU. Increase in wavelengths showed constant absorbance between 700 – 950nm.

In figure 4.25, all infected whole blood samples with drug 5 appear to peak at 400nm with absorbance values between 0.1 and 2.31AU. Increase in wavelengths showed constant absorbance between 770 – 950nm.

Table 4.3: Avg. Peak ā values of drugs and corresponding avg. Peak λ values of different antiviral drugs$_{1-5}$ interacted with different blood components$_{1-4}$ of HIV+ as depicted in the plots above.

Blood Component		Avg. Peak ā values of drugs$_{1-5}$ and corresponding avg. Peak λ values HIV Positive blood components$_{1-4}$ interacted with different Drug$_{1-5}$ samples				
		D1	D2	D3	D4	D5
Serum	ā	2.5000	2.0000	2.3100	2.0000	1.8200
	λ	400	400	400	400	400
White	ā	2.3000	2.4200	2.6100	2.400	2.400
	λ	400	400	400	400	400
Red	ā	2.8000	2.5200	2.3100	2.6200	2.8100
	λ	400	400	400	400	400
Whole	ā	1.8200	2.3100	2.3100	2.500	2.1300
	λ	400	400	400	400	400

Table 4.3: shows average Peak (Max.) ā values of drugs$_{1-5}$ and corresponding average Peak (Max.) λ values of different antiviral drugs interacted with different blood components$_{1-4}$ of HIV+. The average peak absorbance values of different antiviral drugs interacted with different blood components of HIV+ ranged from 1.82 to 2.81AU at a constant 400nm. These fell within the visible range of the UV radiation which is 300-600nm. The serum samples which the virus has to penetrate before getting at the white blood cells, offers appreciable levels of absorbance. The white blood cells likewise attest to the degree of potency of the various drugs by their close values with those of the serum.

4.1.5 Uninfected Components$_{1-4}$ of Blood samples$_{1-10}$ with drugs$_{1-5}$

Again, in relation to the idea for the explanation given under sub-sub-section 4.1.4, the blood-drug interactions (for uninfected blood samples) which have been also exposed to UV radiation test, all depict rise, peak, fall and stable criteria except for all plots that show sharp fall first. This graphical line is most probably due to slight inherent machine error before sample reading. All the same, every biomaterial has its associated surface free energy. But in interaction with another biomaterial, their surface free energies are influenced to encourage either attraction or repulsion that, if its numerical value is negative, implies repulsion but if positive implies attraction for any two and three bio particles.

In fact, the two values of 'blood-drug' and 'drug' with uninfected and infected blood samples would mathematically subtract to give a close prediction for what is in the blood samples as there is yet to be revealed, a functional mechanism of isolating a virus particle like HIV. As earlier stated, any treatment with a drug naturally offers a given degree of absorbance. These for the uninfected blood components with drugs are as shown on figures 4.26 – 4.45.

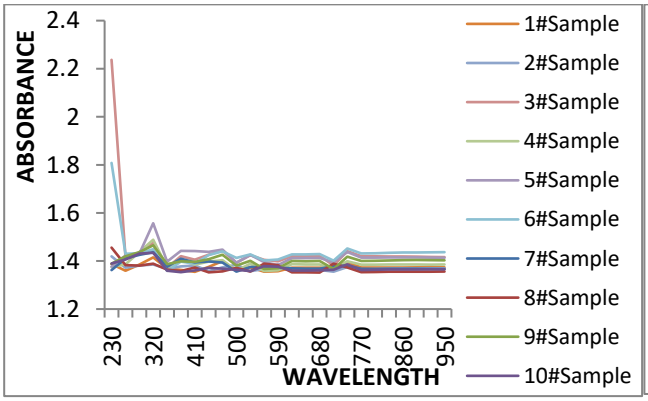

Fig. 4.26: Absorbance Vs Wavelength of Uninfected SERUM$_{1-10}$ with D1.

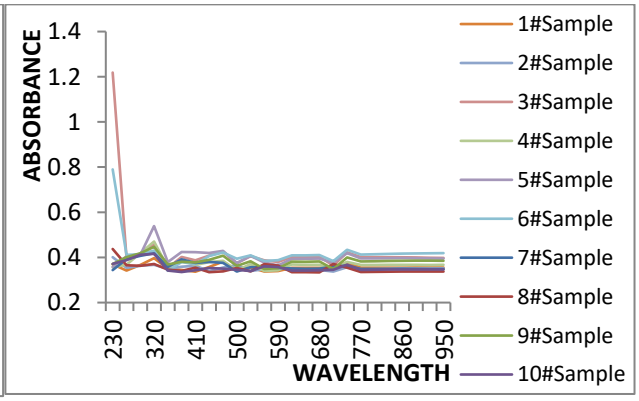

Fig.4.27: Absorbance Vs Wavelength for Uninfected SERUM$_{1-10}$ with D2.

On serum blood component, in figure 4.26, all with drug 1 appear to peak at 300nm with absorbance values between 1.4 and 1.6AU. Increase in wavelengths showed constant absorbance between 740 – 950nm.

In figure 4.27, all uninfected serum blood samples with drug 2 appear to peak at 300nm with absorbance values between 0.35 and 0.55AU. Increase in wavelengths showed constant absorbance between 740 – 950nm.

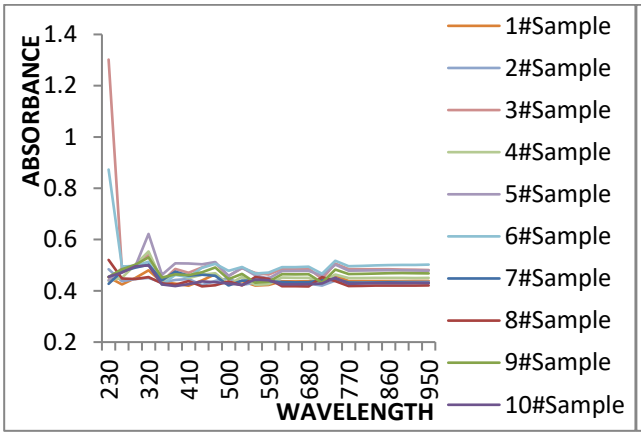

Fig.4.28: Absorbance Vs Wavelength for Uninfected SERUM$_{1\text{-}10}$ with D3.

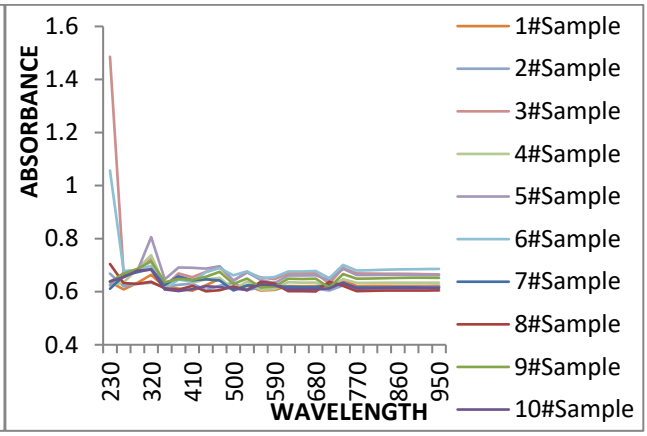

Fig.4.29: Absorbance Vs Wavelength for Uninfected SERUM$_{1\text{-}10}$ with D4.

In figure 4.28, all uninfected serum blood samples with drug 3 appear to peak at 300nm with absorbance values between 0.4 and 0.62AU. Increase in wavelengths showed constant absorbance between 750 – 950nm.

In figure 4.29, all uninfected serum blood samples with drug 4 appear to peak at 300nm with absorbance values between 0.6 and 0.8AU. Increase in wavelengths showed constant absorbance between 750 – 950nm.

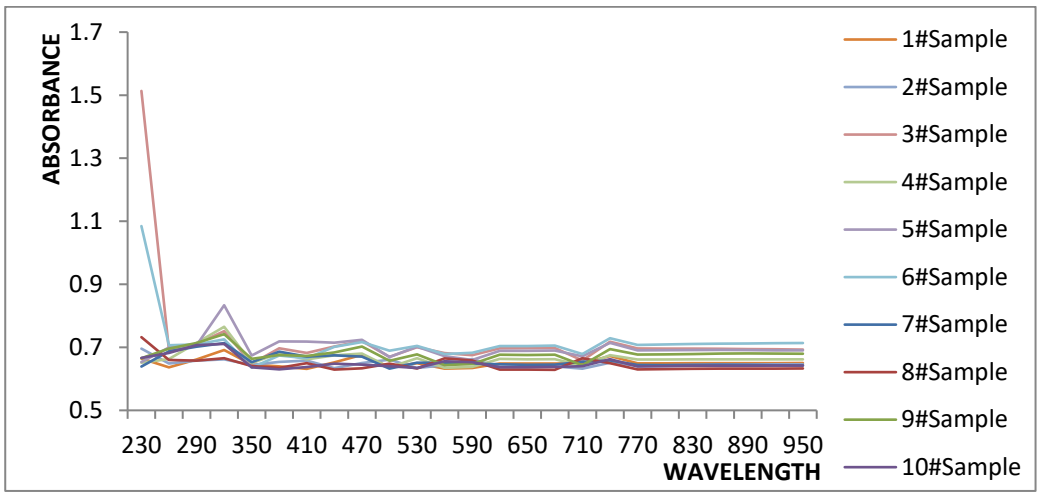

Fig.4.30: Absorbance Vs Wavelength for Uninfected SERUM$_{1\text{-}10}$ with D5.

In figure 4.30, all uninfected serum blood samples with drug 5 appear to peak at 300nm with absorbance values between 0.62 and 0.82AU. Increase in wavelengths showed constant

absorbance between 750 – 950nm. The similarity in the pattern of the curves and the differences in peak â and λ, appear to be due to differences in blood composition.

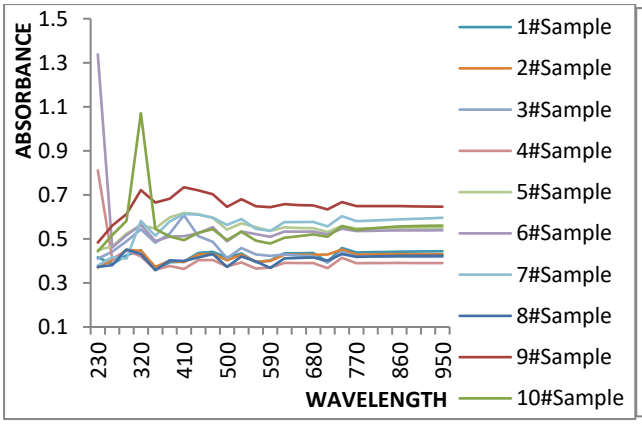

Fig.4.31: Absorbance Vs Wavelength of Uninfected WHITE$_{1\text{-}10}$ with D1.

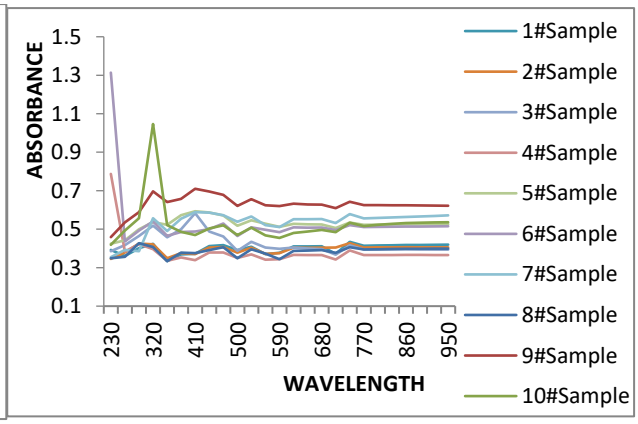

Fig.4.32: Absorbance Vs Wavelength of Uninfected WHITE$_{1\text{-}10}$ with D2.

On white blood component, in figure 4.31, all with drug 1 appear to peak at 300nm with absorbance values between 0.38 and 1.05AU. Increase in wavelengths showed constant absorbance between 750 – 950nm.

In figure 4.32, all uninfected white blood samples with drug 2 appear to peak at 300nm with absorbance values between 0.33 and 1.02AU. Increase in wavelengths showed constant absorbance between 750 – 950nm.

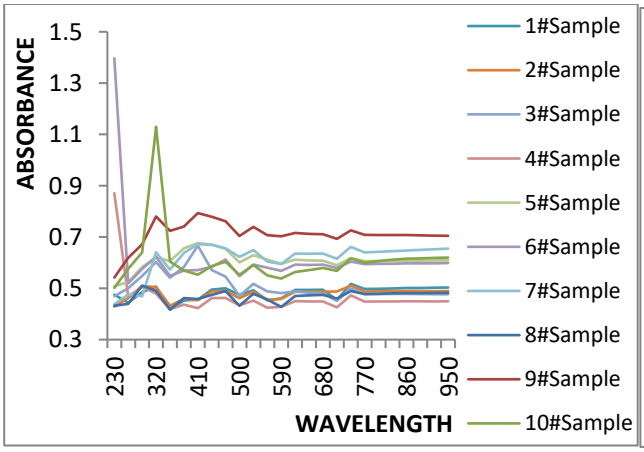

Fig.4.33: Absorbance Vs Wavelength of Uninfected WHITE$_{1\text{-}10}$ with D3.

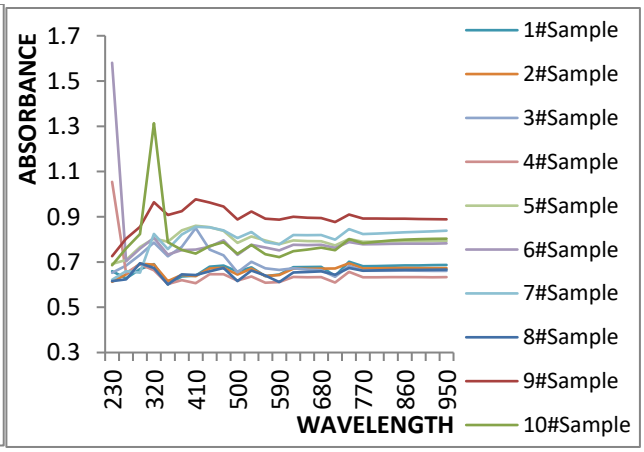

Fig.4.34: Absorbance Vs Wavelength of Uninfected WHITE$_{1\text{-}10}$ with D4.

In figure 4.33, all uninfected white blood samples with drug 3 appear to peak at 300nm with absorbance values between 0.41 and 1.1AU. Increase in wavelengths showed constant absorbance between 750 - 950Å.

In figure 4.34, all uninfected white blood samples with drug 4 appear to peak at 300nm with absorbance values between 0.61 and 1.3AU. Increase in wavelengths showed constant absorbance between 750 – 950nm.

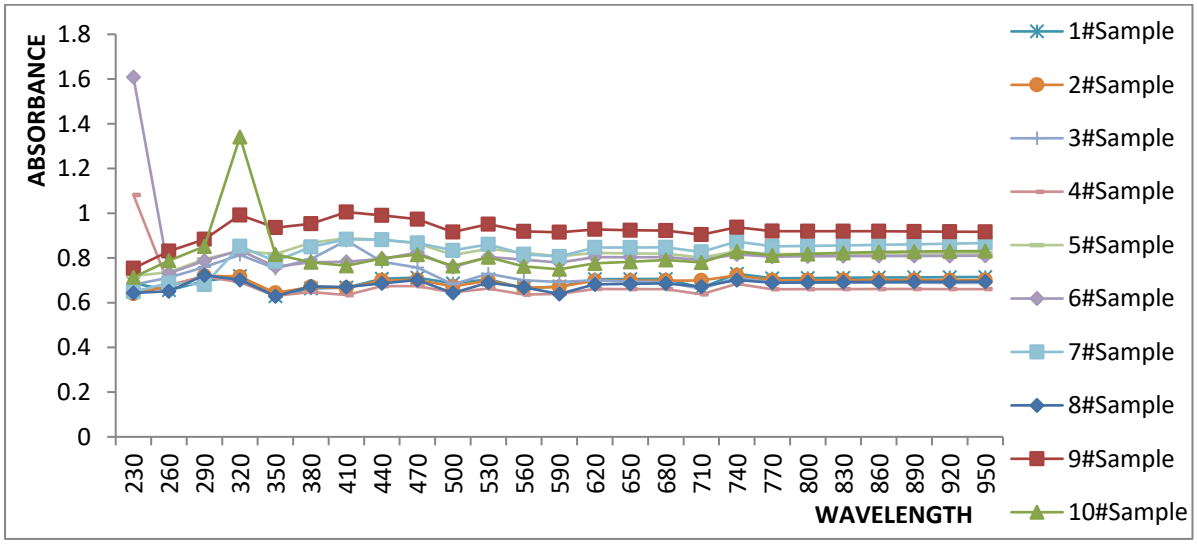

Fig.4.35: Absorbance Vs Wavelength of Uninfected WHITE$_{1\text{-}10}$ with D5.

In figure 4.35, all uninfected white blood samples with drug 5 appear to peak at 300nm with absorbance values between 0.62 and 1.32AU. Increase in wavelengths showed constant absorbance between 750 – 950nm.

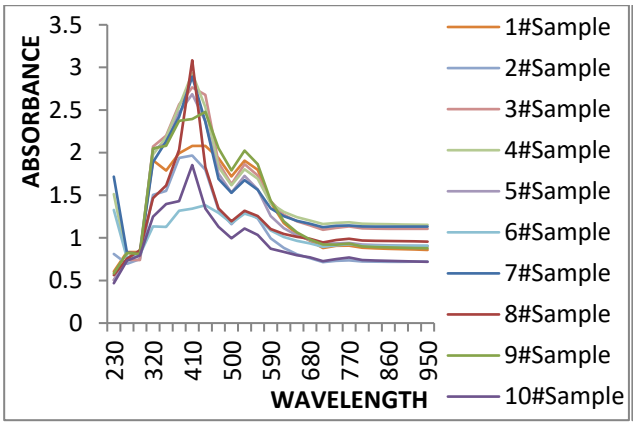

Fig.4.36: Absorbance Vs Wavelength of Uninfected RED$_{1\text{-}10}$ with D1.

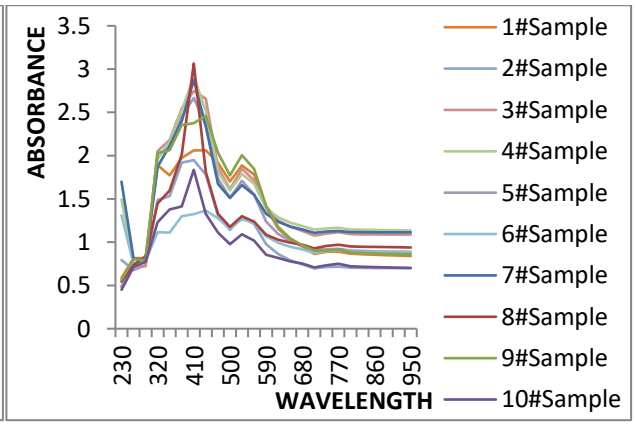

Fig.4.37: Absorbance Vs Wavelength of Uninfected RED$_{1\text{-}10}$ with D2.

On the red blood component, in figure 4.36 above, all with drug 1 appear to peak at 390nm with absorbance values between 0.7 and 3.1AU. Increase in wavelengths showed constant absorbance between 800 – 950nm.

In figure 4.37, all uninfected red blood samples with drug 2 appear to peak at 400nm with absorbance values between 0.45 and 3.1AU. Increase in wavelengths showed constant absorbance between 800 – 950nm.

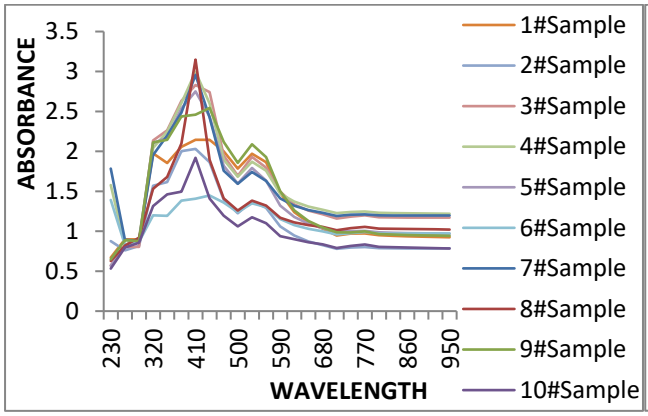

Fig.4.38: Absorbance Vs Wavelength of Uninfected RED$_{1\text{-}10}$ with D3.

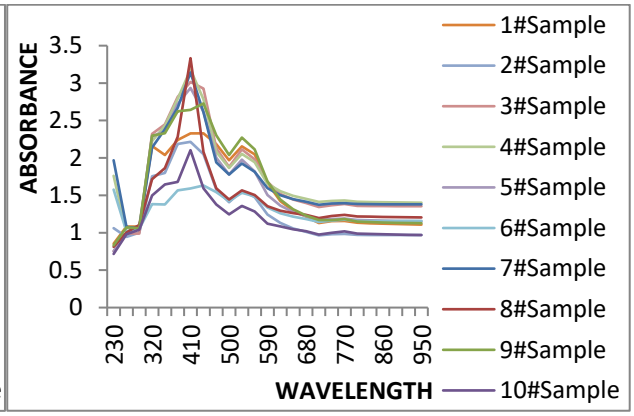

Fig.4.39: Absorbance Vs Wavelength of Uninfected RED$_{1\text{-}10}$ with D4.

In figure 4.38, all uninfected red blood samples with drug 3 appear to peak at 400nm with absorbance values between 0.51 and 3.2AU. Increase in wavelengths showed constant absorbance between 800 – 950nm.

In figure 4.39, all uninfected red blood samples with drug 4 appear to peak at 400nm with absorbance values between 0.7 and 3.4AU. Increase in wavelengths showed constant absorbance between 800 – 950nm.

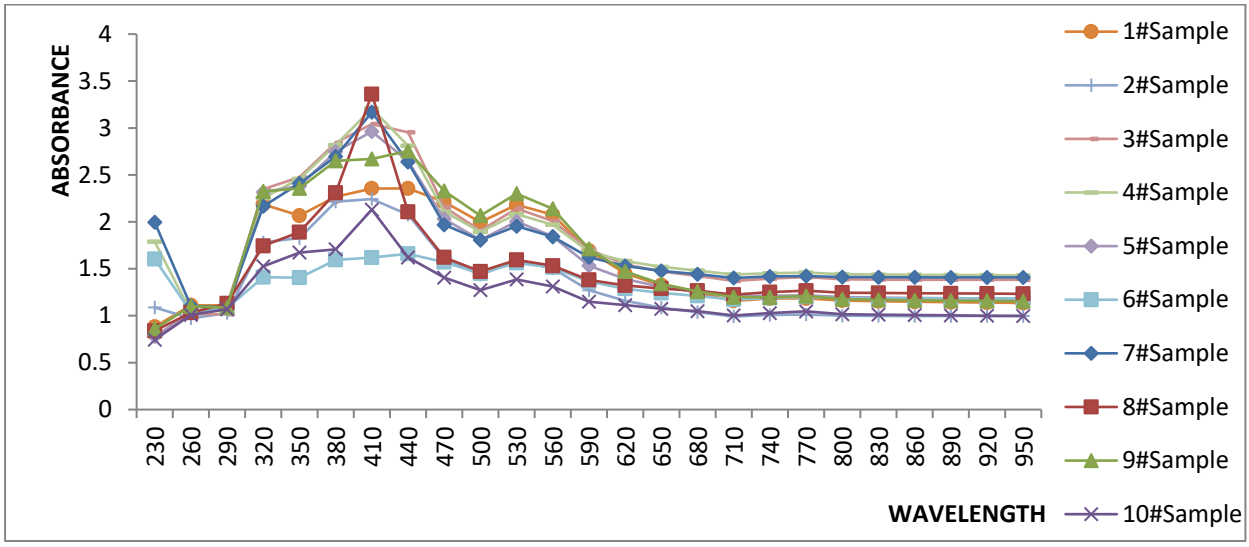

Fig.4.40: Absorbance Vs Wavelength of Uninfected $RED_{1\text{-}10}$ with D5.

In figure 4.40, all uninfected red blood samples with drug 5 appear to peak at 400nm with absorbance values between 0.7 and 3.35AU. Increase in wavelengths showed constant absorbance between 800 – 950nm.

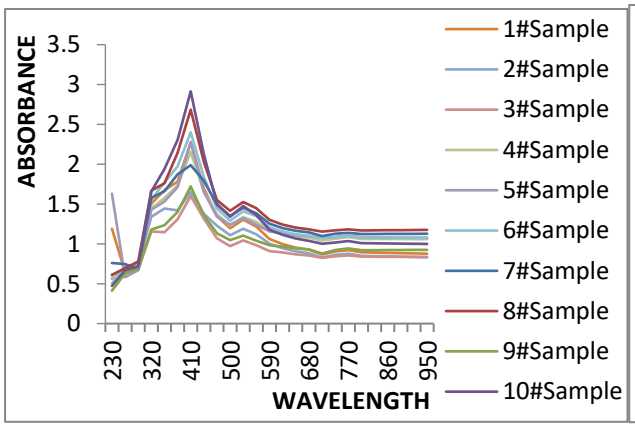

Fig.4.41: Absorbance Vs Wavelength of Uninfected $WHOLE_{1\text{-}10}$ with D1.

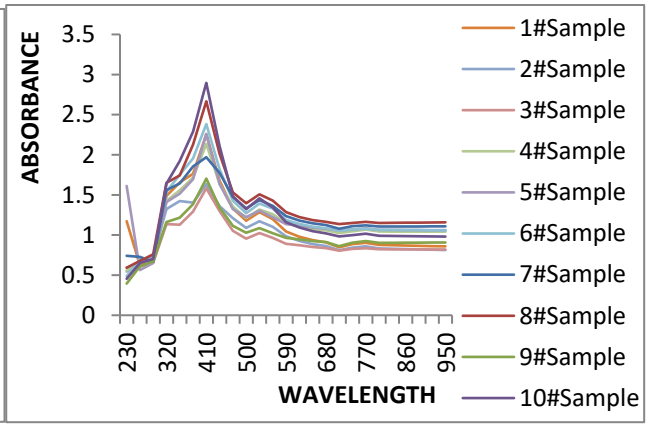

Fig.4.42: Absorbance Vs Wavelength of Uninfected $WHOLE_{1\text{-}10}$ with D2.

On whole blood component mixture, in figure 4.41, all with drug 1 appear to peak at 400nm with absorbance values between 1.05 and 2.9AU. Increase in wavelengths showed constant absorbance between 800 – 950nm.

In figure 4.42, all uninfected whole blood samples with drug 2 appear to peak at 400nm with absorbance values between 1.04 and 2.9nm. Increase in wavelengths showed constant absorbance between 800 – 950AU.

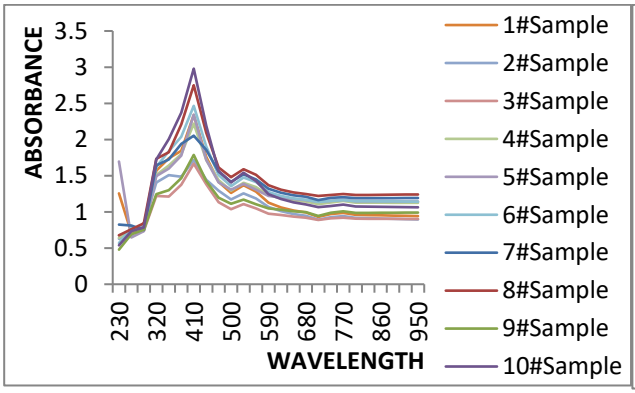

Fig.4.43: Absorbance Vs Wavelength of Uninfected WHOLE$_{1\text{-}10}$ with D3.

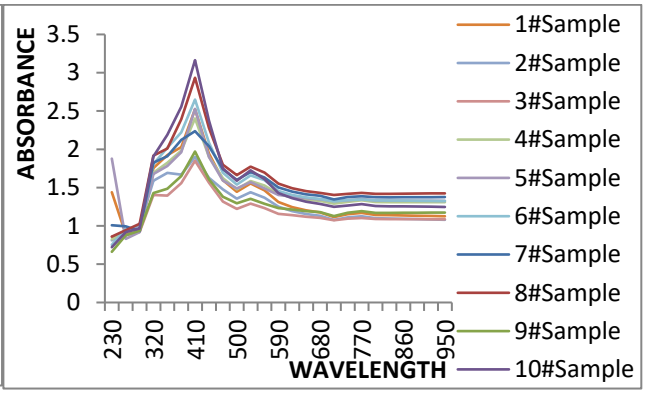

Fig.4.44: Absorbance Vs Wavelength of Uninfected WHOLE$_{1\text{-}10}$ with D4.

In figure 4.43, all uninfected whole blood samples with drug 3 appear to peak at 400nm with absorbance values between 0.4 and 2.95AU. Increase in wavelengths showed constant absorbance between 800 – 950nm.

In figure 4.44, all uninfected whole blood samples with drug 4 appear to peak at 400nm with absorbance values between 0.7 and 3.2AU. Increase in wavelengths showed constant absorbance between 800 – 950nm.

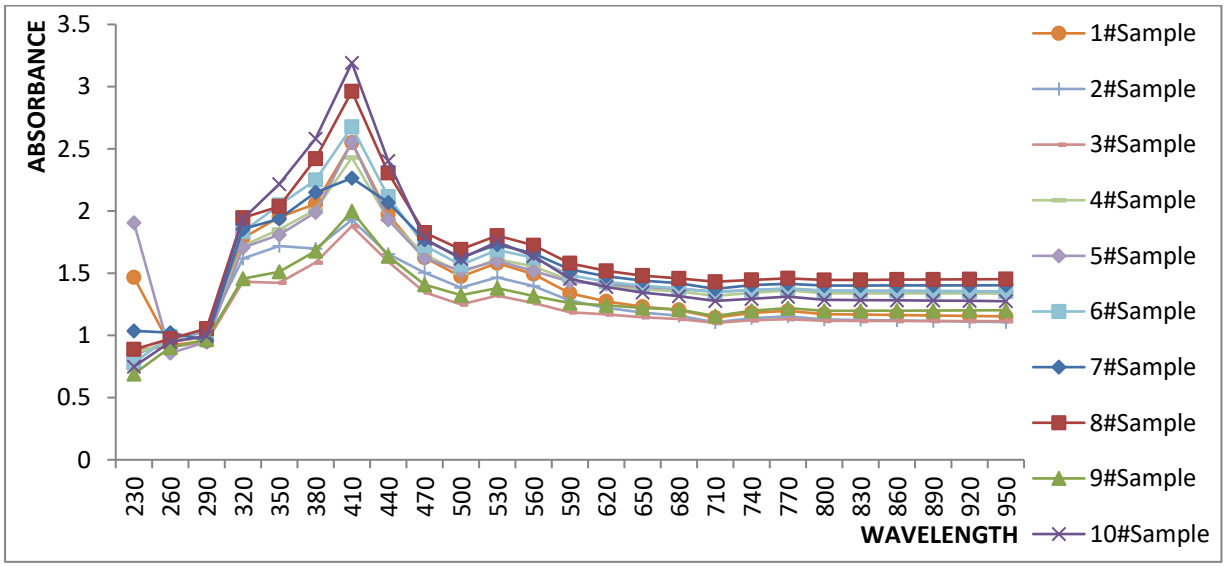

Fig.4.45: Absorbance Vs Wavelength of Uninfected WHOLE$_{1\text{-}10}$ with D5.

In figure 4.45, all uninfected whole blood samples with drug 5 appear to peak at 400nm with absorbance values between 0.7 and 3.2AU. Increase in wavelengths showed constant absorbance between 800 – 950nm.

Table 4.4: Avg. Peak (Max.) ā values of drugs and corresponding avg. Peak (Max.) λ as depicted in the figure plots 4.27 to 4.46.

Blood Component		Avg. Peak ā values of drugs$_{1-5}$ and corresponding avg. Peak λ values HIV Negative blood components$_{1-4}$ interacted with different Drug$_{1-5}$ samples				
		D1	D2	D3	D4	D5
Serum	ā	1.5	0.45	0.15	0.7	0.72
	λ	300	300	300	300	300
White	ā	0.72	0.71	0.76	1.0	0.97
	λ	300	300	300	300	300
Red	ā	1.8	1.78	1.86	2.05	2.03
	λ	390	400	400	400	400
Whole	ā	1.65	1.65	1.68	1.95	1.95
	λ	400	400	400	400	400

At a lower wavelength of 300nm for serum and white components, relative to 400nm for Red and Whole components, the components of Serum and White blood cells shows lower absorbance values. These values stand in comparison with the uninfected blood samples without drugs whose plots are not included in this report for want of space.

Table 4.5: Peak absorbance (â) and Absolute Hamaker constants (A_{11abs}) values with corresponding wavelength (λ) values for each antiviral drug$_{1-5}$ in 1-5mls of sterile H_2O.

Drug Type	Absolute Hamaker Constant, A_{11abs}(x10^{-21}J)						Peak	
	1ml	2mls	3mls	4mls	5mls	A_{11abs} for Drugs in H_2O	Â	λ
D1	1.7117	2.2993	2.2622	1.2774	1.7173	1.8536	0.752	322
D2	0.0036	0.0078	0.1197	0.1447	0.0094	0.0570	0.772	320
D3	0.0312	0.3802	0.0725	0.0254	0.0143	0.1047	0.958	326
D4	1.7764	2.2993	2.2622	1.2774	1.7173	1.8665	0.642	344
D5	0.0040	0.0040	2.0984	0.3956	0.6850	0.6374	0.740	344

From table 4.5, the $A_{11abs.}$ shows that D1 (herbal), D4 (synthetic) and D5 (synthetic) have higher absorbance values compared to D2 and D3. These pointed towards their levels of efficacy as D4 and D5 have been confirmed (Ani, 2015).

Table 4.6: Comparison between Absolute Hamaker constants and Absolute Combined Hamaker constants with Infected Lymphocyte, UNf.Lymphos. & US components (without drugs).

Absolute Hamaker constants			Absolute Combined Hamaker constants		
$A_{11abs.}$	$A_{22abs.}$	$A_{33abs.:US}$	$A_{12abs.}$	$A_{13abs.:US}$	$A_{23abs.:US}$
0.0089	0.4177	0.0034	0.0420	0.0042	0.0087

Table 4.7: Comparison between Absolute Hamaker constants and Absolute Combined Hamaker constants with Inf. Lymphocyte, UNf.Lymphos. & US components (with $drugs_{1-5}$).

Drug Number	Absolute Hamaker constants			Absolute Combined Hamaker constants		
	$A_{11abs.}$	$A_{22abs.}$	$A_{33abs.:US}$	$A_{12abs.}$	$A_{13abs.:US}$	$A_{23abs.:US}$
D1	0.1278	0.1038	0.0487	0.0557	0.0784	0.0334
D2	0.1139	0.1135	0.0477	0.0620	0.0726	0.0369
D3	0.1873	0.1236	0.0913	0.0774	0.1297	0.0510
D4	0.4513	0.1072	0.2797	0.1126	0.3545	0.0873
D5	0.5039	0.1143	0.321	0.2106	0.4013	0.1119

Table 4.8: Comparison between Absolute Hamaker constants and Absolute combined Hamaker constants with Inf. Lymphocyte, UNf.Lymphos. & IS components (without drugs).

Absolute Hamaker constants			Absolute Combined Hamaker constants		
$A_{11abs.}$	$A_{22abs.}$	$A_{33abs.: IS}$	$A_{12abs.}$	$A_{13abs.: IS}$	$A_{23abs.: IS}$
0.0089	0.4177	0.0154	0.0420	0.0087	0.0343

Table 4.9: Comparison between Absolute Hamaker constants and Absolute combined Hamaker constants with Inf. Lymphocyte, UNf.Lymphos. & IS components (with $drugs_{1-5}$).

Drug Number	Absolute Hamaker constants			Absolute Combined Hamaker constants		
	$A_{11abs.}$	$A_{22abs.}$	$A_{33abs.: IS}$	$A_{12abs.}$	$A_{13abs.: IS}$	$A_{23abs.: IS}$
D1	0.1278	0.1038	0.0878	0.0557	0.0528	0.0938
D2	0.1139	0.1135	0.0955	0.0620	0.0504	0.1016
D3	0.1873	0.1236	0.1163	0.0774	0.0717	0.1146

D4	0.4513	0.1072	0.0808	0.1126	0.0932	0.0921
D5	0.5039	0.1143	0.0944	0.1123	0.0908	0.1022

The values pointed towards their levels of efficacy as recorded ahead in this work.

Table 4.10: Comparison between Absolute Combined Hamaker constants and Absolute combined Hamaker coefficients for UNf.Lymphos. &US components (without drugs).

Absolute Combined Hamaker constants			Absolute Combined Hamaker coefficients		
$A_{12abs.}$	$A_{13abs.:US}$	$A_{23abs.:US}$	$A_{132abs.:US}$	$A_{131abs.:US}$	$A_{232abs.:US}$
0.0420	0.0042	0.0087	0.0324	0.0548	0.4036

Table 4.11: Comparison between Absolute Combined Hamaker constants and Absolute Combined Hamaker coefficients for UNf.Lymphos. &US components (with drugs$_{1-5}$).

Drug Number	Absolute Combined Hamaker constants			Absolute Combined Hamaker coefficients		
	$A_{12abs.}$	$A_{13abs.:US}$	$A_{23abs.:US}$	$A_{132abs.:US}$	$A_{131abs.:US}$	$A_{232abs.:US}$
D1	0.0557	0.0784	0.0334	- 0.0385	0.1349	0.0853
D2	0.0620	0.0726	0.0369	- 0.0299	0.1234	0.0873
D3	0.0774	0.1297	0.0510	- 0.0381	0.1333	0.1129
D4	0.1126	0.3545	0.0873	- 0.0511	0.144	0.2123
D5	0.1123	0.4013	0.1119	- 0.053	0.1442	0.258

Table 4.12: Absolute Hamaker constants and Absolute Combined Hamaker constants and Absolute Hamaker coefficients for all blood interacting systems with US as intervening medium (without drugs)

Hamaker variable	Absolute Description	Absolute value
$A_{11abs.}$	Hamaker constant for UNf.Lymphos.- UNf.Lymphos. interaction.	0.0089
$A_{22abs.}$	Hamaker constant for INf.Lymphos-INf.Lymphos.interaction.	0.4177
$A_{33abs.:US}$	Hamaker constant for US-USinteraction.	0.0034

$A_{12abs.}$	Combined Hamaker constant for UNf.Lymphos.-INf.Lympho interaction.	0.0420
$A_{13abs.:US}$	Combined Hamaker constant for UNf.Lymphos.-US interaction.	0.0042
$A_{23abs.:US}$	Combined Hamaker constant for INf.Lymphos.-US interaction.	0.0087
$A_{132abs.:US}$	Combined Hamaker coefficient for UNf.Lymphos.-US-INf.Lymphos. interaction.	0.0324
$A_{131abs.:US}$	Combined Hamaker coefficient for UNf.Lymphos.-US-UNf.Lymphos. interaction.	0.0548
$A_{232abs.:US}$	Combined Hamaker coefficient for INf.LymphoS.-US-INf.Lympho interaction.	0.4036

Table 4.13: Comparison of Absolute Hamaker constants and Absolute Combined Hamaker constants and Absolute Hamaker coefficients for all blood interacting systems with US as the intervening medium (with drugs$_{1-5}$)

Hamaker variable	Absolute Description	Absolute value D1	D2	D3	D4	D5
$A_{11abs.}$	Hamaker constant for UNf.Lymphos.-UNf.Lymphos. interaction.	0.1278	0.1139	0.1873	0.4513	0.5039
$A_{22abs.}$	Hamaker constant for INf.Lymphos.-INf.Lymphos interaction.	0.1038	0.1135	0.1236	0.1072	0.1143
$A_{33abs.:US}$	Hamaker constant for US-US interaction.	0.0487	0.0477	0.0913	0.2797	0.321
$A_{12abs.}$	Combined Hamaker constant for UNf.Lymphos.-INf.Lymphos. interaction.	0.0557	0.0620	0.0774	0.1126	0.1123

$A_{13abs.:US}$	Combined Hamaker constant for UNf.Lymphos.-US interaction.	0.0784	0.0726	0.1297	0.3545	0.4013
$A_{23abs.:US}$	Combined Hamaker constant for INf.Lymphos.-US interaction.	0.0334	0.0369	0.0510	0.0873	0.1119
$A_{132abs.:US}$	Combined Hamaker coefficient for UNf.Lymphos.-US-INf.Lymphos. interaction.	-0.039	-0.029	-0.038	-0.051	-0.053
$A_{131abs.:US}$	Combined Hamaker coefficient for UNf.Lymphos.-US-UNf.Lymphos. interaction.	0.1349	0.1234	0.1333	0.144	0.1442
$A_{232abs.:US}$	Combined Hamaker coefficient for INf.Lympho-US-INf.Lymphos. interaction.	0.0853	0.0873	0.1129	0.2123	0.258

All values were further employed in the calculated combined Hamaker coefficients which are expressions for the thermodynamic interactive term.

4.2 $A_{132abss.}$ versus wavelengths of blood components without drugs (D^-): US as the intervening medium.

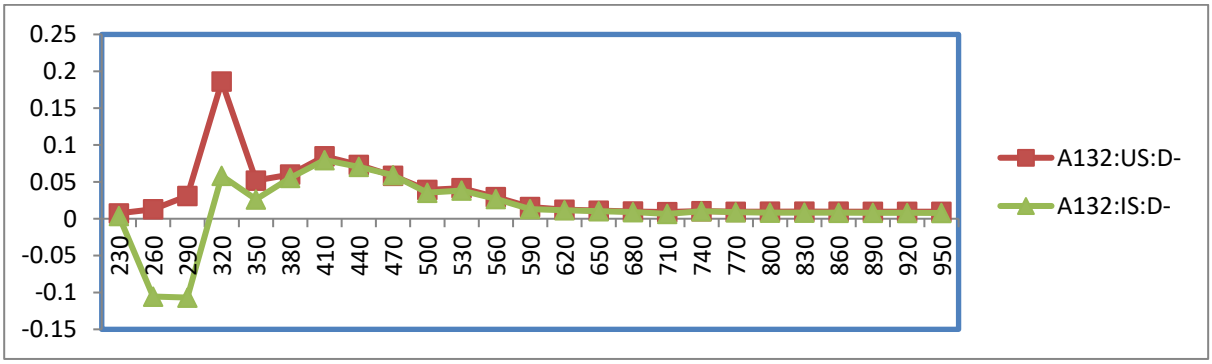

Fig.4.46: $A_{132abs.}$: US (without drugs) and $A_{132abs.}$:IS (without drugs) Vs Wavelengths

Figure 4.46 reveals the natural pattern of the combined Hamaker coefficients for the interacting systems of the twenty samples of HIV negative and positive three main components of blood and the whole blood without drugs. The combined Hamaker coefficients for the interacting system of the HIV positive blood, with uninfected serum (US) increased from zero peaked at 320nm with a value of 0.0154AU. It decreased sharply from 320 to 350nm and continued until it became constant at near zero from 590 to 950nm. The near zero or negative values for the

same $A_{132abs.}$, with infected serum (IS) indicate a van der Waals natural repulsion in the HIV positive systems (whether with US or IS). This in effect is an expected characteristic of the HIV infection. Moreover, the positive values of the combined Hamaker coefficients indicate a van der Waals attraction property of the lymphocytes in the HIV negative system. This is in affirmation that, there would be a surface coating of the lymphocytes with any antiviral drugs, or the binding of antiviral drugs on the surface of the lymphocytes which would be an effective inhibition or blocking of the invading virus. This phenomenon is typical of $A_{131abs.}$ (Figure 4.47) where HIV positive (with IS) exhibits both negative (repulsion) and positive (attraction) values of combined Hamaker coefficients. $A_{232abs.}$ (Figure 4.48) of HIV positive (whether 3 is with US or IS since infected lymphocyte, 2 is already in interaction) shows only positive values indicating attraction the lymphocyte would have with any additive to the serum.

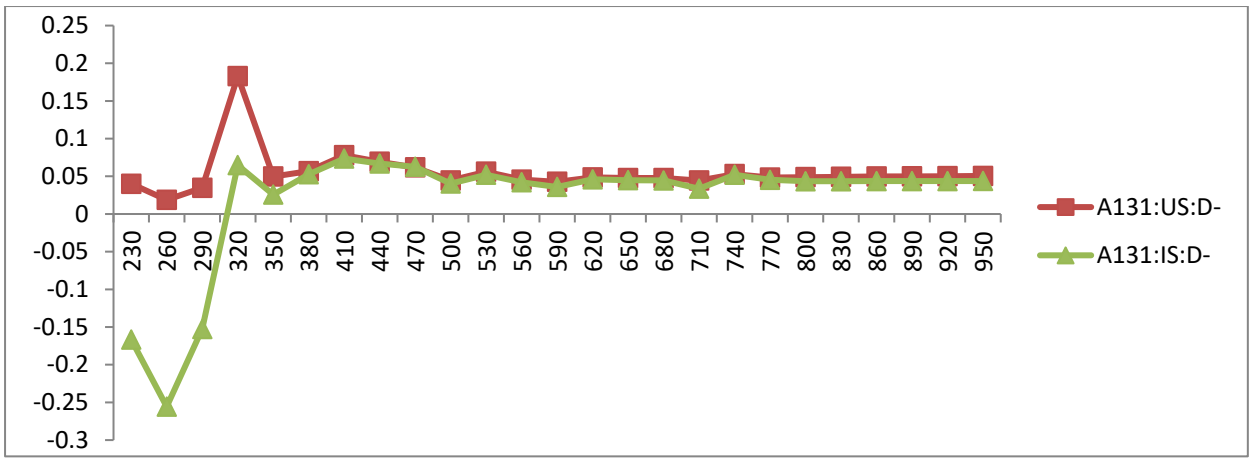

Fig.4.47: $A_{131abs.}$: US (without drugs) and $A_{131abs.}$:IS (without drugs) Vs Wavelengths

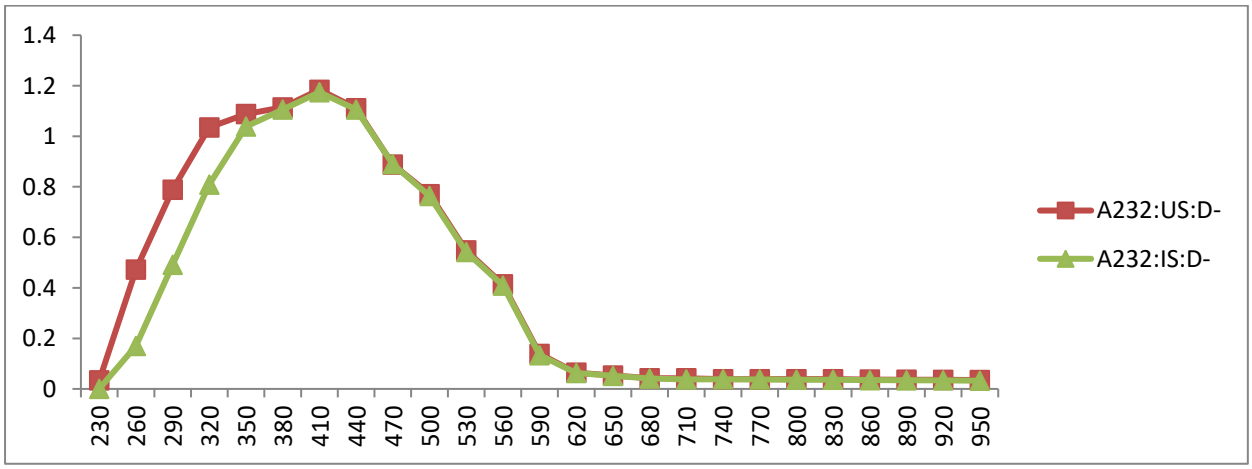

Fig.4.48: $A_{232abs.}$: US (without drugs) and $A_{232abs.}$:IS (without drugs) Vs Wavelengths.

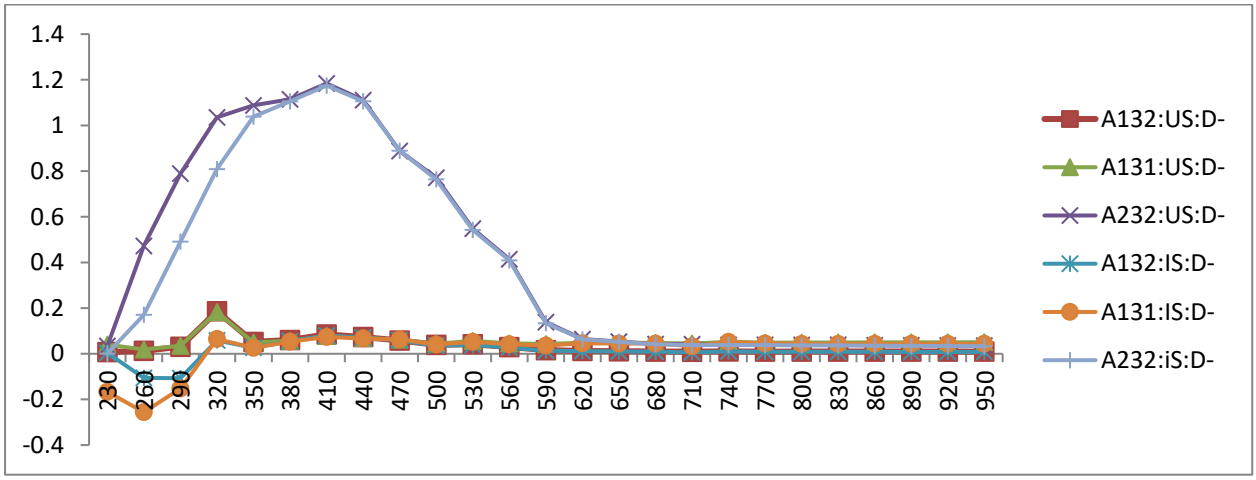

Fig.4.49: Combined plot of $A_{132abs.}$, $A_{131abs.}$, $A_{232abs.}$ (with uninfected serum) and $A_{132abs.}$, $A_{131abs.}$, $A_{232abs.}$ (with infected serum) values of all samples without drugs Vs Wavelengths.

4.3 $A_{132abss.}$ versus wavelengths of blood components (with $drugs_{1-5}$): US as the intervening medium

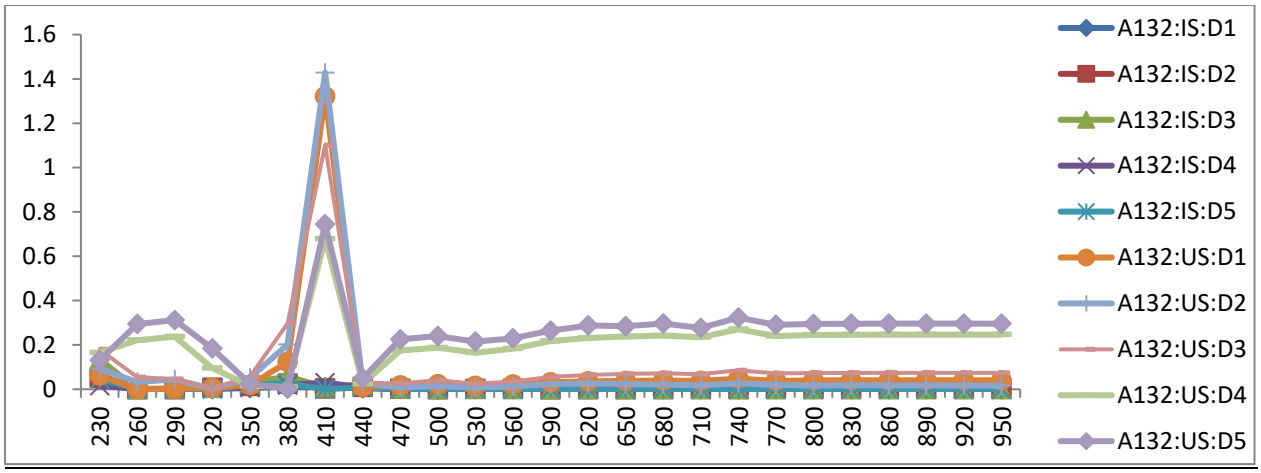

Fig.4.50: $A_{132abs.}$: IS (with $drugs_{1-5}$) and $A_{132abs.}$: US (with $drugs_{1-5}$) Vs Wavelengths

In interactions of HIV positive with drugs, figure 4.50 shows that D1 (Garcinia kola) has a good attractive property which favors coating or binding than repulsive property that encourages repulsion. D2 (Azadirachta indica), D3 (GAM), D4 (EFV) and D5 (ELT) all has attractive tendencies and repulsive natures but for D4 with better repulsive property.

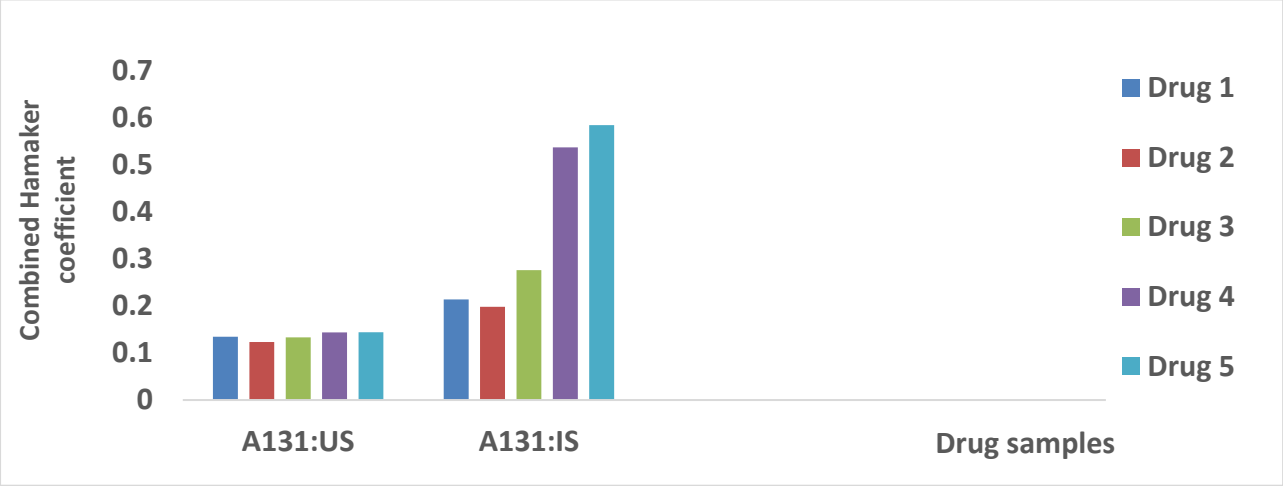

Fig.4.51: $A_{131abs.}$: US (with $drugs_{1-5}$) and $A_{131abs.}$:IS (with $drugs_{1-5}$) Vs Drug samples

In the interactions of HIV negative samples with drugs, figure 4.51 shows that all drugs are with positive signs indicating that they have good attractive properties which favor coating or binding with uninfected lymphocytes. In the presence of a virus particle (A_{131}: IS), D4 and D5 which are synthetic in nature appear to have better qualities than the herbal additives. But in a pure uninfected serum and lymphocyte component samples, all drugs exhibit almost equal potentials for binding.

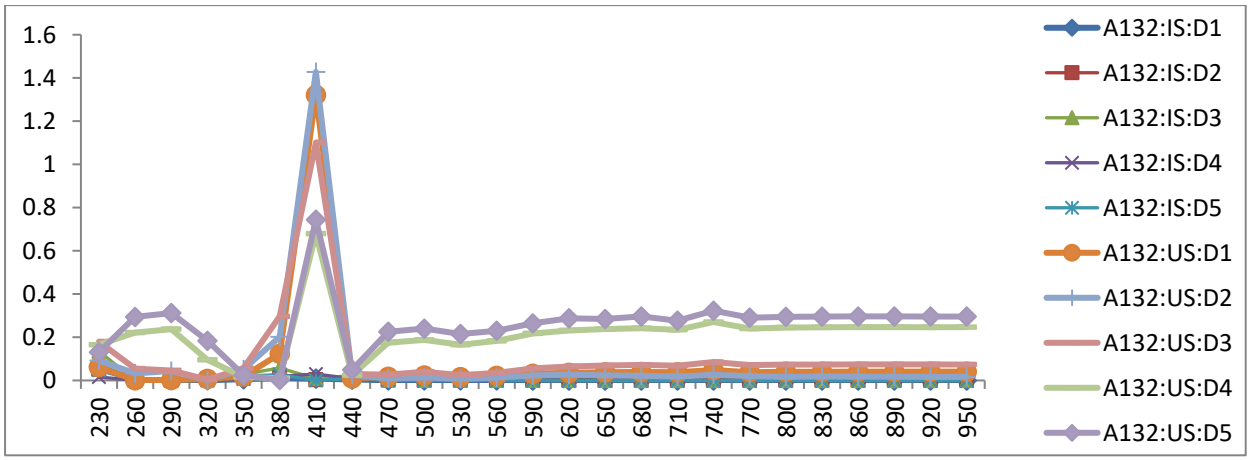

Fig.4.52: $A_{232abs.}$: US (with $drugs_{1-5}$) and $A_{232abs.}$:IS (with $drugs_{1-5}$) Vs Wavelengths.

In figure 4.52, all drugs show good qualities for attraction or coating indicated by the appreciable positive values of the combined Hamaker coefficients in a HIV infected interaction system.

Table 4.14: $A_{11abs.}$ (without drug) and values of $A_{22abs.}$& $A_{33abs.}$ofUNf.Lymphos.-INf.Lymphos. (without drugs), and corresponding $A_{132abs.}$ (with US) of blood samples(without drugs)

Hamaker Variable (x10^{-21}Joules)	Hamaker Values (x10^{-21}Joules)
$A_{11abs.}$	0.0089
$A_{22abs.}$	0.4177
$A_{33abs.:US}$	0.0034
$A_{132abs.:US}$	0.0324

Table 4.15: $A_{11abs.}$ (with $drugs_{1-5}$) and values of $A_{22abs.}$& $A_{33abs.}$ofUS & IS (with $drugs_{1-5}$) and corresponding $A_{132abs.}$ (with IS) of blood samples (with $drugs_{1-5}$)

Hamaker Variable (x10^{-21}Joules)	D1	D2	D3	D4	D5
$A_{11abs.}$	0.1278	0.1139	0.1873	0.4513	0.5042
$A_{22abs.}$	0.1038	0.1135	0.1236	0.1072	0.1143
$A_{33abs.:US}$	0.0483	0.0476	0.0913	0.2797	0.321
$A_{132abs.:US}$	- 0.0385	- 0.0299	- 0.0381	- 0.0511	- 0.053

In table 4.15, the interacting system involving D1, D2, D3, D4 and D5 all gave negative absolute combined Hamaker coefficient $A_{132abs.}$indicating a repulsion between the HIV and the lymphocyte. The newly administered antiviral drugs and the already-existing drug-coated lymphocyte in the HIV positive systems gave a positive $A_{132abs.}$

Table 4.16: Comparison of $A_{11abs.}$ (with $drug_{1-5}$) and values of $A_{22abs.}$& $A_{33abs.}$ of INf.Lymphos.-IS (with $drugs_{1-5}$) and corresponding $A_{132abs.}$ (with IS) of blood samples (with $drugs_{1-5}$)

Hamaker Variable (x10^{-21}Joules)	D1	D2	D3	D4	D5
$A_{11abs.}$	0.1278	0.1139	0.1873	0.4513	0.5042
$A_{22abs.}$	0.1038	0.1135	0.1236	0.1072	0.1143
$A_{33abs.:IS}$	0.0878	0.0955	0.1163	0.0808	0.0944
$A_{132abs.:IS}$	- 0.0013	0.0055	0.0074	0.0081	0.0134

Recalling the conditions for a thermodynamic prediction of the efficacy of drugs against the HIV, the following facts are established with the results on tables 4.15 and 4.16:

1. Positive values of A_{131} (UNf.Lymphos.-US-UNf.Lymphos.) for an interaction between HIV negative blood components and drug samples in serum are all greater than Positive values of $A_{232abs.}$ (INf.Lymphos.-US-INf.Lymphos.) for an interaction between HIV+ blood components and drug samples in serum. Therefore, all experimental drugs have the efficacy to attract lymphocytes and this facilitates binding for surface coating of lymphocytes.
2. Conversely, $A_{131abs.}$ being less than A_{232} implies that the drugs possess stronger binding force which is most effective for coating.
3. $A_{132abs.}$ of -0.0013 for D1 (with IS) being negative equally predicts that D1 can encourage repulsion which would prevent the HIV from being attracted and attached to the lymphocyte. These are in addition to D4 & D5 which have been verified by Ani (2015).
4. $A_{132abs.}$ for D2, D3, D4, D5 being positive predicts that they can encourage attraction which would bind them to the lymphocyte.
5. $A_{132abs.}$ of all drugs (with US) being negative equally predicts that they can encourage repulsion which would prevent the HIV from being attracted and attached to the lymphocyte.

Table 4.17: Comparison of Absolute combined Hamaker coefficients with (Ani, 2015)

Hamaker variable A_{132} (with uninfected serum)	Hamaker Value ($x10^{-21}$Joules)	Hamaker Value ($x10^{-21}$Joules) (Ani, 2015)
D1	-0.0385	-0.03998
D2	-0.0299	-0.05305
D3	-0.0381	-0.05845
D4	-0.0511 (Ani, 2015: D4)	-0.02481
D5	-0.053 (Ani, 2015: D2)	-0.05844

From the table 4.17 it is established that all herbal additives (D1, D2 and D3) to serum would be effective in controlling HIV. Herbal D1 (Akilu) has the same efficacy with Lamivudine/Nevirapine/Zidovudine . Herbal D2 (Dogonyaro) has very close efficacy with Tenofovir/Lamivudine/Efavirenz and Nevirapine and Lamivudine. Herbal D3 (Akilu + Dogonyaro + Mango) has the same efficacy with Efavirenz.

Table 4.18: Mean Values of A_{11}, A_{22} and corresponding $\tilde{A}_{(33:IS)1 \text{ or } 2}$ that yield Zero, Positive and Negative $\tilde{A}_{132s}$ (without drugs). Hamaker variable $x10^{-21}J$ average for TEN blood samples.

Wavelength	A_{11}	A_{22}	$\sqrt{(A_{11})}$	$\sqrt{(A_{22})}$	$(\sqrt{A_{11}} * \sqrt{A_{22}})$	$\tilde{A}_{(33:IS)1} = A_{11} + A_{22} - (\sqrt{A_{11}} * \sqrt{A_{22}})$	$\tilde{A}_{(33:IS)2} = (-)\sqrt{A_{11}} * \sqrt{A_{22}}$	$\tilde{A}_{132:IS} = (\sqrt{(A_{11})} - \sqrt{\tilde{A}_{(33:IS)1}})^* (\sqrt{(A_{22})} - \sqrt{\tilde{A}_{(33:IS)1}})$	$\tilde{A}_{132:IS} = (\sqrt{(A_{11})} - \sqrt{\tilde{A}_{(33:IS)2}})^* (\sqrt{(A_{22})} - \sqrt{\tilde{A}_{(33:IS)2}})$
230	0.1073	0.2227	0.3277	0.4718	0.1546	0.1754	-0.0239	-0.0032	0.03238
260	0.0005	0.4799	0.0241	0.6927	0.0167	0.4637	-0.0002	-0.0074	0.00042
290	0.0018	0.8039	0.0432	0.8966	0.0388	0.7671	-0.0015	-0.0282	0.00271
320	0.0431	1.0859	0.2075	1.0421	0.2163	0.9128	-0.0468	-0.1506	0.10178
350	0.0026	1.0913	0.0513	1.0446	0.0536	1.0403	-0.0029	-0.0529	0.00602
380	0.0039	1.1258	0.0621	1.0610	0.066	1.0637	-0.0044	-0.0658	0.00929
410	0.0068	1.194	0.0825	1.0927	0.0901	1.1107	-0.0081	-0.092	0.01793
440	0.0056	1.1230	0.0749	1.0597	0.07942	1.0492	-0.0063	-0.07702	0.01346
470	0.0048	0.9031	0.0697	0.9503	0.0662	0.8417	-0.0044	-0.0514	0.00839
500	0.0022	0.7754	0.047	0.8805	0.0414	0.7362	-0.0017	-0.0287	0.00304
530	0.0037	0.5555	0.061	0.7453	0.0454	0.5137	-0.0021	-0.0213	0.00322
560	0.0023	0.417	0.048	0.6457	0.031	0.3883	-0.001	-0.0111	0.00136
590	0.0020	0.1404	0.0449	0.3748	0.0168	0.1256	-0.0003	-0.0018	0.00032
620	0.0028	0.0665	0.0529	0.258	0.0136	0.0557	-0.0002	-0.0006	0.00020
650	0.0027	0.0553	0.0520	0.2352	0.0122	0.0458	-0.0002	-0.0004	0.00016
680	0.0027	0.0444	0.0521	0.2106	0.011	0.0361	-0.0001	-0.0003	0.00013
710	0.0020	0.0423	0.0450	0.2058	0.0093	0.0351	-0.0001	-0.0002	0.00009
740	0.0037	0.0416	0.0606	0.2039	0.0124	0.0329	-0.0002	-0.0003	0.00016
770	0.0028	0.0406	0.0528	0.2015	0.0106	0.0327	-0.0001	-0.0002	0.00012
800	0.0029	0.0403	0.0535	0.2008	0.0107	0.0324	-0.0001	-0.0002	0.00012
830	0.0029	0.0406	0.0541	0.2015	0.0109	0.0326	-0.0001	-0.0002	0.00012
860	0.003	0.0390	0.0546	0.1975	0.0108	0.0312	-0.0001	-0.0002	0.00012
890	0.003	0.0384	0.0547	0.1959	0.0107	0.0307	-0.0001	-0.0002	0.00012
920	0.0030	0.0380	0.0549	0.1950	0.0107	0.0303	-0.0001	-0.0002	0.00012
950	0.0030	0.037	0.0552	0.1923	0.0106	0.0294	-0.0001	-0.0002	0.00012
Abs. value						0.3845	-0.0042	**-0.0238**	**0.00808**
SFE of Abs.						28.023	-0.3061	-1.7338	0.58853

The result shows that the Ã(33:IS)1 gives a negative value of -0.0238 and the Ã(33:IS)2 gives a positive value of 0.008 under no drug condition.

4.4 Deductions for the Harmonized Combined Hamaker coefficients

As previously stated, the derivation for a mathematical expression for this relationship is:

$$A_{132harm..} = \phi_t A_{132\max.} \qquad 4.33$$

Where:

$\phi_t \Rightarrow$ Proportionality constant (mean of the difference between $A_{132max.}$ and $A_{132harm.}$)

From equation 4.33:

$$A_{132harm.} \approx 0.4725\left(A_{132\max.}\right) \qquad 4.34$$

Table 4.19: Absolute $A_{132abs.}$, $A_{131abs.}$ & $A_{232abs.}$ values of interacting system with $D_{1\text{-}5}$.

DRUG #	$A_{132abs.}$ ($x10^{-21}J$) (with Inf. Serum) HIV+	$A_{131abs.}$ ($x10^{-21}J$) (withUnf. Serum) HIV-	$A_{232abs.}$ ($x10^{-21}J$) (with Inf.Serum) HIV+
D1	-0.0031	0.1349 >	0.004
D2	0.0055	0.1234 >	0.0058
D3	0.0074	0.1333 >	0.0108
D4	0.0081	0.144 >	0.0037
D5	0.0134	0.1442 >	0.0042

Substituting individual peak values of tables 4.19 in equation 4.34, corresponding harmonized values are obtained.

Table 4.20: Comparison of the values of Absolute combined Hamaker coefficients $A_{132abs.}$ (with infected serum), $A_{131abs.}$ (with uninfected serum) and, their Harmonized combined Hamaker coefficients without antiviral drugs.

With INFECTED serum (HIV+) sample		With UNINFECTED serum (HIV-) sample	
A_{132abs} ($x10^{-21}J$)	A_{132har} ($x10^{-21}J$)	A_{131abs} ($x10^{-21}J$)	A_{131har} ($x10^{-21}J$)
0.0144	0.0089	0.0548	0.0259

Table 4.21: Comparison of the values of Absolute combined Hamaker coefficients $A_{132abs.}$, $A_{232abs.}$ (with infected serum) and $A_{131abs.}$ (with uninfected serum) and, their Harmonized combined Hamaker coefficients of the five antiviral drugs.

Drug sample	With INFECTED serum (HIV+) blood			With UNINFECTED serum (HIV-) sample		
	$A_{132abs.}$ (10^{-21}J)	$A_{132harm.}$ (10^{-21}J)	$A_{232abs.}$ (10^{-21}J)	$A_{232harm}$ (10^{-21}J)	$A_{131abs.}$ (10^{-21}J)	$A_{131harm.}$ (10^{-21}J)
D1*	-0.0031*	-0.0015	0.004	0.0019	0.1349	0.0637
D2*	0.0055	0.0101	0.0058 <	0.0118	0.1234*	0.1044
D3*	0.0074	0.0134	0.0108 <	0.0273	0.1333*	0.1032
D4*	0.0081*	0.0219	0.0037	0.0088	0.144	0.094
D5*	0.0134*	0.0063	0.0042	0.0122	0.1442	0.0614

4.5 Deductions for the Zero, Positive and Negative Combined Hamaker Coefficients of blood-drug interacting systems.

The computed values are seen on the following tables on appendix R and S before the comparisons on Table 4.22 for Unf. and Inf. Samples:

Table R1of appendix R shows the mean values of A_{11}, A_{22} and corresponding A_{33} that yielded zero, positive and negative A_{132} (with drugs$_{1-5}$)

Table R2 of appendix R shows the mean values of A_{11}, A_{22} and corresponding A_{33} that yielded zero, positive and negative A_{132} (without drugs)

Table S1 of appendix S shows the $A_{11abs.}$, $A_{22abs.}$& corresponding $A_{132abss.}$that are Zero or Negative (without drugs).

Table S2 of appendix S shows the $A_{11abs.}$, $A_{22abs.}$& corresponding $A_{132abss.}$that are Zero or Negative (with $drugs_{1-5}$).

Table 4.22: Comparison of $A_{132abs.}$, $A_{131abs.}$, A_{232abs}& their Harmonized Combined Hamaker coefficients with Uninfected Serum.

Hamaker Variable($x10^{-21}J$)	D1 crude compound (Herbal)	D2 crude compound (Herbal)	D3 combined crude compounds (Herbal)	D4 single pure compound (Synthetic ART)	D5 HAART andFDC (Synthetic ART)
$A_{132abs.}$ (HIV Positive)					
Peak value	0.1429	0.1527	0.1187	0.0756	0.0792
Absolute value	-0.0031	0.0055	0.0074	0.0081	0.0134
Harm. value	0.0675	0.0722	0.0561	0.0357	0.0374
$A_{131abs.}$ (HIV Negative)					
Peak value	0.2206	0.2209	0.2180	0.1989	0.1946
Absolute value	0.1349	0.1234	0.1333	0.144	0.1442
Harm. value	0.1042	0.0004	0.1030	0.094	0.092
$A_{232abs.}$ (HIV Positive)					
Peak value	1.3213	1.4283	1.1010	0.6787	0.7442
Absolute value	0.004	0.0058	0.0108	0.0037	0.0042
Harm. value	0.6243	0.6749	0.5202	0.3207	0.3516

In the table 4.22, A_{131} represents the combined Hamaker coefficient for two uninfected lymphocytes and one serum particles. These are for the HIV negative samples which are involved in the determined thermodynamic efficacy of drugs. 'Harm.' Stands for 'harmonized'.

Table 4.23: Comparison of Absolute values of $A_{131abs.}$ with US & Absolute values of $A_{132abs.}$, $A_{232abs.}$ with IS for the five antiviral drugs used.

Hamaker Variable ($x10^{-21}J$)	D1 crude compound (Herbal)	D2 crude compound (Herbal)	D3 combined crude compounds (Herbal)	D4 single compound (Synthetic ART)	D5 HAART andFDC (Synthetic ART)
$A_{131abs.}$	0.1349	0.1234 (Attracts Lymphocytes)	0.1333 (Attracts Lymphocytes)	0.144 (Attracts Lymphocytes)	0.1442 (Attracts Lymphocytes)
$A_{132abs.}$	-0.0031 (repels HIV)	0.0055	0.0074	0.0081	0.0134
$A_{232abs.}$	0.004	0.0058	0.0108	0.0037	0.0042

In the table 4.23, the final comparison is made between HIV- samples interacted with drugs. All drugs appear to have good binding property. But D1 with a negative A_{132abs} which is very closer to zero has a better repelling property against the HIV when covering an UNf.Lymphos.

4.6 Estimation of Blood-Drug coated Effectiveness

This study used the expression in equ.15 below for coating effectiveness: $\hat{a}_{bd}$

$$\eta_a = [(\hat{a}_{bd} - \hat{a}_b)/(\hat{a}_d - \hat{a}_b)] \quad (4.32)$$

Where: $\hat{a}_d$ is peak absorbance for drug film only, $\hat{a}_b$ is peak absorbance for uninfected blood component only and $\hat{a}_{bd}$ is peak absorbance for an uninfected blood component coated by a drug film.

It is assumed that the drug particles dissolved in the serum and its film coated the surface of each blood component. Using relevant average or absolute values for the model in equ.(4.32), with $A_{132abs.}$values for HIV infected blood samples in table 4.20, coating effectiveness were as tabulated in table 4.24.

Table 4.24: Degrees of coating effectiveness, η_a.

Blood Components	Drug Samples				
	D1	D2	D3	D4	D5
Plasma	0.498	0.457	0.458	0.09	0.17
White blood cell	0.57	0.52	0.51	0.56	0.08
Red blood cell	0	-2.45	9.74	-2.21	-3.65

From table 4.24, the effectiveness of coating on the red blood cell is inconsistent with zero, positive and negative signs. These show that the drugs do not have any defined effect on the red blood cells' surfaces (Ozoihu, 2014). The values for effectiveness for the white and plasma cells are all consistently positive for the antiviral drugs used. The highest degree of coating effectiveness for the plasma and WBC are 0.498 and 0.57 of D1 respectively. The higher mean value suggests higher degree of coating. Looking at the values for plasma and white blood components, D1 shows effective coating on the two blood components which are targets of the HIV.

Table 4.25: Details of the Five Antiviral drugs used in the study

Drug No.	Tablets or Powder	Abbreviation	Quantity used	Type of Drug	Manufacture or Extraction Date	Expiration Date	Frequency of Use (dosage)	Batch Number	Pharma-ceutical Company
1	**G**arcinia **K**ola	GK	790mg	Herbal extract	02/2017	-	Once daily	-	Locally sourced
2	**A**zadirachta **I**ndica	AI	970mg	Herbal extract	02/2017	-	Once daily	-	Locally sourced
3	**G**arcinia, **A**zadirachta, **M**angifera	GAM	2800mg: (G.800mg, A.1000mg, M.1000mg)	Herbal extract	02/2017	-	Once daily	-	Locally sourced
4	**Efav**irenz	Efv	600mg	FDC	08/2014	07/2018	Once daily	E121047	HETERO LABS LIMITED
5	**E**favirenz, **L**amivudine, **T**enofovir	ELT	1200mg (E.600mg, L.300mg, T.300mg)	HAART and FDC	09/2014	08/2018	Once daily	E141689	HETERO LABS LIMITED

Table 4.26: Comparison between Blood-Drug interactions for a Surface Thermodynamics Interpretation & Significance.

Drug #	Drug Type	Abrv.	Composition	Quantity Of compo-sition	$A_{132abs.}$ of Infected Blood (with IS or US)	Sign obtained	Nature of Van der Waals' Force	Nature of interac-tion	$A_{131abs.}$ of Uninf. Blood (with US)	Sign obtained	Nature of Van der Waals' Force	Nature of inter-action
1	Harbal extract	GK.	Antiviral Terpenoids, Glycosides and Flavonoids(Kolaviron-a mixture of GB-1, GB-2 & Kolaflavonone biflavonoids)	790mg (crude extract)	-0.0031 or -0.0385	NEGATIVE	Repulsive	Repulsion (HIV therapy)	0.1349> A_{232} of 0.004	Positive	Attractive	Attrac-tion (surface coating)
2	Harbal extract	AI.	Antiviral Flavoniods, Glycosides and Terpenoids (2-acetoxyalphitic acid,	970mg (crude extract)	0.0055 or -0.0299	Near zero or NEGATIVE	Repulsive	Repulsion (HIV therapy)	0.1234> A_{232} of 0.0058	Positive	Attractive	Attrac-tion (surface coating)

			3-acetoxyalphitic acid), 0.1% Phenol									
3	Com-bined Herbal extract	GAM	Gk + AI + Mangifera indica(MI). MI contains Alkaloids, Glycosides (Mangiferin-a glucosyl xanthone). GAM is a sort of a HAHART (Highly Active Herbal Antiretroviral). It therefore contains antiviral Terpenoids, Glycosides and Flavonoids.	2800mg (crude extract)	0.0074 or -0.0381	Near zero or NEGATIVE	Repulsive	Repulsion (HIV therapy)	0.1333> A_{232} of 0.0108	Positive	Attractive	Attrac-tion (surface coating)

4	Single com-pound synthe-tic drug	Efv.	Efavirenz	600mg (pure extract)	-0.0511 or 0.0081	NEGATIVE or Near zero	Repulsive	Repulsion (HIV therapy)	0.144> A_{232} of 0.0037	Positive	Attractive	Attraction (surface coating)
5	HARRT and FDC	ELT	Efavirenz, Lamivudine & Tenofovir	1200mg (pure extract)	0.0134 or -0.053	Near zero or NEGATIVE	Repulsive	Repulsion (HIV therapy)	0.1442> A_{232} of 0.0042	Positive	Attractive	Attraction (surface coating)

The table shows the sign obtained for the combined Hamaker coefficient of both infected A_{132abs} and uninfected A_{131abs} blood-drug interacted systems, the nature of: the van der Waals' forces and interaction involved for HIV management and possible cure.

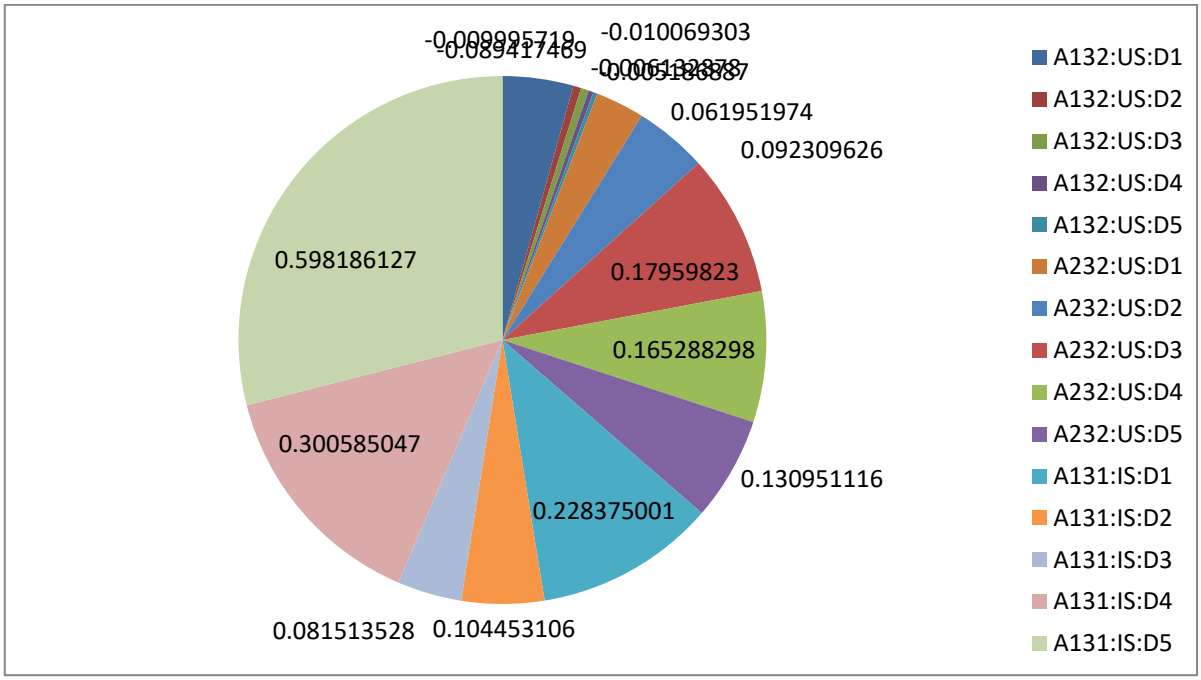

Fig.4.53: Combined plot of ($A_{11abs.}$,$A_{22abs.}$, $A_{33abs.}$), ($A_{132abs.}$,$A_{232abs.}$) with uninfected serum and ($A_{131abs.}$) with infected serum values Vs Wavelengths

In figure 4.53, the combined Hamaker coefficients with appreciable sector areas with positive values show good properties for attraction, while those with negative values can repel the HIV away from the lymphocyte. From the pie chart it indicates that all drugs investigated have good coating abilities which favor repulsion. This is a solution to the virus control and possible complete treatment.

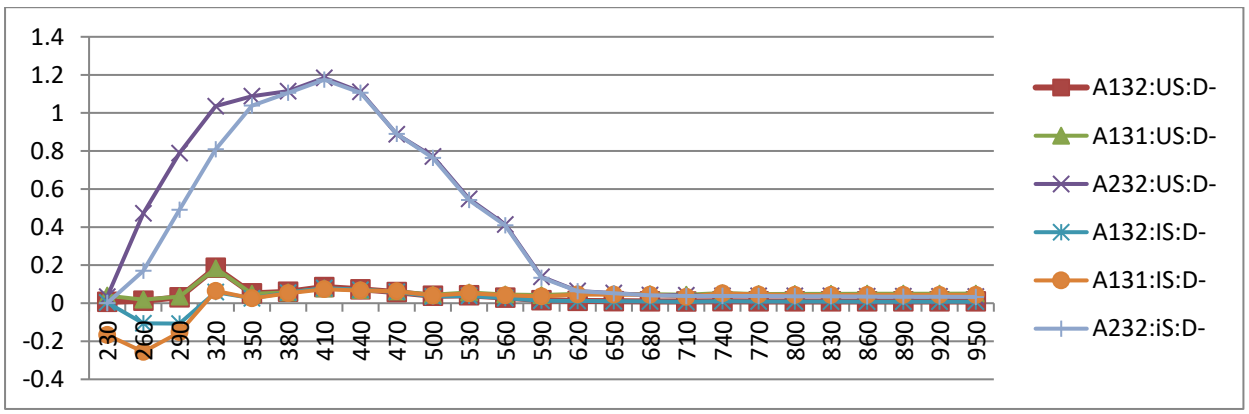

Fig.4.54: Combined plot of $A_{132abs.}$, $A_{131abs.}$, $A_{232abs.}$ (with uninfected serum) and $A_{132abs.}$, $A_{131abs.}$, $A_{232abs.}$ (with infected serum) values of all samples without drugs Vs Wavelengths.

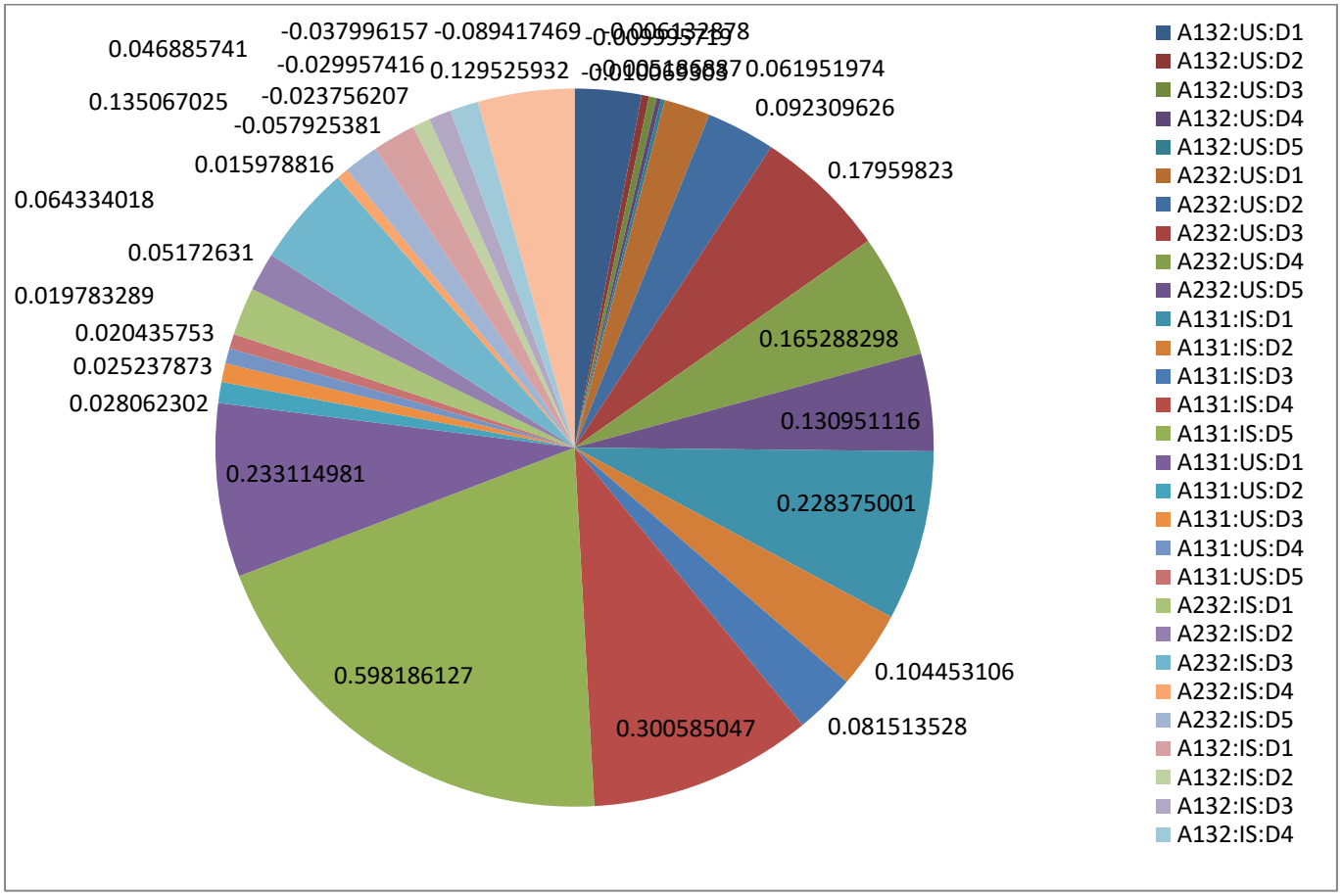

Fig.4.55: Combined plot of $A_{132abs.}$, $A_{131abs.}$, $A_{232abs.}$ (with uninfected serum) and $A_{132abs.}$, $A_{131abs.}$, $A_{232abs.}$ (with infected serum) values of all samples with $drugs_{1-5}$ Vs Wavelengths.

Table 4.27: Summary of the results of Blood-Drug Interactions												
Drug #	Drug Type	Abrv.	Composition	Qty. of composition	A_{132abs} of Inf. Blood	Sign obtained	Nature of Van der Waals' Force	Nature of interaction	$A_{131abs.}$ of Uninf. Blood	Sign obtained	Nature of Van der Waals' Force	Nature of inter-action
Drug 1	Harbal extract	GK.	Antiviral Terpenoids, Glycosides and Flavonoids(Kolavir on-a mixture of GB-1,GB-2 & Kolaflavonone biflavonoids)	790mg	-0.0385	Negative	Repulsive	Repulsion (HIV therapy)	0.1349	Positive	Attractive	Attraction (surface coating)
Drug 2	Harbal extract	AI.	Antiviral Flavoniods, Glycosides and Terpenoids (2-acetoxyalphitic acid, 3-acetoxyalphitic acid), 0.1%Phenol	970mg	-0.0299	Negative	Repulsive	Repulsion (HIV therapy)	0.1234	Positive	Attractive	Attraction (surface coating)
Drug 3	Combined Herbal extract	GAM	Gk + AI + Mangifera indica(MI). MI contains Alkaloids, Glycosides (Mangiferin-a glucosylxanthone)	2800mg	-0.0381	Negative	Repulsive	Repulsion (HIV therapy)	0.1333	Positive	Attractive	Attraction (surface coating)

			. GAM is a sort of a HAHART (Highly Active Herbal Antiretroviral). It therefore contains antiviral Terpenoids, Glycosides and Flavonoids.									
Drug 4	Single com-pound synthetic drug	Efv.	Efavirence	600mg	-0.0511	Negative	Repulsive	Repulsion (HIV therapy)	0.144	Positive	Attractive	Attraction (surface coating)
Drug 5	HARRT and FDC	ELT	Efavirence, Lamivudine & Tenofovir	1200mg	-0.053	Negative	Repulsive	Repulsion (HIV therapy)	0.1442	Positive	Attractive	Attraction (surface coating)

Table 4.28: Comparison between Blood and Drug interactions for a Surface Thermodynamic Interpretation and Significance							
S/n	Type of Interaction	Absorbance values, ā	Hamaker value & sign for interacting system	Van der Waals' Force	Nature of Interaction	Surface Energy of the infected blood	Significance
1	HIV NEGATIVE blood-Drug interactions $A_{131abs.}$ (Unf.Lymph.-Unf.Serum-Unf.Lymph) with Drugs.	Absorbance values increase. Tend to positive. maxima absorbance at a given wavelength	<u>Positive</u> 0.1349(D1) 0.1234 (D2) 0.1333 (D3) 0.1440 (D4) 0.1442 (D5)	Attractive	Attraction	the viral presence lowers the surface energy of infected blood samples	HIV Infection
2	HIV POSITIVE blood-Drug interactions $A_{132abs.}$ (Unf.Lympho.-Unf.Serum-Inf.Lympho) with Drugs.	Absorbance values decrease. Tend to negative. minima absorbance at a given wavelength.	<u>Negative</u> -0.0385 (D1) -0.0299 (D2) -0.0381 (D3) -0.0511 (D4) -0.0530 (D5)	Repulsive	Repulsion	Antiviral treatment increases the surface energy of infected blood samples	Solution to the Virus infection (a therapy)

Table 4.29: Comparison of the Hamaker constant A_{11} for drugs$_{1-5}$ in sterile water and computed corresponding γ_{sv} values.

Drug Number	Absolute $A_{11}(10^{-14}mJ)$	γ_{sv} (mJ/m^2)
D1	1.8536	7.42
D2	0.057	2.28
D3	0.1047	4.19
D4	0.4463	1.79
D5	0.636	2.54

Table 4.30: Comparison of the Hamaker constant A_{22} for INf.Lymphos. (with drugs$_{1-5}$), A_{33} for IS (with drugs$_{1-5}$) and computed corresponding γ_{sv} values.

Drug #	$A_{22}(x10^{-14}mJ)$: INf.Lymphos.	$\gamma_{sv}(mJ/m^2)$:	$A_{33}(x10^{-14}mJ)$: IS	$\gamma_{sv}(mJ/m^2)$
D1	0.1038	7.5640	0.0878	6.3958
D2	0.1135	8.2711	0.0955	6.9586
D3	0.1236	9.0103	0.1163	8.4715
D4	0.1072	7.8085	0.0808	5.8895
D5	0.1143	8.3284	0.0944	6.8816

The γ_{sv} for uninfected serum without drugs has been computed in this report to be 0.2446 mJ/m^2 and γ_{sv} for infected serum without drugs is $1.1189mJ/m^2$. Notice the increase effect of HIV on the surface free energy of serum. From table 4.30, the drugs used for experiments appreciably increased the surface free energies of all the infected serum samples.

Similarly, the γ_{sv} for uninfected lymphocyte without drugs has been computed in this report to be $0.6455mJ/m^2$ and γ_{sv} for infected lymphocyte (that has been on one or more ARt) but without experimental drugs is $30.437mJ/m^2$. Notice the increase effect of the ARts on the surface free energy of infected lymphocyte. From table 4.30, the drugs used for experiments appreciably reduced the surface free energies of all the infected lymphocyte samples.

Table 4.31: Comparison of the Hamaker constant A_{11} for UNf.Lymphos. (with drugs$_{1-5}$), A_{33} for US(with drugs$_{1-5}$) and computed corresponding γ_{sv} values.

Drug #	A_{11}(x10^{-14}mJ): UNf.Lymphos.	γ_{sv}(mJ/m^2):	A_{33}(x10^{-14}mJ): US	γ_{sv}(mJ/m^2)
D1	0.1278	9.3096	0.0487	3.5195
D2	0.1139	8.3011	0.0476	3.4721
D3	0.1873	13.6483	0.0913	6.6509
D4	0.4513	32.886	0.2797	20.3828
D5	0.5042	36.7178	0.321	23.3905

Table 4.32: Comparison of the Hamaker constant A_{11} for UNf.Lymphos. (without drugs), A_{33} for US (without drugs) and computed corresponding γ_{sv} values.

A_{11}(x10^{-14}mJ): UNf.Lymphos.	γ_{sv}(mJ/m^2):	A_{33}(x10^{-14}mJ): US	γ_{sv}(mJ/m^2)
0.0089	0.6455	0.0034	0.2446

Table 4.33: Comparison of the Hamaker constant A_{11} for INf.Lymphos. (without drugs), A_{33} for IS (without drugs) and computed corresponding γ_{sv} values.

A_{22}(x10^{-14}mJ): INf. Lymphos.	γ_{sv}(mJ/m^2):	A_{33}(x10^{-14}mJ): IS	γ_{sv}(mJ/m^2)
0.4177	30.4374	0.0154	1.1189

Table 4.34: Comparison of the Surface Free Energies, γ_{sv} for A_{11} UNf.Lymphos., A_{22} for INf.Lymphos., A_{33} for IS and US (with drugs$_{1-5}$), and computed corresponding γ_{sv} values.

Hamaker Variable (10^{-14}mJ)	HIV Infected (with Drugs)					HIV Uninfected (with Drugs)				
	D1	D2	D3	D4	D5	D1	D2	D3	D4	D5
$A_{11''}$ (Lymphocyte)						9.3	8.30	13.6	32.88	36.71
$A_{22''}$ (HIV)	7.56	8.27	9.01	7.8	8.32					
$A_{33''}$ (Serum)	6.39	6.95	8.47	5.89	6.88	3.52	3.47	6.65	20.3	23.3

Table 4.35: Comparison of the Surface Free Energies, γ_{sv} values for the HIV-Blood interacting systems (without drugs)

Inter-acting System	A_{11} ($x10^{-14}$mJ) (Lymph.)	γ_{sv} (mJ/m^2) (Lympho.)	A_{22} ($x10^{-14}$mJ) (HIV)	γ_{sv} (mJ/m^2) (HIV)	A_{33} ($x10^{-14}$mJ) (Serum)	γ_{sv} (mJ/m^2) (Serum)
Infected Blood	---	---	0.4177	30.437	0.0154	1.1189
Uninfected Blood	0.0089	0.6455	---	---	0.0034	0.2446

A virus has been known to lower the potential level of the naturally occurring surface free energy of a biological blood sample while a drug sample has the efficacy of either increasing or lowering the same SFE. Finally in table 4.35, the Hamaker constants and their corresponding Surface Free Energies are indicating the Constants and SFE for the uninfected lymphocyte and serum. The increased Constant and SFE for the infected lymphocyte and serum is most probably due to the fact that the patients has been on the intake of one or more antiretroviral drugs. Otherwise, HIV would drastically reduce a normal human lymphocyte SFE (of about 0.6455) down to 0.05 or less. It is interesting to note in table 4.35, that all drug samples naturally increased the surface free energies of blood components and this indicates potency of interaction.

Table 4.36: Computed $\Delta F^{adh.}$ Values for HIV- i.e.: Combined Hamaker coefficients (of interacting system with uninfected serum without Drugs)

Combined Hamaker coefficient Variable	Combined Hamaker coefficient Value	ΔF^{adh} (mJ/m^2) ($x10^{-14}$mJ)
A_{131}	0.0548	- 4.384

Table 4.37: Computed $\Delta F^{adh.}$values for HIV+ i.e.: Combined Hamaker coefficients (of interacting systems with Infected serum or Uninfected serum without Drugs)

Combined Hamaker coefficient Variable	Combined Hamaker coefficient Value ($x10^{-14}$mJ)	ΔF^{adh} (mJ/m^2)
$A_{132abs(is)}$	0.0144	- 1.2
$A_{132abs.(us)}$	0.0324	- 2.6
$A_{232abs.(is)}$	0.3645	- 29.2
$A_{232abs.(us)}$	0.4036	-32.3

Table 4.38: Computed $\Delta F^{adh.}$ Values for HIV- i.e.: Combined Hamaker coefficients (of interacting system with uninfected serum with $Drugs_{1-5}$)

Combined Hamaker coefficient	Combined Hamaker coefficient Value ($x10^{-14}$mJ)				
	D1	D2	D3	D4	D5
$A_{131abs.}$ Value	**0.1349**	**0.1234**	**0.1333**	**0.144**	**0.1442**
ΔF^{adh} (mJ/m^2)	-10.8	-9.9	-10.7	-11.4	-11.5

Table 4.39: Computed $\Delta F^{adh.}$ Values for HIV+ i.e.: Combined Hamaker coefficients (of interacting systems with infected serum or uninfected serum with $Drugs_{1-5}$)

Combined Hamaker coefficient	Combined Hamaker coefficient Value ($x10^{-14}$mJ)				
	D1	D2	D3	D4	D5
$A_{132(is)}$ Value	**-0.0031**	**0.0055**	**0.0074**	**0.0081**	**0.0134**
ΔF^{adh} (mJ/m^2)	0.25	- 0.44	- 0.59	- 0.65	- 1.07
$A_{132(us)}$ Value	-0.0385	-0.0299	-0.0381	-0.0511	-0.053
ΔF^{adh} (mJ/m^2)	3.08	2.39	3.05	4.09	4.24
$A_{232(is)}$ Value	**0.004**	**0.0058**	**0.0108**	**0.0037**	**0.0042**

ΔF^{adh} (mJ/m^2)	-0.32	- 0.46	- 0.86	- 0.3	- 0.34
$A_{232(us)}$ Value	0.0853	0.0873	0.1129	0.2123	0.258
ΔF^{adh} (mJ/m^2)	- 6.82	- 6.98	- 9.03	- 16.9	- 20.64

In tables 4.36 to 4.39 all the ΔF^{adh} (mJ/m^2) with a negative sign (obtained with positive coefficients), implies that adhesion is thermodynamically favorable. This is to say that adhesion is naturally governed by attraction van der Waal forces.

The changes in surface free energies of adhesion for:

1. HIV- blood sample without drugs is – 4.384mJ/m^2 (see table 4.36). This means that there is a natural force of adhesion existing between the particles of serum and lymphocyte.

2. HIV positive blood samples ($A_{232abs.}$ or $A_{132abs.}$ (with or without infected or uninfected serum):
    - D1 = between 3.08 and -6.82mJ/m^2
    - D2 = between 3.88 and -6.98mJ/m^2
    - D3 = between 3.05 and -9.03mJ/m^2
    - D4 = between 4.09 and -16.9mJ/m^2
    - D5 = between 4.24 and -20.64mJ/m^2

The interpretation is that the particles of all the drugs being additives in the serum are attracted and adhere to the lymphocyte particle. Without drug, the normal human serum is seen to have a change in free adhesion force with the lymphocyte (and most probably with other blood components), of a – 4.384mJ/m^2 value. This is significantly increased for all infected samples with drugs.

3. HIV negative blood samples, $A_{131abs.}$ (with uninfected serum):
    - D1 = - 10.8mJ/m^2
    - D2 = - 9.9mJ/m^2
    - D3 = - 10.7mJ/m^2

- D4 = - 11.4mJ/m^2
- D5 = - 11.5mJ/m^2

The interpretation is that the particles of all the drugs being additives in the serum and having coated the lymphocyte particle, repels the HIV. The more the values tent to zero, the stronger is their adhesion property.

Table 4.40: Descending order of comparison of ΔF^{adh} (mJ/m^2) beginning with the most effective in adhesion.

Drug Number #	ΔF^{adh} (mJ/m^2) with a negative sign
D2	-9.9
D3	-10.7
D1	-10.8
D4	-11.4
D5	-11.5

Table 4.41: Comparison of A_{132abs} HIV+ with infected serum (that is being treated with one or more of Synthetic drugs) (Ani, 2015) and experimental drugs in interaction.

$A_{132abs.}$ (x10^{-21}Joules):Synthetic (Ani, 2015)		$A_{132abs.(is)}$ (x10^{-21}Joules): Drugs	
D1	0.40951	D1	-0.0031 (Herbal)
D2	0.10270	D2	0.0055 (Herbal)
D3	- 0.25051	D3	0.0074 (Herbal)
D4	0.07160	D4 (Ani's D4)	0.0081(Synthetic)
D5	- 0.10401	D5 (Ani's D2)	0.0134(Synthetic)

Table 4.42: Comparison of A_{131abs} (HIV-) of Synthetic and Herbal drugs in interaction

$A_{131abs.}$ ($x10^{-21}$Joules):Synthetic (Ani.2015)		$A_{131abs.}$ ($x10^{-21}$Joules):Herbal	
D1	0.36760	D1	0.1349
D2	0.46337	D2	0.1234
D3	0.53021	D3	0.1333
D4	0.50971	D4 (Ani, 2015) D4	0.144 (Synthetic)
D5	0.49599	D5 (Ani, 2015) D2	0.1442 (Synthetic)

The A_{132abs} values of HIV+ samples that may be zero or are positive but tending to zero, implies repulsion. The A_{131abs} values of HIV- samples that are zero or positive but tending to zero, imply attraction for binding. Therefore, A_{131abs} values of HIV- samples that are negative but tending to zero imply repulsion. For the HIV- samples different drugs have different natures in interaction. All the antiviral drugs are positive indicating that the drug particles have good adhesive or binding or coating properties on lymphocyte particles.

4.7 Results for Phytochemical and Fourier Transform Infra-red Characterization of the Herbal drugs.

A. Phytochemical Results

Table 4.43: Phytochemical concentrations in the different herbal extracts, expressed in µg/g

Drug No.	Name of Herb/Drug	Name of Specie	Abrv.	Source of Herb	Active Compo-nents	Conc. (µg/g) in 10ml of H_2O	% Compo-sition	% Conc. (µg/g) in 0.2ml of H_2O
D1	Garcinia kola	Garcinia mannii	GK	Ubahu, Okigwe Imo state	Alkaloid	3.42	0.43	0.07
D2	Azaradichta indica	Azaradichta indica	AI	Amachara, Afikpo	Phenol	0.0103	0.001	0.0002
					Flavonoid	0.0533	0.005	0.0011

				Ebonyi state	Tannin	0.0183	0.002	0.0004
D3	Garcinia + Azaradichta + Mangifera	Hybrid formular	**GAM**	As with D1 & D2.	Alkaloid	1.87	0.066	0.037
					Phenol	1.03	0.04	0.021
					Flavonoid	5.33	0.19	0.107
					Tannin	1.83	0.065	0.037
					Alkaloid	0.0084	0.0003	0.0002
D4	Efavirenz	Synthetic	Efv	HETERO LABS. Ltd. India	Efavirenz	600	100	12
D5	Efavirenz + Lamivudine + Tenofovir	Synthetic	ELT	HETERO LABS. Ltd. India	Efavirenz	600	50	12
					Lamivu-dine	300	25	6
					Tenofovir	300	25	6

The table 4.43 shows the different phytochemicals present in 1 g each of the herbal substances, the single active compounds in the two HAARTs used for experiments and the percentage concentrations in 0.2 ml of the 3rd serially diluted drugs' sample used to inoculate collated blood samples.

B. Fourier Transform Infra-red results

- **Garcinia kola**

Table 4.44: Functional Groups present in Garcinia kola

Wave number (cm^{-1})	Functional Group	Stretching Band
768.5974	Aromatic ring	C-H bend
888.3422	"	"
1291.083	Carboxylic acid	O-H
1410.679	Alkanes	CH_2 bend
1622.881	Amides	N-H stretch
1821.905	Ester	C-O bend
2040.11	Nitrile	C-N stretch
2258.835	"	"
2429.158	"	"
2593.207	"	"

2705.259	Aldehydes	C-H stretch
2823.012	“	“
2921.723	Alkanes	CH_2 bend
3039.511	Alkanes	Alkanes
3177.987	Quinine	O-H bend
3378.687	“	O-H bend
3484.47	“	“
3698.836	Amides	C=O stretch
3808.766	“	C=O stretch

In the table 4.44, high peaks occurring at higher wavenumbers indicate high energy band transmissions of those functional groups that are highly interactive. The highest peaking at a high wavenumber indicate a strong active phytochemical and in the case of Garcinia kola, the Alkaloids are known to interact actively with viral particles. The other peaks are possibly Phenols, Flavonoids and Tannins which are equally effective in interacting with viruses especially the HIV. See appendix T for graphical plots of the functional groups that indicate bends and stretches.

- **Azaradichta Indica**

Table 4.45: Functional Groups present in Azaradichta Indica

Wavenumber (cm^{-1})	Functional Group	Stretching Band
710.8826	Aromatic rings	C-H stretch
868.3987	“	“
1014.177	Esters	C-O stretch
1381.042	“	“
1428. 126	Alkanes	CH_2
1616.964	Amides	N-H stretch
1898.87	Esters	C-O stretch
2129.929	Nitriles	C=N stretch
2253.1885	“	C=N stretch
2440.312	“	“
2573.485	“`	“
2648.361	Aldehydes	C-H stretch
2764.288	Aldehydes	C-H stretch

3000.523	Alkanes	“
3212.348	“	“
3307.295	Quinines	O-H stretch
3486.425	“	O-H stretch
3591.526	Amides	C=O stretch
3711.949	“	“

Table 4.45, shows high peaks occurring at higher wavenumbers indicating high energy band transmissions of those functional groups that are highly interactive. The highest peaking at a high wavenumber indicates a strong active phytochemical and in the case of Azaradichta indica, the Phenols, Flavonoids and Tannins are known to interact actively with viral particles. The other peaks are possibly Alkaloids which are equally effective in interacting with viruses especially the HIV. See appendix T for graphical plots of the functional groups that indicate stretches.

- **Mangifera Indica**

Table 4.46: Functional Groups present in Mangifera Indica

Wavenumber (cm^{-1})	Functional Group	Stretching Band
851.9943	Amines	N-H bend
1312.29	Esters	C-O stretch
1437.719	Alkanes	CH_2 bend
1625.077	Amides	N-H stretch
1895.577	Esters	C-O stretch
2023.149	Nitriles	C-N stretch
2104.977	“	“
2217.26	“	“``
2457.086	“	“
2565.551	“`	“
2744.525	Aldehydes	C-H stretch
2914.173	Alkane	C-H bend
3090.849	Quinine	O-H bend
3209.687	“	“
3301.278	“	“
3409.947	Carboxylic acid	O-H bend
3556.461	Amides	C=O stretch

Table 4.46 similarly, shows high peaks occurring at higher wavenumbers indicating high energy band transmissions of functional groups that are highly interactive. The highest peaking at a high wavenumber indicates a strong active phytochemical and in the case of Mangifera indica, the Alkaloids also known to interact actively with viral particles. The other peaks are possibly Phenols, Flavonoids and Tannins which are equally effective in interacting with viruses especially the HIV. See appendix T for graphical plots of the functional groups that indicate bends and stretches.

4.8 Results of Statistical Analysis of Variance (ANOVA)

i. HIV infected ($A_{132abs.}$) blood sample

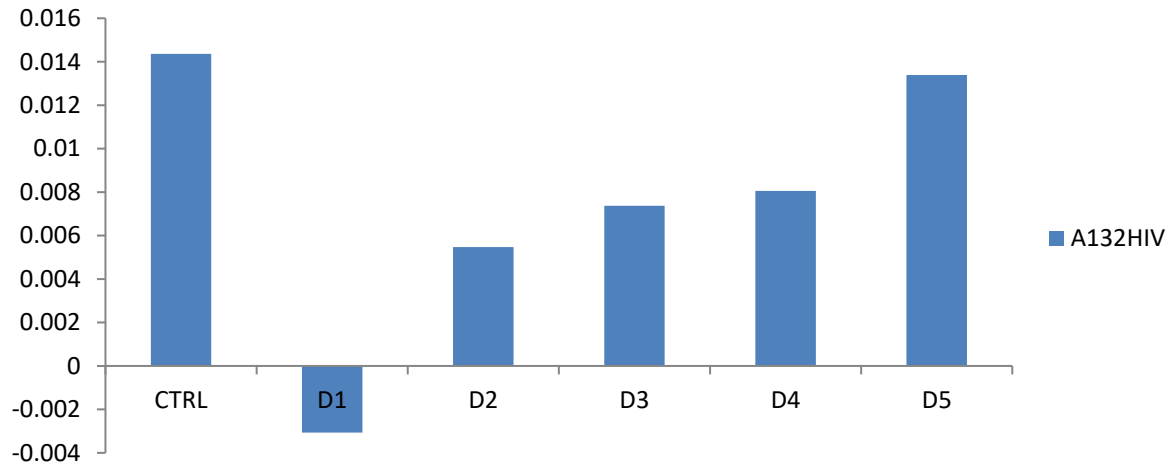

Figure 4.56: HIV+ samples with $Drugs_{1-5}$

Figure 4.56 showed that in a two HIV particles interaction with drugs, D1 on the negative has a repelling potency when compared to a HIV interaction without drug that showed a high level of attraction to a lymphocyte by being on the positive. D2 –D5 have good coating properties at the level of their bars. Notice that D1(Garcinia kola/Akilu) has a unique repelling property. Herbal drugs 2 & 3 compares favorably with antiretroviral synthetic drugs 4 & 5. Actual results are shown on appendix U.

ii. HIV Uninfected ($A_{131abs.}$) blood sample

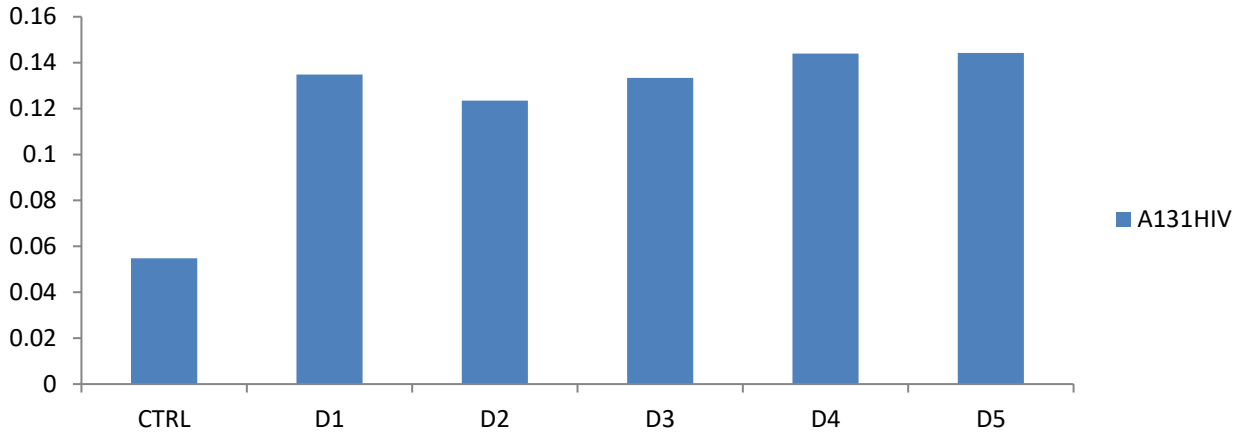

Figure 4.57: HIV- samples with Drugs$_{1-5}$

For a HIV negative blood interaction with drugs, it was expected that all drugs showed positive signs of adhesion to the uninfected lymphocyte well above the control without drugs. All herbal drugs 1, 2 & 3 compared well with synthetic drugs 4 & 5.

iii. HIV infected ($A_{232abs.}$) blood sample

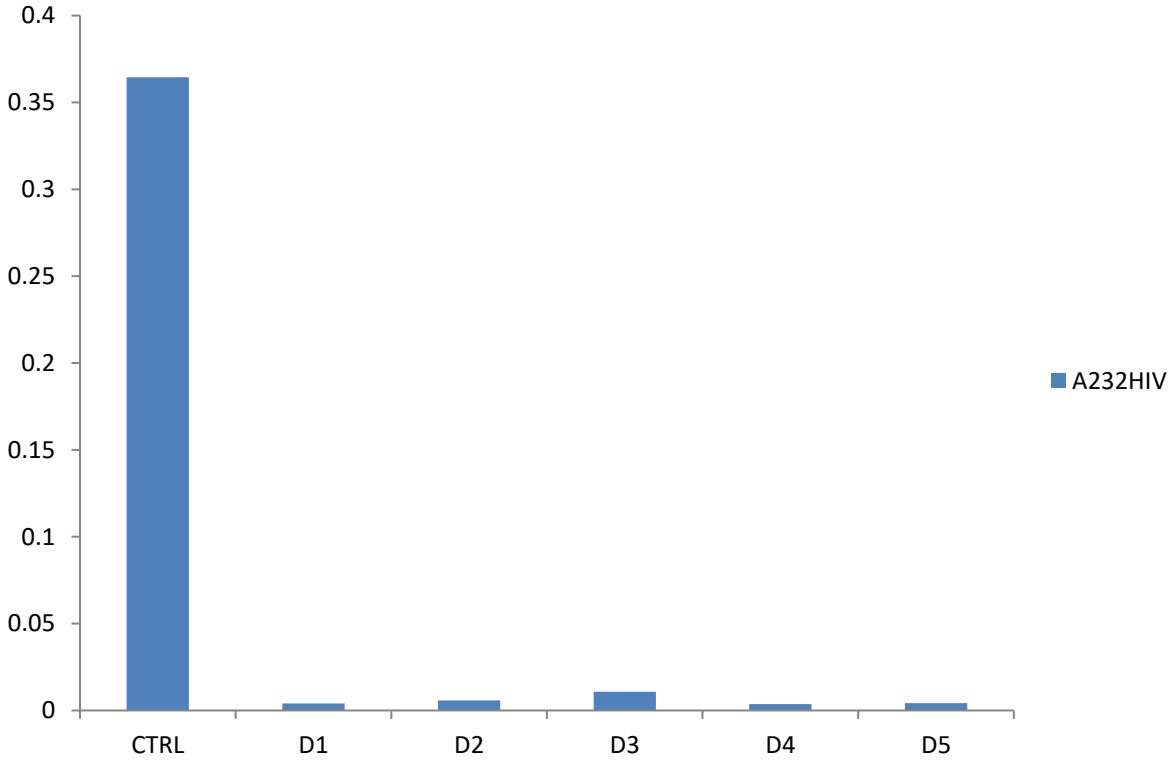

Figure 4.58: HIV+ samples with Drugs$_{1-5}$

similar to the interpretation under figure 4.56, in a 3-HIV particles interaction with drugs, all levels lie low indicating the dangerous effect of the virus. Though the drugs exhibit binding properties, these were not comparable to the interaction with less load of the virus in the blood.

iv. Combined Hamaker coefficients of all interacted blood samples with drugs$_{1\text{-}5}$

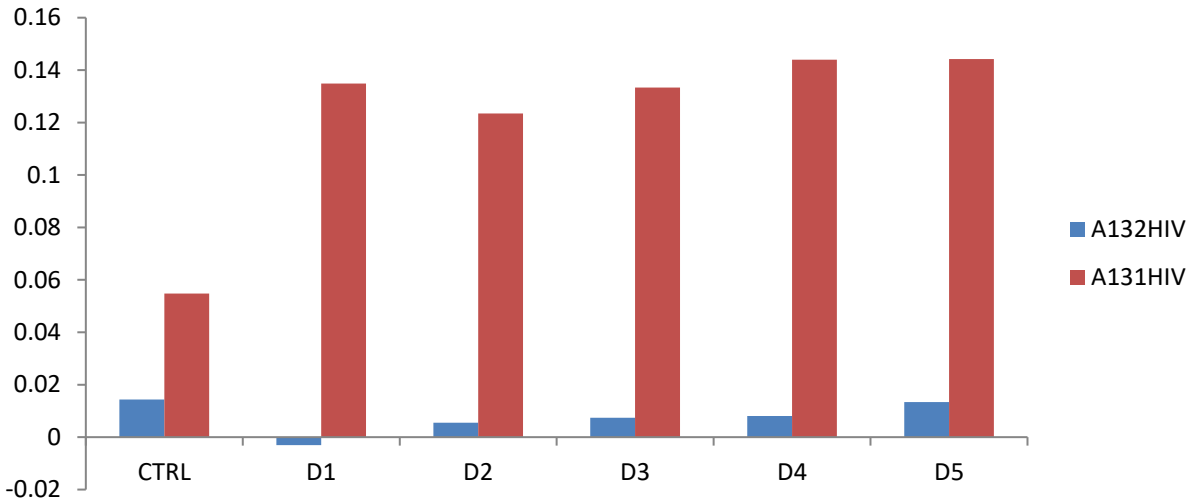

Figure 4.59: HIV+ (A_{132}) & HIV- samples with Drugs$_{1\text{-}5}$

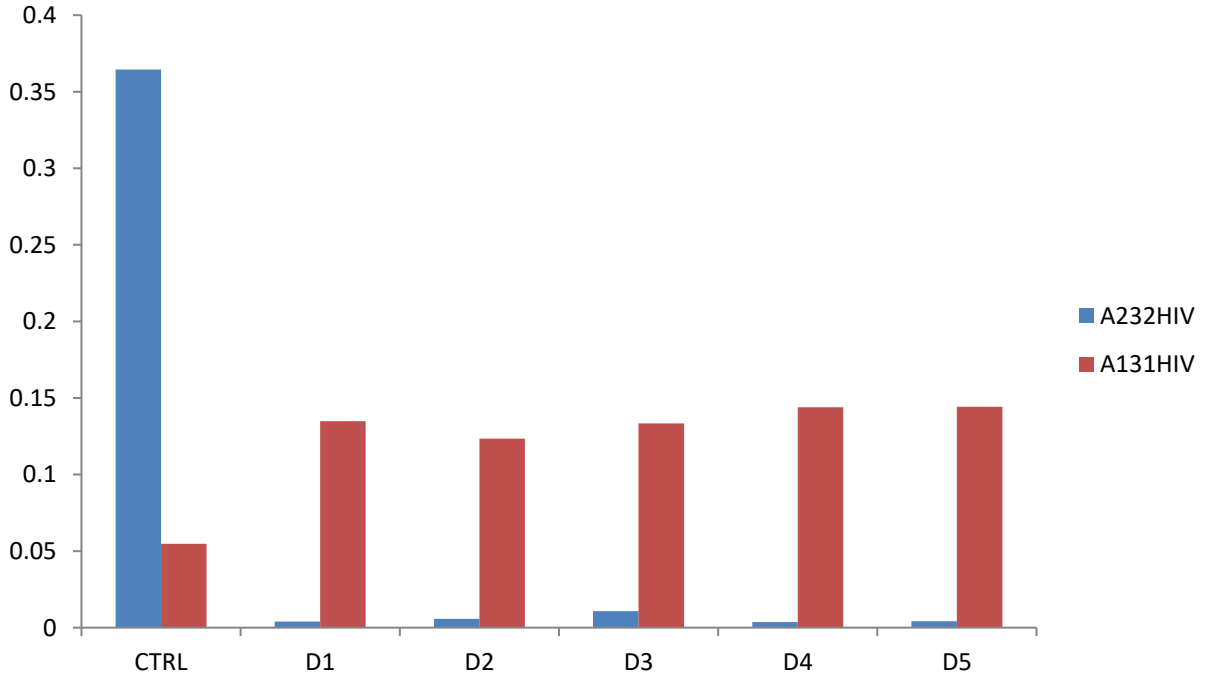

Figure 4.60: HIV+ (A_{232}) & HIV- samples with Drugs$_{1\text{-}5}$

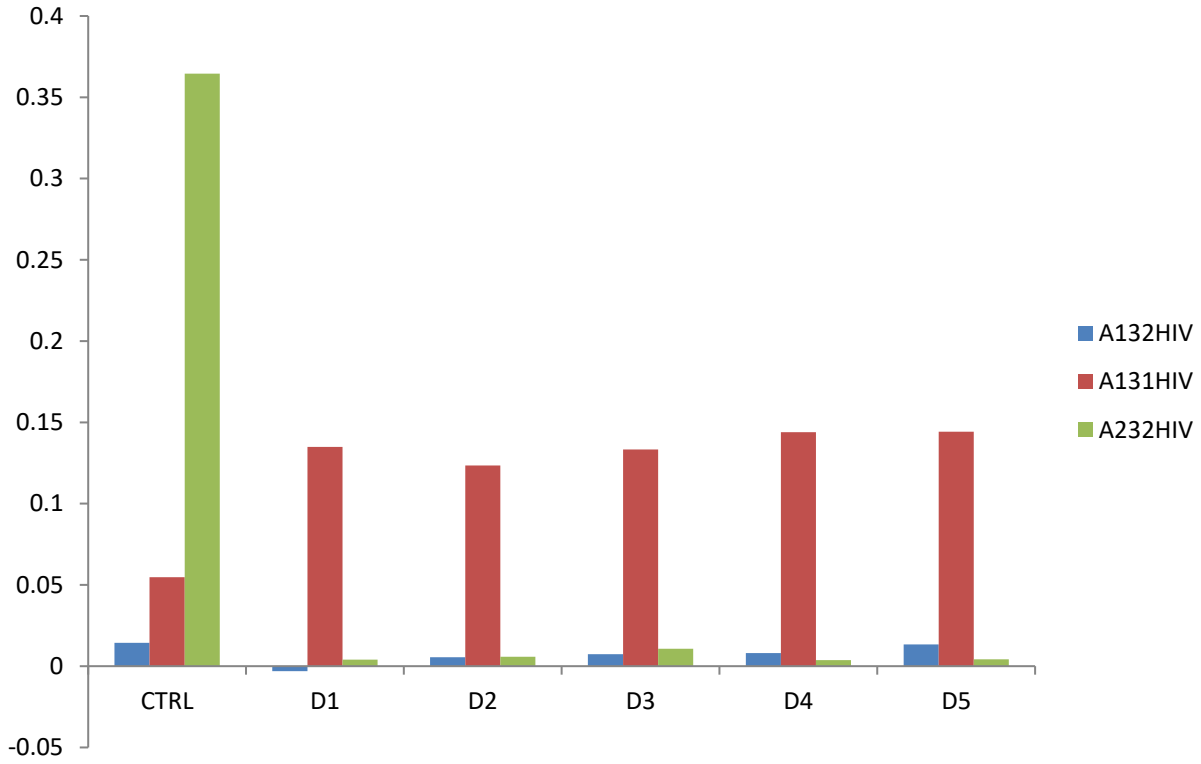

Figure 4.61: HIV+ samples with Drugs$_{1\text{-}5}$

Table 4.47: Summary for ANOVA results

Hamaker parameter variable	Control: D0	D1	D2	D3	D4	D5	$LSD_{0.05}$
A_{132} HIV+	0.0144^{2}_{2}	-0.0031^{1}_{1}	0.0055^{1}_{2}	0.0074^{1}_{2}	0.0081^{1}_{2}	0.0134^{1}_{2}	0.0152
A_{131} HIV-	0.0548^{1}_{1}	0.1349^{2}_{2}	0.1234^{2}_{2}	0.1333^{2}_{2}	0.0144^{2}_{2}	0.01442^{2}_{2}	0.0195
A_{232} HIV+	0.3645^{2}_{2}	0.0040^{1}_{1}	0.0058^{1}_{1}	0.0108^{1}_{1}	0.0037^{1}_{1}	0.0042^{1}_{1}	0.0970
$LSD_{0.05}$	0.1377	0.0134	0.0134	0.0165	0.0144	0.0158	

Superscripts indicate significant difference among parameters at 5% significance level ($P < 0.05$). Subscripts indicate significant difference among parameter levels at 5% significance level ($P < 0.05$).

LSD $\Rightarrow$ Least Significant Difference. Columns 2, 3, 4, 5, 6, 7 are the parameter levels = 6.

The ANOVA result on appendix U showed that there is significant difference among the combined Hamaker coefficients A_{132} HIV+, A_{131} HIV- and A_{232} HIV+ at 5% level of

significance. This implies that at least one of the combined Hamaker coefficients differs significantly. Also, the ANOVA results on appendix U showed that there is significant difference among the combined Hamaker coefficient parameter levels; control, D1, D2, D3, D4 and D5. Since the ANOVA showed significant difference at 5% level of significance, the multiple comparison test (least significant difference test) was performed to determine the combined Hamaker coefficients and their levels that differ significantly from others.

The summary of the statistical result based on the collected experimental data shown on table 4.47 shows evidence of statistical difference due to the different natures of the interacted systems. For the A_{132}HIV+ (assuming 1 virus particle), the result shows significant difference ($p < 0.05$) among the drugs with the control. This implies that the effect of coating by drugs D2 – D5 being positive are the same with the control but with no significant difference in reducing the viral load. D1 has a significant effect in repulsion by being negative and at the same time will have a reducing control on the virus level (from subscript 2 to 1). A_{131}HIV- with D1 – D5 shows improved effects on samples over the control, while A_{232}HIV+ (assuming 2 virus particles) all drugs have lowered effects showing that the virus is dominating their effects.

A novel investigation has been attempted. However, the blood components are not homogeneous substances, that is, they are multi-component systems in their own right. Hence, the isolation of active single particles or even the HIV particle is not within the scope of this research. HIV infected samples were obtained from individuals already being treated with anti-retroviral hence, the underlying effects of the existing ARTs is not considered. The use of optical UV spectrophotometer is with respect to the fact that the interacting particles have dimensions that are different by several orders of magnitude but ideally considered as single particles.

CHAPTER FIVE
CONCLUSION AND RECOMMENDATIONS

5.1 Conclusion

The combined Hamaker coefficient, A_{132abs} obtained for each of the five antiviral drugs interacted with the ten infected human blood components (that are being treated with one or more known synthetic antiretroviral drugs) were: D_1 = - 0.0031 $\times 10^{-21}$Joules, D_2 = 0.0055 $\times 10^{-21}$Joules, D_3 = 0.0074 $\times 10^{-21}$Joules, D_4 = 0.0081$\times 10^{-21}$Joules, D_5 = 0.0134 $\times 10^{-21}$Joules. The interacting systems of uninfected lymphocyte-infected serum-infected lymphocyte and HIV (2) (contained in the infected lymphocyte, since there is not yet a known method of isolating the HIV from the infected lymphocyte)], involving drug 1 gave negative absolute combined Hamaker coefficient values – A_{132abs} indicating a repulsion between the HIV particle (2) in the infected lymphocyte and the particle (1) of uninfected lymphocyte when the intervening serum medium (3) was containing a particle of the drug 1. Equally, the same interacting systems involving drugs 2, 3, 4 and 5 gave positive absolute combined Hamaker coefficient values +A_{132abs} indicating an attraction between the drugs' particles (3) contained in the intervening serum medium and the particles (1) of uninfected lymphocyte thereby causing a repulsion of the HIV particle (2) infested lymphocyte.

Similarly, the combined Hamaker coefficient, A_{131abs} obtained for each of the five antiviral drugs interacting with the ten uninfected human blood components were: D_1 = 0.1349$\times 10^{-21}$Joules, D_2 = 0.1234 $\times 10^{-21}$Joules, D_3 = 0.1333$\times 10^{-21}$Joules, D_4 = 0.144$\times 10^{-21}$Joules, D_5 = 0.1442 $\times 10^{-21}$Joules. The interacted systems of uninfected lymphocyte-uninfected serum-uninfected lymphocyte [assuming one particle each of uninfected lymphocyte (1), drug (3) (contained in the intervening serum medium), and another uninfected lymphocyte (1)], involving drugs 1, 2, 3, 4, 5 all gave positive absolute combined Hamaker coefficient values indicating attraction of the drug particle (3) contained in the serum by uninfected lymphocyte particle (1). This phenomenon is responsible for the coating of a lymphocyte by the drug.

The defined absolute values of the combined Hamaker coefficient, A_{232abs} obtained for each of the five antiviral drugs interacted with ten infected human blood components were: D1 = 0.004 $\times 10^{-21}$Joules, D2 = 0.0058$\times 10^{-21}$Joules, D3 = 0.0108$\times 10^{-21}$Joules, D4 = 0.0037 $\times 10^{-21}$Joules, D5 = 0.0042 $\times 10^{-21}$Joules.

A_{131abs} of D1, D2, D3, D4 and D5 were all greater than their corresponding A_{232abs}. This indicates that D1, D2, D3, D4 and D5 encourage attraction or coating of lymphocyte particles by the drug particles and this protects uninfected lymphocyte particles. This result is hoped to accurately predict the solution mechanism for the HIV scourge.

In summary, the major criteria for drug efficacy using the thermodynamic prediction by the Hamaker models are as follows:

- Negative $A_{132abs.}$ (for any HIV+ sample) $\Rightarrow$ repulsion (of HIV particle$_2$ in lymphocyte, by drug particle$_3$ in serum).
- Positive $A_{132abs.}$ (for any HIV+ sample) $\Rightarrow$ attraction (of uninfected lymphocyte particle$_1$ by drug particle$_3$ in serum)
- Positive $A_{131abs.}$ (for any HIV- sample) > Positive $A_{232abs.}$ (for any HIV+ sample) $\Rightarrow$ attraction (of uninfected lymphocyte particle$_1$ by drug particle$_3$ in serum)
- Positive $A_{131abs.}$ (for any HIV- sample) < Positive $A_{232abs.}$ (for any HIV+ sample) $\Rightarrow$ repulsion (of uninfected lymphocyte particle$_1$, by drug particle$_3$ in serum)

Generally an interaction of three solid particles generates positive and negative forces or charges of which, if any particle 1, 2 or 3 naturally existing with the POSITIVE force, is equal and opposite to any particle 1, 2 or 3 naturally existing with the NEGATIVE force, an attraction force fills the vacuum between the two particles of opposite forces. The particle that possesses the greater surface free energy moves faster in the attraction influence towards the other particle that naturally possesses the lesser surface free energy, just like in a diffusion process. The immediate result of this interaction becomes attachment or coating of the less by the great. At the same interaction time, the third particle possessing a lesser identical force of the same positive force is repelled by the same equal momentum with which it is being attracted to the negative force. This repulsion leaves the third particle in an orbit of constant repulsion as long as the concentration of the surface free energy of the positive force is greater than that of the negative force. This is the concept which Neumann & Omenyi (1981) have established experimentally with bio-particles, (Achebe, 2010) established theoretically with the HIV particle, Ani (2015) established experimentally with known synthetic pharmaceutical antiretroviral drugs on HIV infected and uninfected blood samples, Chukwuneke (2015) established experimentally an attraction interaction between mycobacterium tuberculosis-Human sputum-HIV particles, and potency is being established here experimentally with natural 'herberceutical' antiviral drugs on HIV.

Considering the thermodynamic nature of interactions of all experimental herbal additives, it is believed that they would be effective in controlling HIV in comparison with known antiretroviral drugs used as controls in the same experiment. From calculated values and their interpretations: Herbal D_1: (Akilu) compared favorably with Lamivudine/Nevirapine/Zidovudine (Ani, 2015).

Herbal D_2: (Dogonyaro) is relatively potent as Tenofovir/Lamivudine/Efavirenz, Nevirapine and Lamivudine (Ani, 2015). Herbal D_3: (Akilu + Dogonyaro + Mango) is comparable with the synthetic Efavirenz (Ani, 2015).

5.2 Contributions to Knowledge

The following are contributions this work has made to the body of existing knowledge:

i. The effect of antiviral herbal drugs in an in-vitro interaction with blood samples has been determined using the surface thermodynamics criteria.

ii. The surface free energies and Hamaker coefficients of the individual known herbal drugs have also been determined.

5.3 Recommendations

It would be necessary to carry out repeated and further research on this study area. This will ensure continuity and advancement beyond the frontiers that this work has attained. However, the following recommendations are made:

- Further research based on the Contact Angle approach, (an alternative method to the spectrophotometry and a confirmatory means of determining the absolute combined Hamaker coefficients of the HIV and a drug-coated blood interaction system) should be done for a verification and validation of the results obtained in this study.

- Efforts should be made towards using in-vivo experimentation for a better understanding of drugs' mechanism of action as antivirals. The concept of negative combined Hamaker coefficient A_{132abs} and increased surface free energy of HIV infected systems to determine the efficacy or effectiveness of other herbal antiviral drugs in comparison to existing manufactured synthetic antiretroviral drugs for the treatment of HIV, Ebola virus disease (EVD) and Lassa fever. This should involve a synergy or team of medical personnel like pharmacists, pharmacologists, laboratory scientists, medical doctors, engineers and physicists that would answer various questions about suitability of specified material(s) and toxicity.

- There should be a further study to determine the efficacy or effectiveness of the herbal and synthetic drugs usable for the treatment of other blood-related diseases like malaria

using the concept of Hamaker coefficient approach as a thermodynamic modelling tool to study the interaction processes.

References

Alderman, L.M. (1988): On the maintenance of T-cell populations. Technical report, Los Angeles University of California, department of computer science.

Abbas, A.K. (2003): Cellular and molecular immunology. 5th edition. Philadelphia, PA London W. B. Saunders.

Achebe, C. H. (2010): Human Immunodeficiency Virus (HIV)-Blood Interactions: Surface Thermodynamics Approach. Ph.D. dissertation, Nnamdi Azikiwe University, Awka, Anambra state Nigeria.

Ani, O. I. (2015): Surface Energetics study of the interactions between HIV and Blood cells treated with antiretroviral drugs. Ph.D. dissertation, Nnamdi Azikiwe University, Awka, Anambra state Nigeria.

Baier, R.E., Shafrin, E.G. and Zisman, W.A. (1968): Science journal. Vol.162 p. 1360.

Baier, R.E., Bull, N.Y. (1972): Journal of Academic medicine. Vol.48 p.257

Barre-Sinoussi F., Chermann J.C., Rey, F., Nugeyre, M.T., Chamaret, S., Gruest, J., Dauguet, C., Axler-Blin, C., Vezinet-Brun, F., Rouzioux, C., Rozenbaum, W., and Montagnier, L. (1983): Isolation of a T-Lymphotropic Retrovirus from a patient at risk for acquired immune-deficiency syndrome (AIDS). Science 220: 868-870.

Bragardo, M., Buonfiglio, D. Et al. (1997): Modulation of Lymphocyte interaction with endothelium and homing by HIV-Glycoprotein 120. Journal of immunology. Vol. 159 No.4 pp. 1619-1627.

Berahou (2007); Omar, M.I.Y. (2003): Studies on the antiviral effect of some plant derived compounds. A Ph.D. Thesis, Faculty of Veterinary medicine, Cairo University.

Bai, Yu (2013): Covalent fusion inhibitors targeting HIV-1 gp41 deep pocket. The forum for amino acid, peptide and protein research. Vol.44 No.2 p.701

Churaev, N.V. (1974): Journal of colloidal and interface science. USSR Vol. 36 p. 287

Chattopadhyay U., Das S., Guha S., Ghosal S. (1987): Cancer Lett. Vol.37 p.293

Connor, E.M., Sperling, R.S., Gelber, R., Kiselev, P., Scott, G.O., Sullivan, M.J. (1994): Reduction of maternal-infant transmission of human immunodeficiency virus type 1 with Zidovudine treatment. Padiatric AIDS Clinical trials group protocol076 study group. N England J Med. Vol. 331 pp. 1173-1180

Chaudhury, A. (2005): The Nef protein of HIV-1 induces loss of cell surface stimulatory molecules CD80 and APCs. Journal of Immunology 2005. 175. 4566-4574.

Chukwuneke, J. L. (2016): Mycobacterium tuberculosis (M-TB)-Human sputum interactions: Surface thermodynamics approach. Ph.D. dissertation, Nnamdi Azikiwe University, Awka, Anambra state Nigeria.

Deryagin, B.V. et al. (1954): Journal of colloidal and interface science. USSR Vol. 206 p.1145

Dalgleish, A.G., Beverley,P.C., Clapham, P.R., Crawford, D.H., Weiss, R.A., Alex, R.(1985): The CD4 (T4) antigen is an essential component of the receptor for the AIDS retrovirus. Nature journal 1984 Dec. 20 – 1985 Jan. 2; 312(5996): pp. 763-767

Darbyshire, J. (1995): Perspectives in drug therapy of HIV infection. Drugs 49 Suppl 1: 1-3; discussion 38-40

De, C.E., (2000) "A pharmaceutical being used for treating HIV infection is provided which has the following peptide sequence". Rev. Med. Virol. 10 (4): 255-77.Interscience, New York

Dixon, (2001); Guo et al., (2006); Omar, M.I.Y. (2003): Studies on the antiviral effect of some plant derived compounds. A Ph.D. thesis, Faculty of Veterinary medicine, Cairo University.

Dike, S., Huang, Larry L., Davis, Nicollette, and Omenyi, S. N. (2002): An Estimate of Reasoned Baseline on Patient Load Testing. Journal of American Medical Association.

Donatus, E.O. And Vitus, E. (2008): Evaluation of the Phytochemical Composition of Mango (Mangifera Indica Linn) Stem bark and Leaves. Int'l Journal of Chemical Sci.: 6(2) 705-716.

Dejesus, E., Young, B., Morales-Ramirez, J.O., Sloan, L., Ward, D.J., Flaherty, J.F. (2009): Simplification of antiretroviral therapy to a single-tablet regime consisting of Efavirenz,

Emtricitabine and Tenofovir disoproxilfumarate versus unmodified antiretroviral therapy in virology suppressed HIV-1 infected patients. Journal of Acquired Immune Deficiency Syndrome. Vol. 51 pp. 163-174.

Edoga (2005): Phytochemical constituents of some selected medicinal plants. African journal of Pure and Applied Chemistry. Vol.3 No.11 pp.228-233.

Furman, P.A., Fyfe, J.A., St. Clair, M.H., Weinhold, K., Rideout, J.L., Freeman, G.A. (1986): Phosphorylation of 30-azido-30-deoxythymidineand selection interaction of the 50-triphosphate with human immunodeficiency virus reverse transcriptase. Proc Natl. Acad. of Sci. USA. Vol. 83 pp. 8333-8337.

Fowkes, F.M. (1967): Journal of surface and interfaces. Vol.1 J.J. Burke ed. Syracuse University press, New York pp. 199-197

Fields, B. N., (2007): Field's Virology, 5th edition. Edited by David, M. Knipe; Peter, M. Howley; Diane, et al., Philadephia, PA London.

Freeman Morgan (2019): Through the wormhole. Scientific documentary of the Discovery Family Dstv. © 2019 series on channel Dstv.

Guha S., Ghosal S., Chattopadhyay U. (1996): Chemotherapy. Vol.42 No. 6 pp.443-451.

Gulick, R.M., Mellors, J.W., Havlir, D., Eron, J.J., Meibohm, A., Condra, J.H. (2000): 3-year suppression of HIV viremia with Indinavir, Zidovudine and Lamivudine. Ann Inter Med. Vol. 133 pp.35-39.

Gross (2007): Studies on the antiviral effect of some plant derived compounds. A Ph.D. thesis, Faculty of Veterinary medicine, Cairo University.

Gulluce (2004) in: Omar, M.I.Y. (2003): Studies on the antiviral effect of some plant derived compounds. A Ph.D. Thesis, Faculty of Veterinary medicine, Cairo University.

Garima P., Verma K. K., Munua S. (2014): Evaluation of phytochemical, antibacterial and free radical scavenging properties of Azadirachta indica (Neem) leaves. Int'l J. Of Pharm. & Pharm. Scis. Vol.6 No.2 ISSN: 0975-1491.

Hamaker, H.C. (1937): Phisica. Vol. 4 p. 1058.

Hough, D.B. and White, L.B. (1980): Advanced Colloid interface Science, 14.

Horn, R.G. (1990): Surface forces and their action in ceramic material. Journal of American ceramic society. Vol. 73 No.5 pp. 1117-1135.

Hart, D.N. (1997): Dendritic cells, unique Leukocytes population which control the primary response blood. Journal of immunology. Vol.90 pp.3345-3287.

Haidari (2009): Studies on the antiviral effect of some plant derived compounds. A Ph.D. thesis, Faculty of Veterinary medicine, Cairo University.

Hraba, T. And Dolezal, J. (2009): A mathematical model and CD4 Lymphocyte dynamics in HIV infection. EID vol.2 No.4

Israelachivili, J.N. (1972): Proc. Royal social services A. Vol. 331 p. 39

Igboko A. O., (1983): Phytochemical studies in Garcinia kola (Hekel). Msc. Thesis. University of Nigeria Nsukka (unpublished).

Iwu M.M. (1985): Antihepatotoxic constituents of Garcinia kola seeds. Experiential Vol.41 pp. 699-700

Iwu MM. (1986): Biflavanones of Garcinia: Pharmacological and biological activities. In "Plants Flavonoids in Biology and Medicine: Biochemical, Pharmacological, and Structure-Activity Relationships". Pp. 485-488. Cody V. Middleton E. Harborne JB Eds. Alan R. Liss NY.

Iwu M.M. (1993): Pharmacognotical properties of selected medicinal plants. In: Handbook of African medicinal plants. CRC Press, Boca Raton, Florida: 183

Iwu, M.M. (1993): Ebola cure hope. BBC Health News; Thursday 5th August 1999 at the 16th International Botanical congress in St. Louis USA.

Ibironke GF.,Olaleye SB., Balogun O., and Aremu DA. (1997): Antiucerogenic effect of diets containing seeds of Garcinia kola (Hekel). Phytotherapy research. Vol.11 pp.312-313

Joseph, O. N. (2011): Potential anticancer and antiviral agents from West Africa phytochemicals. University of Nigeria press ISBN: 978-978-53040-4-6

Jon C. Tilbourt and Ted J. Kaptchuk (2008): Herbal medicine research and global health: an ethical analysis. Bulletin of the World Health Organization>Past issue>volume 86; 2008>volume 86, number 8, August 2008, 577 – 656.

Krupp H., (1967): Advances in Colloid Interface science. Vol.1, p. 111

Kruglyakov, P.M. (1974): Journal of colloidal and interface science. USSR Vol. 36 p.145

Kalyan Das (2013): HIV-1 reverse transcriptase and antiviral drug resistance, Part 1. Current opinion in virology. Vol.3 No.2 pp.111-118

London, Van der Waal, J. D. (1873): Thesis Leiden

London, F. (1930): Z. Physics. Vol. 63 pp. 245

Lifshiftz, F.J., Hunt, S.M., Gore, J.M., and Curby, W.A. (1961): Cryobiology. Vol.12 pp.181

Layman, D.J., Muir, W.M., Lee, I.J. (1965): Trans. American society of Artificial Internal Organs. Vol.11 p. 301

Langbein D., (1969): journal of Adhesion. Vol.1, p.237

Levy, J. A. (2000): Acute HIV infection and susceptible cells. USA publication 2000, pp. 63-78

LAD Williams (2006): Ethnomedicine. West Indian Med Journal 2006; vol. 55 No.4 p.215

Li YY, Chen SW, Yang LM, Wang RR, Pang W, Zheng YT (2009): Molecules. Vol.15 No. 1 pp. 138-148.

Maddon P.J., Dalgleish A.G., McDougal J. S., Clapham, P.R., Weiss, R.A., Alex, R. (1986): The T4 gene encodes the AIDS virus receptor and is expressed in the immune system and the brain cell 47. Nature Journal 1985 Dec. 20 – 1986 Jan. 2; 312(5996) pp. 333-348.

Madunagu, B.E., R.U.B. Ebana and E.D. Ekpe (1990): “Antibacterial and Antifungal Activity of some medicinal plants of Akwa Ibom state”. West African Journal.

Mukoyama (1991); Omar, M.I.Y. (2003): Studies on the antiviral effect of some plant derived compounds. A Ph.D. thesis, Faculty of Veterinary medicine, Cairo University.

Martinson, J.A., Roman-Gonzalez, A., Tenorio, A.R. (2007): Dendritic cells from HIV-1 infected individual are less response to toll-like receptor (TLR) ligands. Journal of cell immunology. Vol.250 pp. 75-84

Meyer, J.H. (2007): Impact of HIV on cell survival and antiviral activity of plasmacytoid dendritic cell. Journal of microbiology. Vol.32 pp.19-39

Mamta S., Jyoti, S., Rajeev, N., Dharmendra, S. and Abhishek, G. (2013): Phytochemistry of medicinal plants. Journal of Pharmacognosy and Phytochemistry. Vol.1 No.6 p.168-182

Mazi, E.A. (2013): Physico-Chemical and Nutritive Properties of Bitter Kola (Garcinia Kola). Journal of Nutrition and Food Sci. ISSN: 2155-9600.

Mohammad A.H., Wafa AS. Al-Toubi, Afaf M.Weli, Qasim A. Al-Riyami, Jamal N. Al-Sabahi (2013): Identification and Characterization of chemical compounds in different crude extracts from leaves of Omani neem. Journal of Taibah University for Sci. Vol.7 pp.181-188

Neumann A.W., Absolom D.R., Zingg W., and Van Oss C. J., (1979): Surface Thermodynamics of Leukocyte and Platelet adhesion to polymer surfaces, cell biophysics. Vol.1 (1), pp.79-92

Neumann, A.W., Absolom, D.R., Francis, D.W., Omenyi, S.N., Spelt, J.K., Policova, Z., Thomas, C., Zingg, W. And Van Oss, C.J. (1983): Blood cell and protein surface tensions. Annals New York Academy of Science, pp.276-298

Neumann, A.W., Hope, C.J., Ward, C.A., Herbert, M.A., Dunn, G.W., and Zingg, W. (1975): Journal of Bio medics. Mater Res., vol. 9 pp. 127-142

Neumann, A.W., Van Oss C.J., Omenyi, S.N., Absolom, D.R. and Viser, J. (1983): Advanced colloid interface science. Vol.18 p.133

Neurath (2004) in: Omar, M.I.Y. (2003): Studies on the antiviral effect of some plant derived compounds. A Ph.D. thesis, Faculty of Veterinary medicine, Cairo University.

Nikhal S., Mahajan S. D. (2010): Evaluation of antibacterial and antioxidant activity of Mangifera indica (leaves). Journal of Pharm. Sci. & Research Vol.2 No. 1 pp. 45-47.

Ninham, B.W. and Parsegian, V.A. (1970): Journal of Chemistry and Physics. Vol. 52 p. 4578

Nir, S. (1972): Journal of Theoretical Biology. Vol. 34 p.135

Nwankwo O.J. (2011): Potential anticancer and antiviral agents from West African phytochemicals. University of Nigeria press. ISBN: 978-978-53040-4-6

Omenyi, S.N. (1978): Attraction and repulsion of particles by solidification melts. Ph.D. dissertation, University of Toronto.

Omenyi, S.N., Smith, R.P. and Neumann, A.W. (1980): Journal of Colloid and Interface science. Vol.75 No.1 p.117

Omenyi, S.N., Snyder, R.S. (1982): Enhanced erythrocyte suspension layer stability achieved by surface tension lowering additives. Journal of Dispersion Science and Technology. Vol. 3 pp. 307-333

Omenyi, S. N. And Dike, S. (2002): Unpublished Westcon International Ltd., McLean NV., USA

Omenyi, S. N., (2005): The Concept of Negative Hamaker Coefficient: Nnamdi Azikiwe University, Awka, Anambra state Nigeria, Inaugural Lecture Series No. 8.1, p.23

Okeke, P.N., Okeke, F.N. and Akande, S.F. (2008): Senior secondary physics. Pp. 155-161.

Padday J. F. (1969): Surface and colloid science. Matijevic ed. Vol.1, wiley intersciencs, NY. P.101

Plowden, C. C. (1972): A manual of plants names. 3rd Ed. London Georse Ltd: 239

Pistelli S. and Keith G. (2001): Interactions amongst drugs for HIV and opportunistic infections.

Peter, K. Quashie (2013): HIV drug resistance and the advent of integrase inhibitors. Current infectious disease reports. Vol.15 No.1 pp. 85-100

Joseph Nwankwo, Federal university Ndufu-Alike Ikwo. Oral communications.

Robinson and Zhang (2011): Studies on the antiviral effect of some plant derived compounds. A Ph.D thesis, Faculty of Veterinary medicine, Cairo University.

Sonntag, H. (1972): Kolloid Z.Z. Pol. Vol. 250 p.330

Schulze, H.J. and Cichos, C. (1972): Journal of Chemistry and Physics. Vol. 251 p.145

Scheline R. R. In: “Mammalian metabolism of plants Xenobiotics” (1978): Academic press NY, P. 320

Smith, R.P., Omenyi, S.N., and Neumann, A.W. (1983): Physiochemical aspects of polymer surfaces. Vol.1 pp.155-171. Mittal, A.K (Plenum press, NY)

Skowron, G., Bozette, S.A., Lim, L., Pettinelli, C.B., Schaumburg, H.H., Fischl, M.A. (1993): Alternating and intermittent regimens of Zidovudine and dideoxycytidine in patients with AIDS or AIDS-related complex. Ann Intern Med. Vol 118 pp.321-330

Szekeres, Greg (1999), Bulletin of Experimental Treatment for AIDS, San Francisco AIDS Foundation.

Shortman, K. And Liu, Y.J. (2002): Mouse and human dendritic cell subtypes. National Rev. Immunology. Vol.2 p.151

Song (2005); Omar, M.I.Y. (2003): Studies on the antiviral effect of some plant derived compounds. A Ph.D thesis, Faculty of Veterinary medicine, Cairo University.

Stefano V. A., Bernard S. B., Salif P. S., Serge P. E. And Robert L. M. (2012): The history of antiretroviral therapy and of its implementation in resource limited areas of the world. AIDS 2012, 26: 1231-1241.

Triboulet R., Mari B., Lin YL.,Chable-Bessia C., et al., (2007). Suppression of microRNA-silencing pathway by HIV-1 during virus replication. Science, 2007. 315, 1579-1582.

US department of health and human services (2012) edition.

UNAIDS (2016): The Joint United Nations programme on HIV/AIDS general assembly. UNAIDS South Africa, June 2016 report.

Vroman, L. And Adams, A.L. (1967): Thromb. Diath. Haemorrh. Vol.18 p.510

Vissers J., (1972): Advances in Colloid and Interface sciences. Vol.3, p. 331

Visser, J. (1975): in: Surface and colloidal science. Vol.8 E. Matijevis ed., vol.1 Wiley-Interscience, New York p.101

Van der Scheer A. And Smolders C. A. (1978): Dynamic aspects of contact angle measurements on adsorbed protein layers. Journal of colloid and interface sciences. Vol.63, pp.7-15

Van Oss C.J., and Grossberg, A.L. (1979): in: Principles of Immunology, Rose, N.R., Milgram, F. and Van Oss C.J. Macmillan, New York, chapter 5.

Van Oss, C.J., Absolom, D.R., and Neumann, A.W. (1979): Separ science and technology. Vol. 14, no. 4

Visser, J. (1981): Advances in interfacial science. Elsevier Scientific Publishing Co., Amsterdam. Vol. 15 pp. 157-169

Van der W., Louis, Stephanus, Abdul-Majeed, Bin, A.A. (2011): The use of a herbal composition for the treatment of a person infected with HIV. WO 2011039574

Vanden, B. (1986) in: Okeke, et al (2005) in: Omar, M.I.Y. (2003): Studies on the antiviral effect of some plant derived compounds. A Ph.D. thesis, Faculty of Veterinary medicine, Cairo University.

Wittman, F. (1971): Physics. Vol. 245 p.354

World Health Organization (WHO), (2003) report.

Wu, L. And Kewal-Ramani, V. N. (2006): Dendritic-cell interaction with HIV infection and viral dissemination. National Rev. Immunology. Vol.6 pp.859-868

Wanke, D. (2007); Stefano, V.A., Bernard, S.B., Salif, P.S., Serge, P.E. and Robert, L.M. (2012): The history of antiretroviral therapy and of its implementation in resource limited areas of the world. AIDS report 2012, vol.26 pp. 1231-1241.

Wang, J. H. (2009): Intercellular adhesion molecule (ICAM)-1, but not ICAM 2 and 3, is important for dendritic cell-mediated human immunodeficiency virus type-1 transmission. Journal of virology.Vol.83 pp. 4195-4204.

Webster's comprehensive dictionary of the English language. The new international Deluxe Encyclopedic 2010 edition.

Wensing, A. M. (2010): Fifteen years of HIV protease inhibitors: raising the barrier to resistance. Antiviral research. Vol.85 No.1 pp.59-74

www.HIVanotomy. Accessed 15/2/2016.

Xi-Jing Q., Yong-Zhe Z., Ping Z., and Zhong-Tian Q. (2016): Entry inhibitors: New advances in HCV treatment. www.nature.com/emi Accessed 24/6/2016

Yildirim, I. (2002): Studies of the interactions between talc and stikies during paper recycling. SME annual meeting and exhibition, Cincinnati society for mining, metallurgy and exploration.

Zisman, W. A. (1964): Advances in chemistry series. No. 43. American Chemistry Society, Washington DC.

Zheng M. S., Lu Z.Y. (1990): China Medical Journal (Engl.) Vol.103 No.2 pp.160-165

Zhentian (1999): Studies on the antiviral effect of some plant derived compounds. A Ph.D. Thesis, Faculty of Veterinary medicine, Cairo University.

Zheng, H. (2009): Reversal of HIV-1 latency with anti-microRNA inhibitors. Journal of Biochemistry cell biology. Vol.41 pp.451-454

A P P E N D I C E S